The role of hepatic inflammation in the development of hepatic steatosis and insulin resistance

Funke, Anouk

The Role of Hepatic Inflammation in the Development of Hepatic Steatosis and Insulin Resistance

Anouk Funke

Research
The work described in this thesis was performed at the Department of Molecular Genetics at the University Medical Center Groningen, University of Groningen, Groningen, the Netherlands

Funding
The studies described in this thesis were supported by SenterNovem (an IOP Genomics IGE05012 from Agentschap NL).

Printing of this thesis was financially supported by
University of Groningen, Groningen, the Netherlands
University Medical Center Groningen, Groningen, the Netherlands
Graduate School for Drug Exploration (GUIDE)
Greiner Bio-One B.V.
Hycult Biotech

Cover design: Anouk Funke
Page Layout: Anouk Funke
Printed by: CPI Wöhrmann Print Service

ISBN: 978-90-367-6557-2

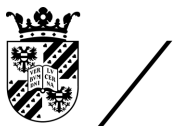

rijksuniversiteit
groningen

The Role of Hepatic Inflammation in the Development of Hepatic Steatosis and Insulin Resistance

Proefschrift

ter verkrijging van het doctoraat in de
Medische Wetenschappen
aan de Rijksuniversiteit Groningen
op gezag van de
Rector Magnificus, dr. E. Sterken,
in het openbaar te verdedigen op
woensdag 6 november 2013
om 11.00 uur

door

Anouk Funke

geboren op 3 oktober 1982

te Emmen

Promotor:	Prof. dr. M.H. Hofker
Copromotor:	Dr. D.P.Y. Koonen
Beoordelingscommissie:	Prof. dr. A.K. Groen Prof. dr. P.C.N. Rensen Prof. dr. R.J. Porte

Paranimfen:	Bianca Funke
	Marijke Schreurs

Contents

Chapter 1

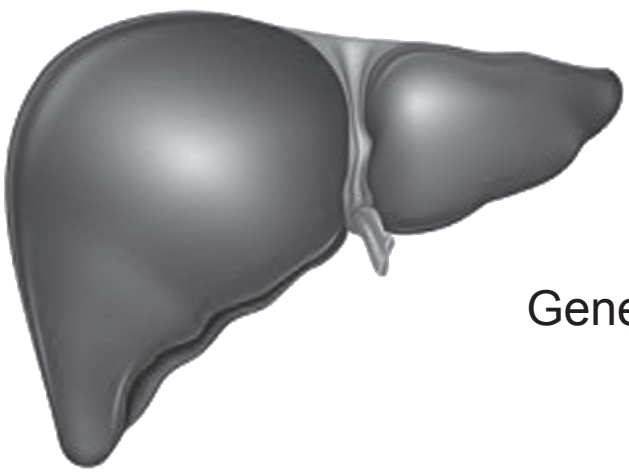

General Introduction

Obesity and the metabolic syndrome

For years, obesity has been a public health problem that remained limited to the developing countries. However, over the last decade obesity rates have reached pandemic proportions worldwide and obesity has developed into a global health problem. Now, for the first time in history the world has more overweight than underweight people (1). Moreover, children are increasingly at risk of becoming obese (2,3). In parallel with the obesity epidemic, obesity-related disorders, such as the metabolic syndrome are rising. The metabolic syndrome is characterized by a cluster of several metabolic disorders that are highly prevalent in developing countries, such as central obesity, dyslipidemia, insulin resistance and hypertension (4) (Fig. 1).

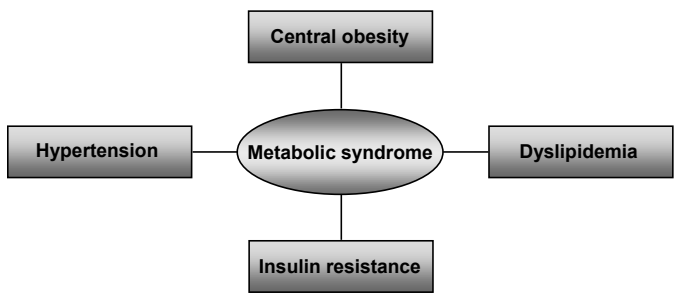

Figure 1. *The metabolic disorders that are clustered in the metabolic syndrome.*

Since 1920 these disorders have been clustered and different names have been given such as syndrome X, insulin resistance syndrome, Reaven's syndrome, and CHAOS (5). The presence of the metabolic syndrome is known to increase the risk for the development of type 2 diabetes (T2D) (6) and is highly predictive of new-onset T2D (7,8). In addition, the metabolic syndrome is associated with other diseases, including non-alcoholic fatty liver disease affecting up to a third of the population worldwide and has been shown to significantly enhance the risk of developing cardiovascular disease (9,10).

Although insulin resistance plays a crucial role in the pathogenesis of all of these disorders, its etiology is still poorly understood. There is growing evidence connecting obesity and its associated pathologies including non-alcoholic fatty liver disease (NAFLD) to the presence of a chronic low-grade inflammatory state (11,12). According to this commonly held view, inflammation leads to aberrant insulin receptor substrate (IRS) phosphorylation and reduced AKT phosphorylation, causing impaired glucose tolerance and insulin resistance. The liver is an important metabolic organ, which is affected by adiposity/obesity (13). The production of pro-inflammatory cytokines, by resident macrophages in the liver, contributes to hepatic inflammation and has been linked to disruption of (hepatic) insulin signaling (11). However, the contribution of hepatic inflammation to the etiology of fatty liver disease and insulin resistance is still elusive. This thesis describes the role of hepatic inflammation in the development of NAFLD and insulin resistance, as it represents a possible, but untapped opportunity,

to develop novel therapies. This introduction aims to provide the background information on which the studies performed in this thesis are founded.

The liver as a central organ

Already in the ancient times, the Greek physician Galen considered the liver as the most essential organ of the human body stating that the liver was “the principal organ of sanguification” (14). Although the role of the liver was somewhat overstated by the ancient Greeks, it is now known that the liver is a major metabolic organ that plays a central role in whole body metabolism by its ability to metabolize carbohydrates, lipids and proteins (15). Its main functions are glycogen storage, decomposition of red blood cells, plasma protein synthesis, and hormone production (15). The liver also produces and secretes bile to support the digestion and uptake of lipids from the intestine (15). In addition, the liver has also a detoxification function; it serves as a first pass organ. About 30% of the total blood passes through the liver every minute (16). Moreover, the liver is an important part of the bodies immune response and is important in acute phase responses and innate immunity (17,18).

The liver is comprised of parenchymal cells, the hepatocytes (19,20), and a variety of non-parenchymal resident cells. These include Kupffer cells, endothelial cells, stellate cells and immune cells (17). Hepatocytes are the so-called “liver cells”, and represent approximately two thirds of the total cells in the liver (16). Hepatocytes perform critical metabolic, endocrine, and secretory functions, which includes the synthesis of carbohydrates, cholesterol, bile salts, fatty acids, triglycerides, phospholipids, and proteins (reviewed in (21)). In hepatocytes, free fatty acids (FFA) are converted to triglycerides (TG) or oxidized as fuel. Mitochondrial β-oxidation of FFA will produce both energy for the cell and ketone bodies that are used as fuel for the brain. Stellate cells are the main cellular source of extracellular matrix proteins in the liver and represent 5 to 8% of the total liver mass (22). Moreover, Kupffer cells and lymphocytes account for the bulk of immune cells in the liver. Lymphocyte subpopulations include the innate (natural killer (NK) and NKT cells) and adaptive immune systems (T and B cells) (16). NKT cells account for up to 30% of the total lymphocytes in the liver (reviewed in (23)). Finally, liver endothelial cells form a lining of the hepatic sinusoids and separate the sinusoid lumen from the hepatocyte. An important function of the endothelial cells is to free the bloodstream from a variety of macromolecular waste products by endocytosis (24).

NAFLD

Non-alcoholic fatty liver disease (NAFLD) is tightly associated with insulin resistance, affecting up to 90% of the obese population (25). Driven by the obesity-epidemic, NAFLD has become the main cause of chronic liver in Western countries. Although, NAFLD is considered to be the hepatic manifestation of the metabolic syndrome, NAFLD is a strong, independent predictor for the development of T2D (26). NAFLD describes a wide spectrum of liver disorders, including hepatic steatosis, non-alcoholic steatohepatitis (NASH), advanced fibrosis, cirrhosis and ultimately liver cancer/failure (Fig. 2) (27,28).

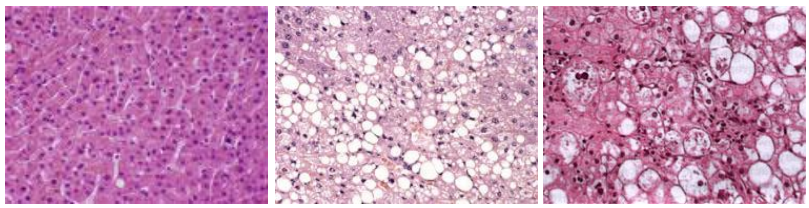

Normal liver | Fatty liver disease (NAFLD) | NASH

Figure 2. *Histological pictures of a normal liver, a liver with NAFLD and NASH.*

The *hallmark* of NAFLD is intrahepatic fat accumulation (steatosis) (29) and the accumulation of certain lipid species (e.g. diacylglycerol, long-chain acyl-CoA, ceramides) is thought to directly interfere with hepatic insulin signaling by inducing serine phosphorylation of IRS-1 (30). Hepatic steatosis arises from an imbalance between TG acquisition and removal (26). Causes of increased lipid content in hepatic steatosis may include 1) increased dietary fat associated with overeating or calorie dense foods that reach the liver as chylomicron particles from the intestine; 2) increased TG synthesis in the liver from fatty acids formed from *de novo* lipogenesis; 3) excess fatty acid influx into the liver from lipolysis of adipose tissue in obese and insulin resistant states and subsequent conversion to TG; 4) diminished export of lipids from the liver in very-low-density lipoproteins (VLDL); and 5) reduced mitochondrial oxidation of fatty acids (Fig. 3).

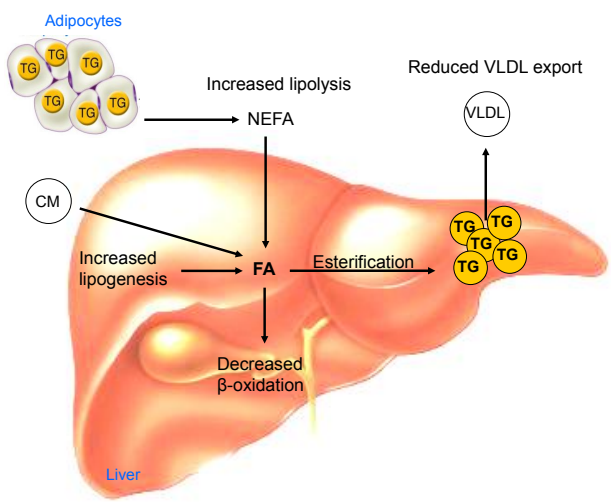

Figure 3. *Metabolic defects leading to the development of hepatic steatosis. Hepatic steatosis arises from an imbalance between triglyceride (TG) acquisition and removal. Several mechanisms can lead to the development of hepatic steatosis. (Adapted from Postic et al, JCI 2008).*

Hepatic steatosis may have a macro- or micro-vesicular appearance depending on size and number of fat droplets within the hepatocyte (31). The diagnosis of steatosis is made when the lipid content in the liver exceeds the 95th percentile for lean, healthy individuals (i.e.,> 55 mg per g of liver) or if the presence of cytoplasmic TG droplets is more than 5% of hepatocytes (32,33). A preliminary diagnosis of NAFLD can be made in patients with elevated liver enzymes, although a definitive diagnosis can only be made by liver biopsy (34).

NASH

Hepatic steatosis can progress to non-alcoholic steatohepatitis (NASH), the more advanced stage of NAFLD (26). NASH was originally defined by Ludwig and colleagues as a condition indistinguishable by histology from alcoholic steatohepatitis, although most patients carried the hallmarks of obesity and the metabolic syndrome (35). About one-third of individuals with NAFLD who undergo liver biopsy, upon elevated levels of ALT/AST, have evidence of NASH (36). NASH can be distinguished from simple steatosis by the presence of hepatocyte injury including hepatocyte ballooning and cell death, an inflammatory infiltrate, and/or collagen deposition (fibrosis). It is not known whether steatosis always precedes NASH or whether inflammation occurs independently of hepatic steatosis (26). However, the inflamed liver preludes further disease progression and allows for later stages of the disease to develop, such as liver fibrosis, cirrhosis and eventually liver failure or hepatocellular carcinoma (37,38). Moreover, the inflammatory component in addition to steatosis carries a higher risk of cardiovascular disease and mortality than simple steatosis (39). Approximately 25–30% of the patients with simple steatosis will develop NASH (40). In addition, 20-30% of the NASH patients progresses to severe fibrosis within 10 years (36). Moreover, 10 to 29% of the individuals with NASH will develop cirrhosis within 10 years (41). Cirrhosis can ultimately progress to liver cancer; 4 to 27% of individuals with NASH-induced cirrhosis develop hepatocellular carcinoma (42).
An increasing amount of evidence supports a central role for pro-inflammatory cytokines, particularly TNF-α in the development of NASH (43). TNF-α levels are elevated in the liver and blood of patients with NASH, and inhibition of TNF-α by administration of recombinant TNF-α has been demonstrated to improve NAFLD in rodents (reviewed in (44)). Hepatic inflammation in NASH has also been reported to induce hepatic and systemic insulin resistance (13), making NASH an important contributing factor to the development of T2D. The factors causing progression of NAFLD to fibrosis and cirrhosis have not been defined in humans, in part because of the relative inaccessibility of liver tissue thus impeding detailed studies.

Role of Kupffer cells in development of NASH

Kupffer cells were discovered in 1876 by Karl Wilhelm von Kupffer (45). Kupffer cells are now defined as specialized tissue macrophages in the hepatic sinusoid and are derived from circulating monocytes that arise from bone marrow progenitors (46). It has been calculated that up to 50% of the circulating monocytes are destined for the liver (47). Kupffer cells represent 10-15% of the total liver cell population (24), and comprise of 80-90% of all tissue macrophages in the body (48). Kupffer cells are

responsible for the rapid repression and clearance of exogenous particulates and immunoreactive materials that are perceived by the body to be foreign and harmful (24). Like other macrophages, Kupffer cells sense endogenous molecular signals that may result from the perturbed homeostasis of the host. Activated Kupffer cells are able to: 1) initiate interactions with hepatocytes and other liver cells through the release of active mediators, including cytokines, chemokines, eicosanoids, proteolytic enzymes, reactive oxygen species and nitric oxide; 2) recruit and retain neutrophils and NK T lymphocytes, NK cells and blood monocyte-derived macrophages; 3) engulf, ingest and eliminate solid particles, including micro-organisms, apoptotic cells and cellular debris; and 4) process and present antigens to attract cytotoxic and regulatory T cells, thereby contributing to adaptive immunity (16,17,24,49,50). All of these functions need to be rigorously controlled to avoid escalation of the inflammatory response. Therefore, Kupffer cells have been thought to contribute to the pathogenesis of many different kinds of liver injury (51,52). In addition, the production of pro-inflammatory cytokines secreted by Kupffer cells in the liver is linked to disruption of hepatic insulin signaling (11). Indeed, Kupffer cell activation upon high fat feeding has been linked to NASH and the development of hepatic insulin resistance (53,54). Therefore, inflammation and hepatic insulin resistance can be exacerbated through the release of locally acting cytokines by activated Kupffer cells (55,56).

Therapy

Given the close relationship between obesity, the metabolic syndrome and NAFLD, treatment of NASH is mainly aimed to target several parameters of the metabolic syndrome, such as obesity, hyperlipidemia and insulin resistance. Steatosis itself is generally considered a rather benign and reversible condition (4). However, the presence of inflammation in a fatty liver represents an irreversible step and has a poor prognosis (4). Despite the rapidly growing recognition of NAFLD/NASH over the past decade, therapy directed at treating or preventing the disease remains limited to weight loss.

Simple lifestyle modifications, such as body weight management and regular physical exercise are the primary therapy options for patients with the metabolic syndrome (6). Weight loss has been shown to reduce steatosis (57). However, its effect on inflammation and fibrosis, is still unclear (58,59). In line with this, bariatric surgery, which alleviates NAFLD (60), is associated with increased insulin sensitivity in human patients (61). The quick improvement of insulin resistance after bariatric surgery may be due to decreased intrahepatic fat accumulation in response to caloric restriction (62,63). This suggests that targeting NAFLD and NASH may be an attractive strategy to improve insulin resistance and T2D.

In addition to lifestyle changes and bariatric surgery, current therapies used for NASH include insulin sensitizers such as metformin and thiazolidinediones (TZDs). The primary mode of action of TZDs is through binding and activation of the nuclear receptor PPAR-γ to improve insulin sensitivity (64,65). Unfortunately, discontinuation of TZDs treatment after 48 weeks abolishes the therapeutic effects on NASH, resulting in increased liver fat, inflammation, and aggravation of histopathological scores (66,67). Metformin improves insulin sensitivity by acting on hepatic and skeletal

muscle glucose uptake and metabolism (68). Given the fact that hypertriglyceridemia and low HDL levels are defining elements of the metabolic syndrome, lipid-lowering agents are also possible candidates for NASH treatment. For example, statins and fibrates, or a combination of the two, are considered to be good treatment options for NASH. Fibrates are ligands of PPAR-α and are an effective therapy promoting lipid oxidation, lowering serum TG levels, and increasing serum HDL by stimulating lipoprotein lipase and regulating apolipoprotein expression (69,70). Statins lower serum lipid concentrations by inhibiting HMG-CoA reductase, the key enzyme in cholesterol biosynthesis (71). However, the use of lipid-lowering drugs is controversial because of their potential hepatotoxicity in patients with underlying hepatic disease (reviewed in (72)).
As none of the above treatments have shown convincing benefits, new therapy options should be considered. At the moment liver transplantation remains the only curative treatment for end-stage liver failure.

The role of adipose tissue and systemic inflammation in the etiology of insulin resistance

As early as the 1950s and 1960s, studies have suggested an association between inflammation, T2D and obesity, but the mechanistic links were unknown. Obese subjects were found to have elevated circulating concentrations of systemic markers of inflammation including fibrinogen and acute-phase reactants (73,74). However, these findings failed to influence thoughts about the pathogenesis of T2D. Experiments with the adipose tissue-derived pro-inflammatory cytokine TNF-α showed that TNF-α was able to induce insulin resistance (75). In the last decades, it has become increasingly clear that obesity and the concomitant development of inflammation are major players in the etiology of insulin resistance. It was a groundbreaking idea that a cytokine, which was produced by the adipose tissue, had not only local but also systemic effects on metabolism. It did not take long before other cytokines and bioactive substances produced by the adipose tissue were discovered, which include leptin, IL-6, resistin, and monocyte chemoattractant protein-1 (MCP-1) (76,77).
As part of the chronic inflammatory process, locally secreted chemokines attract pro-inflammatory macrophages into the adipose tissue where they form crown-like structures around dead or dying adipocytes. These tissue macrophages then release cytokines that further activate the inflammatory program in neighboring adipocytes, thereby exacerbating inflammation and insulin resistance. A major mechanistic breakthrough into the understanding of how obesity and inflammation are connected was by the discovery of adipose tissue being infiltrated with increased numbers of macrophages in obese mice and humans (78). Pharmacological or genetic inhibition of pathways that are involved in the inflammatory response have been found to protect experimental animals and humans from diet-induced insulin resistance (56,79). Two transcription factor-signaling pathways have been linked to the pro-inflammatory effects of obesity and insulin resistance: the NF-κB pathway, which is activated by inhibitor of NF-κB (IκB) kinase β (IKKβ), and the c-Jun NH_2-terminal kinase (JNK) pathway. Genetic disruption of NF-κB and JNK signaling pathways has been shown to protect against insulin resistance.

Cross-talk and insulin resistance

In obese subjects and rodent models of obesity and T2D, inflammation and insulin resistance does not remain restricted to the adipose tissue. Also the liver and skeletal muscle are affected (Fig. 4). Upon obesity, the hepatic inflammatory pathway can be activated by steatosis and/or the increased hepatocyte stress pathway responses. Obesity overloads the functional capacity of the endoplasmic reticulum (ER), triggering intracellular ER stress. Moreover, ER stress leads to the activation of inflammatory signaling pathways and contributes to the development of insulin resistance (80,81). Moreover, Kupffer cells are activated and lead to the production of locally acting cytokines, which further exacerbate inflammation and hepatic insulin resistance (reviewed in (82)). In skeletal muscle, obesity results in increased FFA uptake and also the activation and recruitment of macrophages and eventually leading to the development of skeletal muscle insulin resistance.

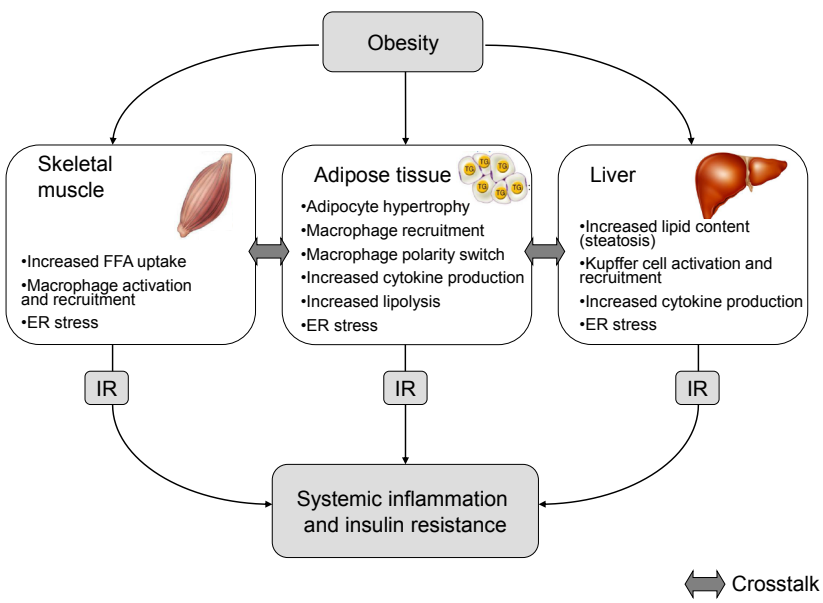

Figure 4. *Obesity and the development of inflammation and insulin resistance. Obesity-induced changes in different metabolic organs resulting in localized inflammation and insulin resistance. Endocrine-mediated cross-talk between insulin target tissues contributes to insulin resistance in distant tissues. Systemic inflammation and insulin resistance are the net effect of these changes. (Adapted from de Luca et al, FEBS Letters 2008).*

It is known that obesity-induced adipose tissue inflammation has an effect on liver metabolism and insulin resistance (83,84). Activated adipose tissue macrophages secrete different cytokines that can leak out of the tissue, resulting in raised circulating levels and produce endocrine effects on distant organs, such as the liver and skeletal muscle, eventually leading to exacerbation of systemic insulin resistance (reviewed in (82)). However, it has been suggested that cross-talk between the adipose tissue and liver is bidirectional. Of note, the liver produces and secretes cytokines (i.e., CRP, SAA, IL-6) that end up in the circulation and may impair insulin sensitivity in

other organs through endocrine effects (85,86). In line with this, Kupffer cell depletion studies have been shown to prevent hepatic insulin resistance, but also protects against adiposity, adipose tissue inflammation and whole-body insulin resistance induced by a HFD (87). Therefore, it has been suggested that endocrine-mediated cross-talk between insulin target tissues contributes to insulin resistance in distant tissues. Further studies are needed to decipher the communication between the metabolic active tissues to assess the role of obesity-induced inflammation and the development of insulin resistance. Recent data showed that increased hepatic and skeletal muscle inflammation only became apparent after establishment of obesity (88). In line with this, obesity is a confounding factor in the development of inflammation–induced insulin resistance, making it difficult to assess inter-organ effects.

Moreover, cell-cell interactions are also important in the development of obesity-induced insulin resistance. One study showed that deletion of IKKβ in the hepatocytes resulted in insulin sensitivity in the liver; however these mice became insulin resistant in muscle and adipose tissue. In contrast, deletion of IKKβ in myeloid cells led to a global improvement in insulin sensitivity. Therefore, it has been suggested that myeloid cells are responsible for the major form of cross-talk between insulin-responsive tissues involving pro-inflammatory cytokines (89). More studies should be performed assessing the role of different cell types in the development of obesity-induced insulin resistance.

Study objectives

Considerable evidence now points towards a crucial role for inflammation as a causal factor in obesity-induced insulin resistance and T2D (reviewed in (85)). Mouse models show that in the absence of other confounding factors, hepatic inflammation alone is sufficient to cause hepatic and systemic insulin resistance (13). However, the exact role of hepatic inflammation and the involvement of Kupffer cells in the development of insulin resistance remains to be elucidated. In this thesis, we used 3 different mouse models, i.e., *Ldlr*$^{-/-}$ mice, *Myd88*$^{-/-}$ mice, and *Csf1*$^{op/+}$ mice (Fig. 5) to investigate the role of hepatic inflammation in the etiology of NAFLD and insulin resistance. The models and specific hypotheses that will be tested are described below.

(1) Low-density lipoprotein receptor (Ldlr knock out mouse model)

Mice deficient for the low-density lipoprotein receptor (*Ldlr*$^{-/-}$) (90) exhibit many features of the metabolic syndrome when fed a western style or diabetogenic diet, including obesity, insulin resistance, dyslipidemia, inflammation and atherosclerosis (91,92). When triggered with a high-fat cholesterol (HFC) diet (21% milk butter, 0.2% cholesterol), *Ldlr*$^{-/-}$ mice also display many features of human NAFLD, including NASH (93,94). This is in contrast to C57BL/6 mice that develop hepatic steatosis and insulin resistance without further progression towards NASH (95).

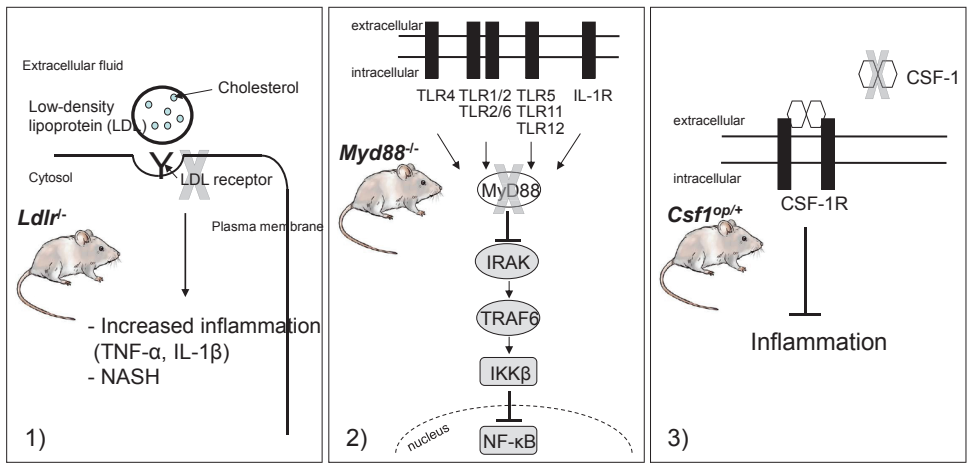

Figure 5. *The different mouse models used in this thesis. 1) Ldlr$^{-/-}$ mouse; 2) Myd88$^{-/-}$ mouse; and 3) Csf1$^{op/+}$ mouse. Deletion of the LDLR leads to enhanced hepatic inflammation and NASH. Myd88$^{-/-}$ mice show reduced NF-κB-mediated inflammation. Heterozygous mice deficient for CSF1 (Csf1$^{op/+}$ mice) exhibit reduced inflammation.*

The function of the LDL receptor (LDLR) is clearing of LDL and lipoprotein remnants containing ApoE and ApoB (96,97). Moreover, the LDLR is thought to play a role in regulating hepatic lipoprotein production (98). Deletion of the LDLR would lead to elevated levels of LDL. In humans, mutations in the LDL receptor leads to one of the most severe forms of human hyperlipidemia, familial hypercholesterolemia, causing elevated levels of the atherogenic lipoprotein LDL and atherosclerosis (90). Notably, *Ldlr$^{-/-}$* mice are hyperlipidemic and show a lipoprotein profile resembling dyslipidemia in human obesity and T2D. Whereas, *Ldlr$^{-/-}$* mice develop moderate hypercholesterolemia on a chow diet, on a high-fat/high-cholesterol diet *Ldlr$^{-/-}$* mice rapidly develop severe hyperlipidemia and extensive atherosclerosis (90).

Although *Ldlr$^{-/-}$* mice are now a well established model to study NASH (93,94,99), it is not known what the metabolic consequences are in terms of insulin resistance. Therefore, we aimed to unravel the extent to which hepatic inflammation contributes to the development of hepatic and systemic insulin resistance in the absence and presence of obesity using hyperlipidemic *Ldlr$^{-/-}$* mice (**Chapter 2**).

(2) Myeloid differentiation factor response gene 88 (Myd88)

Toll-like receptors (TLRs) are potential “sensors” that may link obesity to inflammation and insulin resistance. Myeloid differentiation primary response gene 88 (Myd88) is a key intracellular adaptor protein in the TLR and IL-1 signaling cascade linked to NASH and insulin resistance (100-104). Since both TLR and IL-1 signal through Myd88 to activate NF-κB, it is likely that Myd88 plays an essential role in the pathogenesis of NAFLD/NASH and insulin resistance.
TLRs are part of a family of pattern-recognition receptors (PRRs) that detect microbial components and activate the immune system, providing a first line of host

defense against infections (105-107). Each TLR recognizes different pathogens (viruses, bacteria, fungi, parasites) via PAMPs (pathogen-associated molecular patterns) and initiate the immune response. TLR2 and TLR4, have an important role in inflammation associated with both atherosclerosis and insulin resistance (108). TLRs signal via various adaptor molecules, including Myd88 (106,107). Mice deficient for Myd88 have previously been show to be protected against the development of atherosclerosis (109) and therefore represents a good model to study the role of Myd88 on the development of NAFLD and insulin resistance. Furthermore, we will investigate the contribution of hematopoietic-cell-derived Myd88 on the development of obesity-induced inflammation and insulin resistance (**Chapter 3**).

(3) Macrophage colony stimulating factor (MCSF)/Osteopetrotic (Op)

Mice which are insufficient for colony-stimulating factor 1 (Csf1) have impaired macrophage development. Therefore this model is ideally suited to investigate the role of macrophages in NAFLD and insulin resistance.
The colony-stimulating factors (CSFs) are a family of cytokine growth factors originally identified by their ability to support the proliferation and differentiation of hematopoietic progenitor stem cells into mature monocytes/macrophages and granulocytes (110). The CSF family comprises of macrophage CSF (M-CSF or CSF-1), granulocyte-macrophage CSF (GM-CSF or CSF-2), and granulocyte CSF (G-CSF or CSF-3). M-CSF functions as a chemotactic factor for monocytes, regulates the effector functions of mature monocytes and macrophages, and modulates the inflammatory responses by stimulating the production of other cytokines and growth factors (111).
Osteopetrotic (*op/op*) mice lack M-CSF due to a point mutation (thymidine insertion) in the coding region of the M-CSF gene (112). Lack of M-CSF in *op/op* mice results in impaired growth and differentiation of monocytes and their precursors in bone marrow (112,113). Homozygous mice insufficient for Csf1 (*Csf1*$^{op/op}$) show a severe deficiency of osteoclasts, resulting in impaired bone remodeling, skeletal deformities (domed skulls), and absence of teeth, impairing consumption of solid food (114). Chronic injection of recombinant M-CSF partially corrects the phenotypic defects in *Csf1*$^{op/op}$ mice (115). In contrast to *Csf1*$^{op/op}$ mice, heterozygous mice insufficient for Csf1 (*Csf1*$^{op/+}$ mice) do not exhibit growth or skeletal defects and do not lack teeth making dietary intervention studies and obesity research possible (114,116). CSF-1 has been shown to play an important role in chronic diseases and inflammatory disease states, including atherosclerosis (111,117,118). Therefore, Csf1 insufficient mice allow us to study the hypothesis that macrophages via Csf1 regulation contribute to the pathogenesis of obesity-related disorders, including insulin resistance and T2D (**Chapter 4**).

(4) N-(5-adamantane-1-yl-methoxy-pentyl)-deoxynojirimycin (AMP-DNM)

Glycosphingolipids (GSLs) are known to be involved in the development of

insulin resistance (119,120). Moreover, it has been demonstrated that inhibitors of glucosylceramide (GlcCer) synthase lead to inhibition of GSL biosynthesis (121). Furthermore, these GlcCer synthase inhibitors have been shown to hold great promise as novel therapeutics in metabolic disease. *N*-(5-adamantane-1-yl-methoxy-pentyl)-deoxynojirimycin (AMP-DNM), an inhibitor of GlcCer synthase, improved glucose tolerance and enhanced insulin signaling in rodent models of type 2 diabetes (122-124). Moreover, AMP-DNM-treated mice exhibited improved adipocyte function, reduced adipose tissue and liver inflammation and diminished and corrected hepatic steatosis (123-126). Since food intake is reduced in AMP-DNM-treated animals, we assessed the role of AMP-DNM as a caloric restriction mimetic and the therapeutic potential of AMP-DNM in metabolic disease (**Chapter 5**).

Finally, in **Chapter 6** we will discuss the major findings of this thesis, place them in the context of the current state of the field, and address the clinical implications of the results.

References

1. Popkin BM. The world is fat. Sci Am 2007;297(3):88-95.
2. Mendez MA, Monteiro CA, Popkin BM. Overweight exceeds underweight among women in most developing countries. Am J Clin Nutr 2005;81(3):714-721.
3. Sherry B, Mei Z, Scanlon KS, Mokdad AH, Grummer-Strawn LM. Trends in state-specific prevalence of overweight and underweight in 2- through 4-year-old children from low-income families from 1989 through 2000. Arch Pediatr Adolesc Med 2004;158(12):1116-1124.
4. Parekh S, Anania FA. Abnormal lipid and glucose metabolism in obesity: implications for nonalcoholic fatty liver disease. Gastroenterology 2007;132(6):2191-2207.
5. Sarafidis PA, Nilsson PM. The metabolic syndrome: a glance at its history. J Hypertens 2006;24(4):621-626.
6. Grundy SM. Metabolic syndrome: connecting and reconciling cardiovascular and diabetes worlds. J Am Coll Cardiol 2006;47(6):1093-1100.
7. Hanson RL, Imperatore G, Bennett PH, Knowler WC. Components of the “metabolic syndrome” and incidence of type 2 diabetes. Diabetes 2002;51(10):3120-3127.
8. Laaksonen DE, Lakka HM, Niskanen LK, Kaplan GA, Salonen JT, Lakka TA. Metabolic syndrome and development of diabetes mellitus: application and validation of recently suggested definitions of the metabolic syndrome in a prospective cohort study. Am J Epidemiol 2002;156(11):1070-1077.
9. Jeppesen J, Hansen TW, Rasmussen S, Ibsen H, Torp-Pedersen C, Madsbad S. Insulin resistance, the metabolic syndrome, and risk of incident cardiovascular disease: a population-based study. J Am Coll Cardiol 2007;49(21):2112-2119.
10. Meigs JB, Rutter MK, Sullivan LM, Fox CS, D’Agostino RB, Sr., Wilson PW. Impact of insulin resistance on risk of type 2 diabetes and cardiovascular disease in people with metabolic syndrome. Diabetes Care 2007;30(5):1219-1225.
11. Tilg H, Moschen AR. Insulin resistance, inflammation, and non-alcoholic fatty liver disease. Trends Endocrinol Metab 2008;19(10):371-379.
12. Osborn O, Olefsky JM. The cellular and signaling networks linking the immune system and metabolism in disease. Nat Med 2012;18(3):363-374.
13. Cai D, Yuan M, Frantz DF, Melendez PA, Hansen L, Lee J, et al. Local and systemic insulin resistance resulting from hepatic activation of IKK-beta and NF-kappaB. Nat Med 2005;11(2):183-190.
14. Adamson JD. The Liver as the Organ of Sanguification. Can Med Assoc J 1928;18(2):147-150.
15. Meshkani R, Adeli K. Hepatic insulin resistance, metabolic syndrome and cardiovascular disease. Clin Biochem 2009;42(13-14):1331-1346.
16. Racanelli V, Rehermann B. The liver as an immunological organ. Hepatology 2006;43(2 Suppl 1):S54-S62.
17. Gao B, Jeong WI, Tian Z. Liver: An organ with predominant innate immunity. Hepatology 2008;47(2):729-736.
18. Dong Z, Wei H, Sun R, Tian Z. The roles of innate immune cells in liver injury and regeneration. Cell Mol Immunol 2007;4(4):241-252.
19. David H. The hepatocyte. Development, differentiation, and ageing. Exp Pathol Suppl 1985;11:1-148.
20. Rappaport AM, Borowy ZJ, Lougheed WM, Lotto WN. Subdivision of hexagonal liver lobules into a structural and functional unit; role in hepatic physiology and pathology. Anat Rec 1954;119(1):11-33.
21. Kmiec Z. Cooperation of liver cells in health and disease. Adv Anat Embryol Cell Biol 2001;161:III-151.
22. Gabele E, Brenner DA, Rippe RA. Liver fibrosis: signals leading to the amplification

of the fibrogenic hepatic stellate cell. Front Biosci 2003;8:d69-d77.
23. Shoelson SE, Herrero L, Naaz A. Obesity, inflammation, and insulin resistance. Gastroenterology 2007;132(6):2169-2180.
24. Smedsrod B, De Bleser PJ, Braet F, Lovisetti P, Vanderkerken K, Wisse E, et al. Cell biology of liver endothelial and Kupffer cells. Gut 1994;35(11):1509-1516.
25. Marchesini G, Bugianesi E, Forlani G, Cerrelli F, Lenzi M, Manini R, et al. Nonalcoholic fatty liver, steatohepatitis, and the metabolic syndrome. Hepatology 2003;37(4):917-923.
26. Cohen JC, Horton JD, Hobbs HH. Human fatty liver disease: old questions and new insights. Science 2011;332(6037):1519-1523.
27. Angulo P. Nonalcoholic fatty liver disease. N Engl J Med 2002;346(16):1221-1231.
28. Matteoni CA, Younossi ZM, Gramlich T, Boparai N, Liu YC, McCullough AJ. Nonalcoholic fatty liver disease: a spectrum of clinical and pathological severity. Gastroenterology 1999;116(6):1413-1419.
29. Marchesini G, Brizi M, Bianchi G, Tomassetti S, Bugianesi E, Lenzi M, et al. Nonalcoholic fatty liver disease: a feature of the metabolic syndrome. Diabetes 2001;50(8):1844-1850.
30. Samuel VT, Shulman GI. Mechanisms for insulin resistance: common threads and missing links. Cell 2012;148(5):852-871.
31. Reddy JK, Rao MS. Lipid metabolism and liver inflammation. II. Fatty liver disease and fatty acid oxidation. Am J Physiol Gastrointest Liver Physiol 2006;290(5):G852-G858.
32. Adams LA, Angulo P, Lindor KD. Nonalcoholic fatty liver disease. CMAJ 2005;172(7):899-905.
33. Szczepaniak LS, Nurenberg P, Leonard D, Browning JD, Reingold JS, Grundy S, et al. Magnetic resonance spectroscopy to measure hepatic triglyceride content: prevalence of hepatic steatosis in the general population. Am J Physiol Endocrinol Metab 2005;288(2):E462-E468.
34. Clark JM, Diehl AM. Nonalcoholic fatty liver disease: an underrecognized cause of cryptogenic cirrhosis. JAMA 2003;289(22):3000-3004.
35. Ludwig J, Viggiano TR, McGill DB, Oh BJ. Nonalcoholic steatohepatitis: Mayo Clinic experiences with a hitherto unnamed disease. Mayo Clin Proc 1980;55(7):434-438.
36. Argo CK, Northup PG, Al-Osaimi AM, Caldwell SH. Systematic review of risk factors for fibrosis progression in non-alcoholic steatohepatitis. J Hepatol 2009;51(2):371-379.
37. Portincasa P, Grattagliano I, Palmieri VO, Palasciano G. The emerging problem of nonalcoholic steatohepatitis (NASH). Rom J Gastroenterol 2005;14(1):43-51.
38. Byrne CD. Fatty liver: role of inflammation and fatty acid nutrition. Prostaglandins Leukot Essent Fatty Acids 2010;82(4-6):265-271.
39. Bhatia LS, Curzen NP, Calder PC, Byrne CD. Non-alcoholic fatty liver disease: a new and important cardiovascular risk factor? Eur Heart J 2012;33(10):1190-1200.
40. McCullough AJ. Pathophysiology of nonalcoholic steatohepatitis. J Clin Gastroenterol 2006;40 Suppl 1:S17-S29.
41. Argo CK, Caldwell SH. Epidemiology and natural history of non-alcoholic steatohepatitis. Clin Liver Dis 2009;13(4):511-531.
42. Starley BQ, Calcagno CJ, Harrison SA. Nonalcoholic fatty liver disease and hepatocellular carcinoma: a weighty connection. Hepatology 2010;51(5):1820-1832.
43. Feldstein AE. Novel insights into the pathophysiology of nonalcoholic fatty liver disease. Semin Liver Dis 2010;30(4):391-401.
44. Tilg H. The role of cytokines in non-alcoholic fatty liver disease. Dig Dis 2010;28(1):179-185.
45. Szymanska R, Schmidt-Pospula M. Studies of liver's reticuloendothelial cells by

Tadeusz Browicz and Karl Kupffer. A historical outline. Arch Hist Med (Warsz) 1979;42(3):331-336.
46. Gale RP, Sparkes RS, Golde DW. Bone marrow origin of hepatic macrophages (Kupffer cells) in humans. Science 1978;201(4359):937-938.
47. Crofton RW, Diesselhoff-den Dulk MM, van Furth R. The origin, kinetics, and characteristics of the Kupffer cells in the normal steady state. J Exp Med 1978;148(1):1-17.
48. Bouwens L, Baekeland M, De Zanger R, Wisse E. Quantitation, tissue distribution and proliferation kinetics of Kupffer cells in normal rat liver. Hepatology 1986;6(4):718-722.
49. Burgio VL, Ballardini G, Artini M, Caratozzolo M, Bianchi FB, Levrero M. Expression of co-stimulatory molecules by Kupffer cells in chronic hepatitis of hepatitis C virus etiology. Hepatology 1998;27(6):1600-1606.
50. Decker K. Biologically active products of stimulated liver macrophages (Kupffer cells). Eur J Biochem 1990;192(2):245-261.
51. Enomoto N, Ikejima K, Yamashina S, Hirose M, Shimizu H, Kitamura T, et al. Kupffer cell sensitization by alcohol involves increased permeability to gut-derived endotoxin. Alcohol Clin Exp Res 2001;25(6 Suppl):51S-54S.
52. Rivera CA, Bradford BU, Hunt KJ, Adachi Y, Schrum LW, Koop DR, et al. Attenuation of CCl(4)-induced hepatic fibrosis by GdCl(3) treatment or dietary glycine. Am J Physiol Gastrointest Liver Physiol 2001;281(1):G200-G207.
53. Feng B, Jiao P, Nie Y, Kim T, Jun D, van Rooijen N, et al. Clodronate liposomes improve metabolic profile and reduce visceral adipose macrophage content in diet-induced obese mice. PLoS One 2011;6(9):e24358.
54. Lanthier N, Molendi-Coste O, Horsmans Y, van Rooijen N, Cani PD, Leclercq IA. Kupffer cell activation is a causal factor for hepatic insulin resistance. Am J Physiol Gastrointest Liver Physiol 2010;298(1):G107-G116.
55. Popa C, Netea MG, van Riel PL, van der Meer JW, Stalenhoef AF. The role of TNF-alpha in chronic inflammatory conditions, intermediary metabolism, and cardiovascular risk. J Lipid Res 2007;48(4):751-762.
56. Schenk S, Saberi M, Olefsky JM. Insulin sensitivity: modulation by nutrients and inflammation. J Clin Invest 2008;118(9):2992-3002.
57. Luyckx FH, Lefebvre PJ, Scheen AJ. Non-alcoholic steatohepatitis: association with obesity and insulin resistance, and influence of weight loss. Diabetes Metab 2000;26(2):98-106.
58. Kotronen A, Yki-Jarvinen H. Fatty liver: a novel component of the metabolic syndrome. Arterioscler Thromb Vasc Biol 2008;28(1):27-38.
59. Ueno T, Sugawara H, Sujaku K, Hashimoto O, Tsuji R, Tamaki S, et al. Therapeutic effects of restricted diet and exercise in obese patients with fatty liver. J Hepatol 1997;27(1):103-107.
60. Mummadi RR, Kasturi KS, Chennareddygari S, Sood GK. Effect of bariatric surgery on nonalcoholic fatty liver disease: systematic review and meta-analysis. Clin Gastroenterol Hepatol 2008;6(12):1396-1402.
61. Bradley D, Magkos F, Klein S. Effects of bariatric surgery on glucose homeostasis and type 2 diabetes. Gastroenterology 2012;143(4):897-912.
62. Isbell JM, Tamboli RA, Hansen EN, Saliba J, Dunn JP, Phillips SE, et al. The importance of caloric restriction in the early improvements in insulin sensitivity after Roux-en-Y gastric bypass surgery. Diabetes Care 2010;33(7):1438-1442.
63. Kirk E, Reeds DN, Finck BN, Mayurranjan SM, Patterson BW, Klein S. Dietary fat and carbohydrates differentially alter insulin sensitivity during caloric restriction. Gastroenterology 2009;136(5):1552-1560.
64. Shulman GI. Cellular mechanisms of insulin resistance. J Clin Invest 000;106(2):171-

176.
65. Yki-Jarvinen H. Thiazolidinediones. N Engl J Med 2004;351(11):1106-1118.
66. Lutchman G, Modi A, Kleiner DE, Promrat K, Heller T, Ghany M, et al. The effects of discontinuing pioglitazone in patients with nonalcoholic steatohepatitis. Hepatology 2007;46(2):424-429.
67. Neuschwander-Tetri BA, Brunt EM, Wehmeier KR, Oliver D, Bacon BR. Improved nonalcoholic steatohepatitis after 48 weeks of treatment with the PPAR-gamma ligand rosiglitazone. Hepatology 2003;38(4):1008-1017.
68. Reynaert H, Geerts A, Henrion J. Review article: the treatment of non-alcoholic steatohepatitis with thiazolidinediones. Aliment Pharmacol Ther 2005;22(10):897-905.
69. Cook WS, Yeldandi AV, Rao MS, Hashimoto T, Reddy JK. Less extrahepatic induction of fatty acid beta-oxidation enzymes by PPAR alpha. Biochem Biophys Res Commun 2000;278(1):250-257.
70. Neve BP, Fruchart JC, Staels B. Role of the peroxisome proliferator-activated receptors (PPAR) in atherosclerosis. Biochem Pharmacol 2000;60(8):1245-1250.
71. Onofrei MD, Butler KL, Fuke DC, Miller HB. Safety of statin therapy in patients with preexisting liver disease. Pharmacotherapy 2008;28(4):522-529.
72. Bhardwaj SS, Chalasani N. Lipid-lowering agents that cause drug-induced hepatotoxicity. Clin Liver Dis 2007;11(3):597-613, vii.
73. Fearnley GR, Vincent CT, Chakrabarti R. Reduction of blood fibrinolytic activity in diabetes mellitus by insulin. Lancet 1959;2(7111):1067.
74. Ogston D, McAndrew GM. Fibrinolysis in obesity. Lancet 1964;2(7371):1205-1207.
75. Hotamisligil GS, Shargill NS, Spiegelman BM. Adipose expression of tumor necrosis factor-alpha: direct role in obesity-linked insulin resistance. Science 1993;259(5091):87-91.
76. Fried SK, Bunkin DA, Greenberg AS. Omental and subcutaneous adipose tissues of obese subjects release interleukin-6: depot difference and regulation by glucocorticoid. J Clin Endocrinol Metab 1998;83(3):847-850.
77. Steppan CM, Bailey ST, Bhat S, Brown EJ, Banerjee RR, Wright CM, et al. The hormone resistin links obesity to diabetes. Nature 2001;409(6818):307-312.
78. Weisberg SP, McCann D, Desai M, Rosenbaum M, Leibel RL, Ferrante AW, Jr. Obesity is associated with macrophage accumulation in adipose tissue. J Clin Invest 2003;112(12):1796-1808.
79. Wellen KE, Hotamisligil GS. Inflammation, stress, and diabetes. J Clin Invest 2005;115(5):1111-1119.
80. Nakatani Y, Kaneto H, Kawamori D, Yoshiuchi K, Hatazaki M, Matsuoka TA, et al. Involvement of endoplasmic reticulum stress in insulin resistance and diabetes. J Biol Chem 2005;280(1):847-851.
81. Ozcan U, Cao Q, Yilmaz E, Lee AH, Iwakoshi NN, Ozdelen E, et al. Endoplasmic reticulum stress links obesity, insulin action, and type 2 diabetes. Science 2004;306(5695):457-461.
82. de Luca C, Olefsky JM. Inflammation and insulin resistance. FEBS Lett 2008;582(1):97-105.
83. Sabio G, Das M, Mora A, Zhang Z, Jun JY, Ko HJ, et al. A stress signaling pathway in adipose tissue regulates hepatic insulin resistance. Science 2008;322(5907):1539-1543.
84. De Taeye BM, Novitskaya T, McGuinness OP, Gleaves L, Medda M, Covington JW, et al. Macrophage TNF-alpha contributes to insulin resistance and hepatic steatosis in diet-induced obesity. Am J Physiol Endocrinol Metab 2007;293(3):E713-E725.
85. Gregor MF, Hotamisligil GS. Inflammatory mechanisms in obesity. Annu Rev Immunol 2011;29:415-445.

86. Olefsky JM, Glass CK. Macrophages, inflammation, and insulin resistance. Annu Rev Physiol 2010;72:219-246.
87. Lanthier N, Molendi-Coste O, Cani PD, van Rooijen N, Horsmans Y, Leclercq IA. Kupffer cell depletion prevents but has no therapeutic effect on metabolic and inflammatory changes induced by a high-fat diet. FASEB J 2011;25(12):4301-4311.
88. Lee YS, Li P, Huh JY, Hwang IJ, Lu M, Kim JI, et al. Inflammation is necessary for long-term but not short-term high-fat diet-induced insulin resistance. Diabetes 2011;60(10):2474-2483.
89. Arkan MC, Hevener AL, Greten FR, Maeda S, Li ZW, Long JM, et al. IKK-beta links inflammation to obesity-induced insulin resistance. Nat Med 2005;11(2):191-198.
90. Ishibashi S, Brown MS, Goldstein JL, Gerard RD, Hammer RE, Herz J. Hypercholesterolemia in low density lipoprotein receptor knockout mice and its reversal by adenovirus-mediated gene delivery. J Clin Invest 1993;92(2):883-893.
91. Schreyer SA, Vick C, Lystig TC, Mystkowski P, LeBoeuf RC. LDL receptor but not apolipoprotein E deficiency increases diet-induced obesity and diabetes in mice. Am J Physiol Endocrinol Metab 2002;282(1):E207-E214.
92. Subramanian S, Han CY, Chiba T, McMillen TS, Wang SA, Haw A, III, et al. Dietary cholesterol worsens adipose tissue macrophage accumulation and atherosclerosis in obese LDL receptor-deficient mice. Arterioscler Thromb Vasc Biol 2008;28(4):685-691.
93. Bieghs V, van Gorp PJ, Wouters K, Hendrikx T, Gijbels MJ, van Bilsen M, et al. LDL receptor knock-out mice are a physiological model particularly vulnerable to study the onset of inflammation in non-alcoholic fatty liver disease. PLoS One 2012;7(1):e30668.
94. Wouters K, van Gorp PJ, Bieghs V, Gijbels MJ, Duimel H, Lutjohann D, et al. Dietary cholesterol, rather than liver steatosis, leads to hepatic inflammation in hyperlipidemic mouse models of nonalcoholic steatohepatitis. Hepatology 2008;48(2):474-486.
95. Collins S, Martin TL, Surwit RS, Robidoux J. Genetic vulnerability to diet-induced obesity in the C57BL/6J mouse: physiological and molecular characteristics. Physiol Behav 2004;81(2):243-248.
96. Brown MS, Goldstein JL. A receptor-mediated pathway for cholesterol homeostasis. Science 1986;232(4746):34-47.
97. Goldstein JL, Brown MS. Lipoprotein receptors and the control of plasma LDL cholesterol levels. Eur Heart J 1992;13 Suppl B:34-36.
98. Twisk J, Gillian-Daniel DL, Tebon A, Wang L, Barrett PH, Attie AD. The role of the LDL receptor in apolipoprotein B secretion. J Clin Invest 2000;105(4):521-532.
99. Subramanian S, Goodspeed L, Wang S, Kim J, Zeng L, Ioannou GN, et al. Dietary cholesterol exacerbates hepatic steatosis and inflammation in obese LDL receptor-deficient mice. J Lipid Res 2011;52(9):1626-1635.
100. de Roos B, Rungapamestry V, Ross K, Rucklidge G, Reid M, Duncan G, et al. Attenuation of inflammation and cellular stress-related pathways maintains insulin sensitivity in obese type I interleukin-1 receptor knockout mice on a high-fat diet. Proteomics 2009;9(12):3244-3256.
101. Matsuki T, Horai R, Sudo K, Iwakura Y. IL-1 plays an important role in lipid metabolism by regulating insulin levels under physiological conditions. J Exp Med 2003;198(6):877-888.
102. Rivera CA, Adegboyega P, van Rooijen N, Tagalicud A, Allman M, Wallace M. Toll-like receptor-4 signaling and Kupffer cells play pivotal roles in the pathogenesis of non-alcoholic steatohepatitis. J Hepatol 2007;47(4):571-579.
103. Miura K, Kodama Y, Inokuchi S, Schnabl B, Aoyama T, Ohnishi H, et al. Toll-like receptor 9 promotes steatohepatitis by induction of interleukin-1beta in mice. Gastroenterology 2010;139(1):323-334.

104. Shi H, Kokoeva MV, Inouye K, Tzameli I, Yin H, Flier JS. TLR4 links innate immunity and fatty acid-induced insulin resistance. J Clin Invest 2006;116(11):3015-3025.
105. Akira S, Uematsu S, Takeuchi O. Pathogen recognition and innate immunity. Cell 2006;124(4):783-801.
106. Kawai T, Akira S. The role of pattern-recognition receptors in innate immunity: update on Toll-like receptors. Nat Immunol 2010;11(5):373-384.
107. Medzhitov R. Toll-like receptors and innate immunity. Nat Rev Immunol 2001;1(2):135-145.
108. Jialal I, Kaur H. The Role of Toll-Like Receptors in Diabetes-Induced Inflammation: Implications for Vascular Complications. Curr Diab Rep 2012;12(2):172-179.
109. Bjorkbacka H, Kunjathoor VV, Moore KJ, Koehn S, Ordija CM, Lee MA, et al. Reduced atherosclerosis in MyD88-null mice links elevated serum cholesterol levels to activation of innate immunity signaling pathways. Nat Med 2004;10(4):416-421.
110. Metcalf D. The Florey Lecture, 1991. The colony-stimulating factors: discovery to clinical use. Philos Trans R Soc Lond B Biol Sci 1991;333(1266):147-173.
111. Pixley FJ, Stanley ER. CSF-1 regulation of the wandering macrophage: complexity in action. Trends Cell Biol 2004 Nov;14(11):628-638.
112. Yoshida H, Hayashi S, Kunisada T, Ogawa M, Nishikawa S, Okamura H, et al. The murine mutation osteopetrosis is in the coding region of the macrophage colony stimulating factor gene. Nature 1990;345(6274):442-444.
113. Wiktor-Jedrzejczak W, Bartocci A, Ferrante AW, Jr., hmed-Ansari A, Sell KW, Pollard JW, et al. Total absence of colony-stimulating factor 1 in the macrophage-deficient osteopetrotic (op/op) mouse. Proc Natl Acad Sci U S A 1990;87(12):4828-4832.
114. Kodama H, Nose M, Niida S, Yamasaki A. Essential role of macrophage colony-stimulating factor in the osteoclast differentiation supported by stromal cells. J Exp Med 1991;173(5):1291-1294.
115. Kodama H, Yamasaki A, Nose M, Niida S, Ohgame Y, Abe M, et al. Congenital osteoclast deficiency in osteopetrotic (op/op) mice is cured by injections of macrophage colony-stimulating factor. J Exp Med 1991;173(1):269-272.
116. Sugita S, Kamei Y, Oka J, Suganami T, Ogawa Y. Macrophage-colony stimulating factor in obese adipose tissue: studies with heterozygous op/+ mice. Obesity (Silver Spring) 2007;15(8):1988-1995.
117. Chitu V, Stanley ER. Colony-stimulating factor-1 in immunity and inflammation. Curr Opin Immunol 2006;18(1):39-48.
118. Hamilton JA. Colony-stimulating factors in inflammation and autoimmunity. Nat Rev Immunol 2008;8(7):533-544.
119. Tagami S, Inokuchi JJ, Kabayama K, Yoshimura H, Kitamura F, Uemura S, et al. Ganglioside GM3 participates in the pathological conditions of insulin resistance. J Biol Chem 2002;277(5):3085-3092.
120. Yamashita T, Hashiramoto A, Haluzik M, Mizukami H, Beck S, Norton A, et al. Enhanced insulin sensitivity in mice lacking ganglioside GM3. Proc Natl Acad Sci U S A 2003;100(6):3445-3449.
121. Aerts JM, Hollak C, Boot R, Groener A. Biochemistry of glycosphingolipid storage disorders: implications for therapeutic intervention. Philos Trans R Soc Lond B Biol Sci 2003;358(1433):905-914.
122. Aerts JM, Ottenhoff R, Powlson AS, Grefhorst A, van Eijk M, Dubbelhuis PF, et al. Pharmacological inhibition of glucosylceramide synthase enhances insulin sensitivity. Diabetes 2007;56(5):1341-1349.
123. Bijl N, Sokolovic M, Vrins C, Langeveld M, Moerland PD, Ottenhoff R, et al. Modulation of glycosphingolipid metabolism significantly improves hepatic insulin sensitivity and reverses hepatic steatosis in mice. Hepatology 2009;50(5):1431-1441.
124. van Eijk M, Aten J, Bijl N, Ottenhoff R, van Roomen CP, Dubbelhuis PF, et al.

Reducing glycosphingolipid content in adipose tissue of obese mice restores insulin sensitivity, adipogenesis and reduces inflammation. PLoS One 2009;4(3):e4723.
125. Langeveld M, van den Berg SA, Bijl N, Bijland S, van Roomen CP, Houben-Weerts JH, et al. Treatment of genetically obese mice with the iminosugar N-(5-adamantane-1-yl-methoxy-pentyl)-deoxynojirimycin reduces body weight by decreasing food intake and increasing fat oxidation. Metabolism 2012;61(1):99-107.
126. Lombardo E, van Roomen CP, van Puijvelde GH, Ottenhoff R, van Eijk M, Aten J, et al. Correction of liver steatosis by a hydrophobic iminosugar modulating glycosphingolipids metabolism. PLoS One 2012;7(10):e38520.

Chapter 2

Cholesterol-induced hepatic inflammation does not contribute to the development of insulin resistance in male LDL receptor knockout mice

Anouk Funke, Marijke Schreurs, Marcela Aparicio-Vergara, Fareeba Sheedfar, Nanda Gruben, Niels J. Kloosterhuis, Ronit Shiri-Sverdlov, Albert K. Groen, Bart van de Sluis, Marten H. Hofker, Debby P.Y. Koonen

Conditionally accepted by Atherosclerosis

Abstract

Objective It is generally assumed that hepatic inflammation in obesity is linked to the pathogenesis of insulin resistance. Several recent studies have shed doubt on this view, which questions the causality of this association. This study focuses on Kupffer cell-mediated hepatic inflammation as a possible driver of insulin resistance in the absence and presence of obesity.

Methods We used male mice deficient for the low-density lipoprotein receptor (*Ldlr*$^{-/-}$) and susceptible to cholesterol-induced hepatic inflammation. Whole body and hepatic insulin resistance was measured in mice fed 4 diets for 2 and 15 weeks, *i.e.*, chow, high-fat (HF), HF-cholesterol (HFC; 0.2% cholesterol) and HF without cholesterol (HFnC). Biochemical parameters in plasma and liver were measured and inflammation was determined using immunohistochemistry and RT-PCR.

Results At 2 weeks, we did not find significant metabolic effects in either diet group, except for the mice fed a HFC diet which showed pronounced hepatic inflammation ($p<0.05$) but normal insulin sensitivity. At 15 weeks, a significant increase in insulin levels, HOMA-IR, and hepatic insulin resistance was observed in mice fed a HFC, HFnC, and HF diet compared to chow-fed mice ($p<0.05$). Regardless of the level of hepatic inflammation (HFC > HF, HFnC; $p<0.05$) insulin resistance in mice fed HFC was no worse compared to mice on a HFnC and HF diet.

Conclusion These data show that cholesterol-induced hepatic inflammation does not contribute to the development of insulin resistance in male *Ldlr*$^{-/-}$ mice. This study suggests that Kupffer cell-driven hepatic inflammation is a consequence, not a cause, of metabolic dysfunction in obesity.

Introduction

Chronic inflammation, particularly when it occurs in metabolically important organs such as the liver and adipose tissue, is considered to play a crucial role in the etiology of many metabolic diseases, including type 2 diabetes, non-alcoholic fatty liver disease (NAFLD) and cardiovascular disease (1,2). As in adipose tissue, obesity leads to an increase in pro-inflammatory gene expression in the liver (3). Pro-inflammatory pathways in Kupffer cells are activated in obesity and the production of inflammatory cytokines secreted by these liver macrophages is linked to disruption of hepatic insulin signaling and reduced insulin sensitivity in mice (2-4). For instance, LIKK mice with hepatocyte specific expression of the IκB kinase β (IKKβ), an upstream kinase that activates NF-κB, a master regulator of inflammation, exhibit profound hepatic insulin resistance with moderate systemic insulin resistance (3). In line with this, mice lacking IKKβ in hepatocytes retain liver insulin sensitivity in response to high-fat feeding, obesity or aging (5). Although these and many other studies suggest that insulin resistance is causally linked to hepatic inflammation (3,5,6), recent studies show a disconnection between insulin resistance and hepatic inflammation (7-11). Moreover, obesity is a confounding factor in most studies making it difficult to dissect the role of hepatic inflammation in the development of insulin resistance.

As Kupffer cells have been studied less extensively than adipose tissue macrophages in the context of obesity and insulin resistance (12) and Kupffer cell depletion studies have shown controversial findings (8,13-15), we aimed to study the role of Kupffer cell-driven hepatic inflammation in the development of insulin resistance in the onset and presence of obesity. We used mice deficient for the low-density lipoprotein receptor (*Ldlr*$^{-/-}$) (16), a humanized mouse model exhibiting many features of the metabolic syndrome when fed a western style or diabetogenic diet, including obesity, insulin resistance, dyslipidemia, inflammation and atherosclerosis (17,18). When triggered with low levels of cholesterol (0.15-0.2%), *Ldlr*$^{-/-}$ mice also display many features of human NAFLD, including Kupffer cell-driven hepatic inflammation (19-21). This is in contrast to C57BL/6 mice that develop hepatic steatosis and insulin resistance without hepatic inflammation and further progression towards non-alcoholic steatohepatitis (22). Importantly, we have previously shown that dietary cholesterol can provoke hepatic inflammation within 7 days, in the absence of obesity (21), thereby serving as an attractive model to unravel the role of Kupffer cell-driven hepatic inflammation in the development of insulin resistance.

Materials and methods

Mice and Diet Intervention. All procedures were performed with approval of the University of Groningen Ethical Committee for Animal Experiments, which adheres to the principles and guidelines established by the European Convention for the Protection of Laboratory Animals. Experiments were carried out on male *Ldlr*$^{-/-}$ mice (Jackson Laboratory, Bar Harbor, USA, ME), housed individually in a temperature- and light-controlled facility with *ad libitum* access to food and water.

At the age of 8-10 weeks, mice were divided into 4 groups of 6-8 mice: (1) mice fed

chow diet (2181, RMH-B, Hope Farms, Woerden, the Netherlands); (2) mice fed a high-fat-diet containing 36% (w/w) fat from lard and 0.03% (w/w) cholesterol (HF; diet 4031.45, Abdiets, Woerden, the Netherlands.); (3) mice fed HF-diet containing 21% milk butter and 0.2% cholesterol (HFC; diet 0035, Scientific Animal Food and Engineering, Villemoisson-sur-orge, France); and (4) mice fed HF-diet containing 21% milk butter and 0% cholesterol (HFnC; diet 0136, Scientific Animal Food and Engineering, Villemoisson-sur-orge, France). Mice were kept on these diets for 2 and 15 weeks and experiments were carried out simultaneously using diets from the same batch number. After 2 and 15 weeks animals were killed for the collection of blood, liver and muscle samples.

Dual-Energy X-ray Absorptiometry (DEXA) scan analysis. Fat and lean mass was determined in the same mice at 2 and 15 weeks following dietary intervention using Dual-Energy X-ray Absorptiometry (p-DEXA, Norland Stratec Medizintechnik GmbH, Birkenfeld, Germany). Mice were scanned under fed conditions while anesthesized using isoflurane and data was analyzed according to the manufacturer's instructions.

Oral Glucose Tolerance Test. Mice were fasted for 9 hours and a glucose bolus (2 g/kg of 20% glucose solution) was given by oral gavage. Glucose levels were measured with an OneTouch Ultra glucometer (Lifescan Benelux, Beerse, Belgium) before and 15, 30, 60, 90, and 120 minutes after the gavage.

Insulin Signalling Studies in vivo. The mice were fasted overnight and subjected to an intraperitoneal injection with saline or human recombinant insulin (0.75 U/kg body weight, Actrapid, Novo Nordisk Canada inc., Ontario, Canada) 15 minutes before killing. Tissues were isolated and snap-frozen in liquid nitrogen.

Analysis of plasma parameters. Insulin was determined in plasma from overnight fasted mice using the Mercodia ultrasensitive mouse insulin-linked immunosorbent assay (Orange Medica, Tilburg, the Netherlands). NEFA, triglycerides (TG), and total cholesterol (TC) were determined by commercially available kits (NEFA: NEFA-HR, Wako Chemicals GmbH, Neuss, Germany; TG: Hitachi, Roche, Woerden, the Netherlands; TC: cholesterol CHOD-PAP, Roche, Woerden, the Netherlands).

Liver Lipids. Total liver lipids were extracted according to Bligh and Dyer (23). Total cholesterol and triglycerides were quantified using commercially available kits (Cholesterol CHOD-PAP, Roche, Woerden, the Netherlands and Triglycerides Hitachi, Roche, Woerden, the Netherlands), respectively.

Liver Histology. Paraffin embedded sections of the liver (4 µm) were stained with Hematoxillin/Eosin (H/E). Frozen-cut liver sections (5 µm) were fixated in liquid nitrogen and stained with antibodies against Cd68 (FA11, Abcam, Cambridge, UK), to detect activated hepatic macrophages and Kupffer cells (24), and Cd11b (M1/70, Abcam, Cambridge, UK) to identify monocytes/macrophages including Cd11b+ Kupffer cells with cytokine-producing capacity (24). Microscopy was performed with a Leica DM 3000 microscope with a DFC420 camera (Leica Microsystems, Rijswijk, the Netherlands). The slides where scanned with a NanoZoomer 2.0-HT slide

scanner (Hamamatsu, Herrsching am Ammersee, Germany) and analyzed using Imagescope software (Aperio, Vista, USA).

RT-PCR. Total RNA was isolated from the liver with TRIzol reagent (Sigma Alderich, Zwijndrecht, the Netherlands) and total RNA (1 µg) from each individual mouse was converted into cDNA with Quantitect Reverse Transcription kit (QIAGEN, Venlo, the Netherlands). Real time PCR (RT-PCR) was performed using a 7900HT system (Applied Biosystems, Warrington, UK) and values were corrected using the housekeeping gene Cyclophillin A (*Ppia*). The following primers were used: *Mcp-1* forward GCTGGAGAGCTACAAGAGGATCA, reverse ACAGACCTCTCTCTTGAGCTTGGT; *Cmklr1*, forward AACAGCCACTACCAGAACAAC, reverse CGTGACTGGAAATACCTTCTC; *Tnf-α*, forward CATCTTCTCAAAATTCGAGTGACAA, reverse TGGGAGTAGACAAGGTACAACCC and *Il-1β*, forward TGCAGCTGGAGAGTGTGG, reverse TGCTTGTGAGGTGCTGATG; *Ppia* forward TTCCTCCTTTCACAGAATTATTCCA, reverse CCGCCAGTGCCATTATGG.

Immunoblot Analysis. Tissues were homogenized in ice-cold buffer (liver: NaCl 150 mM, Tris-HCl pH 7.5 50 mM, EDTA 5 mM, Pyrophophate 30 mM, NaF 50 mM, Triton X-100, PMSF 100 mM, phosphatase inhibitor cocktails; skeletal muscle: as shown previously (25)). Equal amounts of protein were separated by SDS-PAGE, and transferred to Polyvinylidene Difluoride membranes (GE Healthcare Life Sciences, Diegem, Belgium). Phosphorylated and total AKT antibodies were purchased from Cell Signaling Technology (Leiden, the Netherlands). Immune-complexes were visualized by chemiluminescence (GE Healthcare Life Sciences, Diegem, Belgium) and quantified by densitometry (imageJ software, National Institute of Health).

Statistical Analysis. Data are expressed as means ± SEM for the indicated number of observations. Statistical significance between groups was determined using a two-tailed Mann-Whitney U test. Multiple comparison analysis was performed using two-way ANOVA with a Bonferroni post hoc test to correct for multiple testing. Two-way ANOVA for repeated measurements was used to test for comparisons in body weight and fat mass between the 2- and 15-week time points. Values of $p<0.05$ were considered statistically significant. The software used for the analysis was GraphPad Prism (version 5.00 for Windows, GraphPad Software, San Diego, CA, USA).

Results

Dietary cholesterol triggers Kupffer cell activation.

To confirm Kupffer cell involvement following cholesterol supplementation to the diet, immunostaining against Cd68 and Cd11b was performed in liver sections of *Ldlr*$^{-/-}$ mice fed chow, HF, HFC and HFnC diet for 2 and 15 weeks. Indeed, macrophage size and number (Fig. 1A) was significantly increased in the livers of 2-week HFC-fed mice when compared to mice fed chow, HF and HFnC diet ($p<0.05$, ANOVA). Consistent with this, the number of Cd11b+-macrophages was significantly increased in *Ldlr*$^{-/-}$ mice after 2 weeks of HFC feeding when compared to mice fed chow, HF and HFnC diet (Supplemental Fig. 1; $p<0.05$, ANOVA). Consistent with this, HFC feeding resulted in a concomitant increase in the expression level of monocyte chemotactic protein-1 (*Mcp-1*, Fig. 1B) and chemokine-like receptor 1 (*Cmklr1,* Fig. 1B; $p<0.05$ vs chow, HF, HFnC, ANOVA), genes known to be involved in monocyte/macrophage migration and infiltration (12,26).

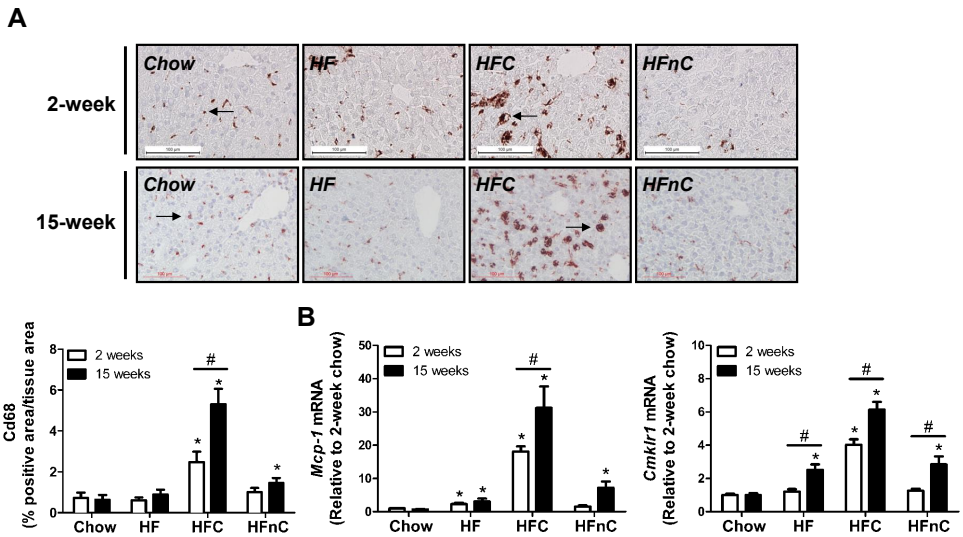

Figure 1. *Dietary cholesterol triggers Kupffer cell activation. (**A**) Representative pictures of Cd68 staining and morphometric analysis of Cd68 stained liver sections from Ldlr*$^{-/-}$ *mice fed a chow, HF, HFC or HFnC diet for 2 and 15 weeks. Original magnification x 200. Kupffer cells are indicated with arrows. (**B**) RT-PCR analysis of hepatic Mcp-1 and Cmklr1 mRNA expression. Data is expressed as fold induction versus 2-week chow-fed Ldlr*$^{-/-}$ *mice. Data are expressed as means ± SEM, n = 6 in each group. * P<0.05 vs chow-fed mice (Mann-Whitney U Test); # P<0.05 2- vs 15-week diet period (two-way ANOVA).*

Similar to 2 weeks of HFC feeding, feeding mice a HFC diet for 15 weeks resulted in a marked increase in Kupffer cell size and number (Fig. 1A), and Cd11b cell count (Supplemental Fig. 1) when compared to mice fed chow, HF and HFnC diet for 15 weeks ($p<0.05$, ANOVA). In addition, Kupffer cell number was significantly enhanced in liver sections of *Ldlr*$^{-/-}$ mice subjected to 15 weeks of HFC feeding compared to 2 weeks of HFC feeding (Fig. 1A). However, the number of Cd11b+-macrophages in liver sections of *Ldlr*$^{-/-}$ mice fed a HFC diet did not change overtime (Supplemental

Fig. 1). Furthermore, hepatic *Mcp-1* and *Cmklr1* levels were increased in 15-week HFC-fed mice compared to 2-week HFC-fed mice (Fig. 1B). 15 weeks of high-fat feeding with low levels of cholesterol (HF, HFnC) also led to a significant increase in both *Mcp-1* and *Cmklr1* expression compared to chow-fed *Ldlr*$^{-/-}$ mice (Fig. 1B). However, this increase was relatively small compared to mice fed a HFC diet for 15 weeks (*Mcp-1*, HF vs HFC p<0.01; HFnC vs HFC p<0.01; *Cmklr*, HF *vs* HFC p<0.01; HFnC vs HFC p<0.01).

Hepatic inflammation is sustained after long-term HFC feeding in Ldlr$^{-/-}$ *mice.*

To assess whether enhanced Kupffer cell activation translates into increased hepatic inflammation, we performed gene expression analysis for the inflammatory mediators *Tnf-α and Il-1β* in the livers of *Ldlr*$^{-/-}$ mice at both time points. The expression of these genes was significantly increased in *Ldlr*$^{-/-}$ mice fed a HFC diet for 2 weeks when compared to mice fed chow, HF and HFnC diet (Fig. 2A, B; p<0.05, ANOVA). Mice fed a HF diet containing 0.03% cholesterol also showed a significant up regulation of these genes above chow levels (Fig. 2A, B), but this was only modest compared to HFC-fed mice (*Tnf-α*, HF vs HFC p<0.01; *Il-1β*, HF vs HFC p<0.01). Moreover, hepatic inflammation was absent in the mice fed a HFnC diet for 2 weeks, highlighting the specificity of our cholesterol supplementation model in inducing hepatic inflammation.

In addition, 15 weeks of HFC feeding led to a similar significant increase in inflammatory gene expression compared to 2 weeks of HFC feeding (Fig. 2A, B). However, it did not further increase the levels of these genes above the 2-week time point. 15 weeks of HF-feeding also led to significant increase in hepatic inflammation, albeit less pronounced compared to HFC feeding (*Tnf-α*, HF vs HFC p<0.01; *Il-1β*, HF vs HFC p<0.05). Similar results were obtained for 15 weeks of HFnC feeding in mice, although *Il-1β* did not reach statistical significance (*Tnf-α,* HFnC vs HFC p<0.05).

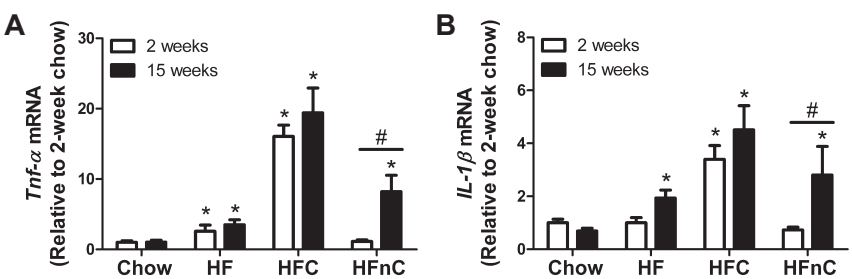

Figure 2. *Kupffer cell-mediated hepatic inflammation is sustained after long-term HFC feeding in Ldlr*$^{-/-}$ *mice. (**A**) RT-PCR analysis of Tnf-α and (**B**) Il-1β mRNA expression in livers from Ldlr*$^{-/-}$ *mice fed a chow, HF, HFC or HFnC diet for 2 and 15 weeks. Data is expressed as fold induction versus 2-week chow-fed Ldlr*$^{-/-}$ *mice. Data are expressed as means ± SEM, n = 6 in each group. * P<0.05 vs chow-fed mice (Mann-Whitney U Test); # P<0.05 2- vs 15-week diet period (two-way ANOVA).*

Dietary cholesterol does not lead to overt changes in adiposity in Ldlr$^{-/-}$ mice.

As body weight adversely affects insulin sensitivity, *Ldlr*$^{-/-}$ mice were subjected to DEXA scan analysis to determine fat mass at the end of the 2- and 15-week diet period. After 2 weeks, body weight (Fig. 3A) and fat mass (Fig. 3B) did not differ significantly amongst the 4 diet groups. At the end of the 15-week diet period body weight (Fig. 3A) and fat mass (Fig. 3B) were significantly increased in mice fed a HFC and HF diet compared to the 15-week chow controls and the respective 2-week time points (Fig. 3A, B). However, body weight was lower in 15-week HFC-fed mice compared to HF-fed mice ($p<0.05$), although fat mass did not differ significantly between these groups (Fig. 3B; HFC vs HF $p=0.20$). In addition, body weight was significantly lower in HFnC-fed mice compared to both HFC- and HF-fed mice (Fig. 3A; HFnC vs HFC $p<0.05$; HFnC vs HF $p<0.01$). Plasma and liver cholesterol levels were increased in *Ldlr*$^{-/-}$ mice fed a HFC, HF and HFnC diet compared to chow-fed mice at either time point (Supplemental Table 1, 2). In addition, plasma and liver cholesterol levels were markedly increased in HFC-fed mice compared to mice fed HFnC and HF diet. Plasma triglycerides (TG) were elevated in all mice following HF feeding at 2 and 15 weeks compared to chow controls and no differences were observed between HFC-, HFnC- and HF-fed mice at both time points (Supplemental Table 1, 2). Furthermore, hepatic TG levels were significantly increased in mice fed a HFC, HF and HFnC diet compared to chow-fed mice at the 2-week time point (Supplemental Table 1) and did not differ at the 15-week time point (Supplemental Table 2).

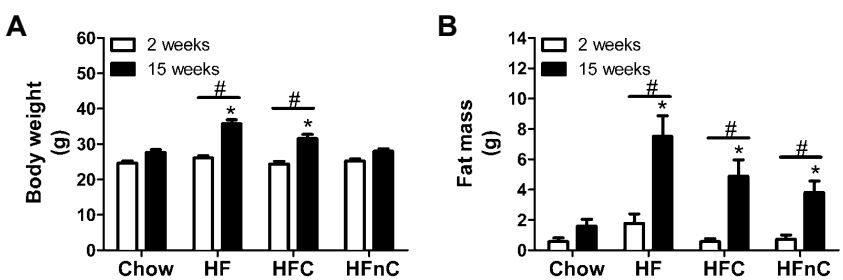

Figure 3. *Dietary cholesterol does not lead to overt changes in adiposity in Ldlr$^{-/-}$ mice. (**A**) Body weight of Ldlr$^{-/-}$ mice fed a chow, HF, HFC or HFnC diet for 2 (n = 12 in each group) and 15 weeks (n = 12 in each group). (**B**) Fat mass was determined by DEXA scan analysis (n = 6 in each group). Data are expressed as means ± SEM. * P<0.05 vs chow-fed mice (Mann-Whitney U Test); # P<0.05 2- vs 15-week diet period (two-way ANOVA for repeated measurements).*

Hepatic inflammation does not induce insulin resistance in lean Ldlr$^{-/-}$ mice.

To investigate whether hepatic inflammation may affect glucose metabolism, we assessed glucose tolerance, plasma insulin levels, and the calculated HOMA-IR index as markers of insulin resistance. At 2 weeks, *Ldlr*$^{-/-}$ mice fed a HFC diet did not exhibit elevated fasted insulin levels compared to mice fed a HF and HFnC diet (Fig. 4A) nor was their glucose tolerance negatively affected (Fig. 4B). Consistent

with this, HOMA-IR was not significantly increased in the mice fed a HFC diet (Fig. 4C) compared to chow-, HF-, or HFnC-fed mice, suggesting that cholesterol-induced hepatic inflammation does not induce the development of systemic insulin resistance. In addition, no differences were observed in phosphorylation status of AKT in either skeletal muscle or liver (Fig. 4D) in the *Ldlr*$^{-/-}$ mice fed a HFC diet compared to chow-, HF-, or HFnC-fed mice, suggesting that insulin signalling in these metabolically active tissues was not impaired.

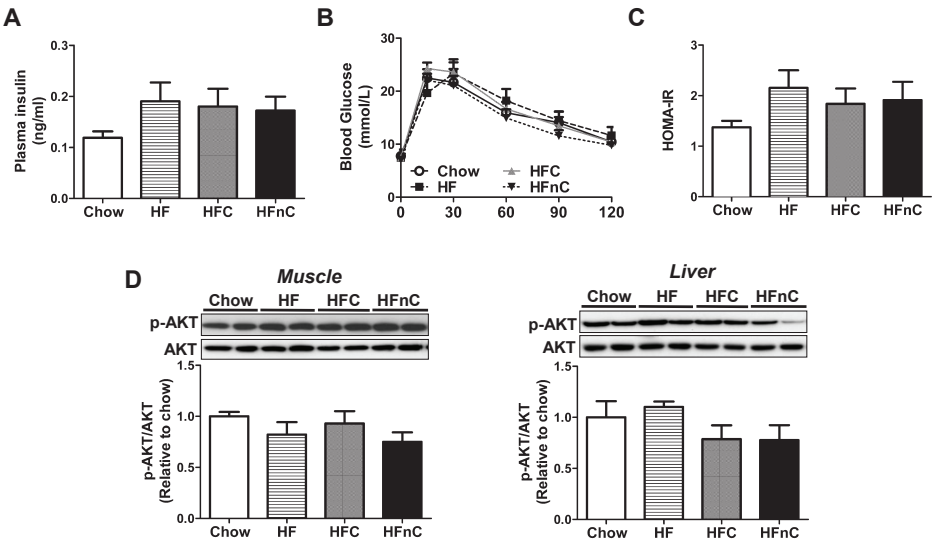

Figure 4. *Hepatic inflammation does not induce insulin resistance in lean Ldlr*$^{-/-}$ *mice. (**A**) Plasma insulin levels in Ldlr*$^{-/-}$ *mice fed a chow, HF, HFC or HFnC diet for 2 weeks (n = 6 in each group). (**B**) Blood glucose levels during an oral glucose tolerance test (n = 6 in each group). (**C**) HOMA-IR as a surrogate marker of insulin resistance (n = 6 in each group). (**D**) Western blot analysis of phosphorylated and total AKT in skeletal muscle and liver after an insulin injection (n = 8 in each group). * P<0.05 vs chow-fed mice (Mann-Whitney U Test). Data are expressed as means ± SEM.*

Hepatic inflammation does not aggravate insulin resistance in obese Ldlr$^{-/-}$ *mice.*

Although our data indicate that Kupffer cell-mediated hepatic inflammation may not increase the susceptibility towards the development of insulin resistance during the onset of obesity, it may still aggravate insulin resistance in obese *Ldlr*$^{-/-}$ mice. However, glucose tolerance was not affected in *Ldlr*$^{-/-}$ mice fed either HFC or HFnC diet, and was only impaired in mice fed the diabetogenic HF diet (Fig. 5A). In spite of this, fasted insulin levels (Fig. 5B) and HOMA-IR (Fig. 5C) were all significantly increased compared to the chow controls but did not differ between the HFC-, HFnC-, and HF-fed groups. Whereas, insulin signalling in skeletal muscle did not seem to be impaired after 15 weeks of HFC-, HFnC- and HF-feeding compared to chow-fed mice, hepatic insulin resistance was observed in mice on a HFC diet but again was no worse compared to mice on a HFnC and HF diet (Fig. 5D). This was indicated by a similar reduction in insulin-stimulated AKT phosphorylation in the livers of these mice (Fig. 5D).

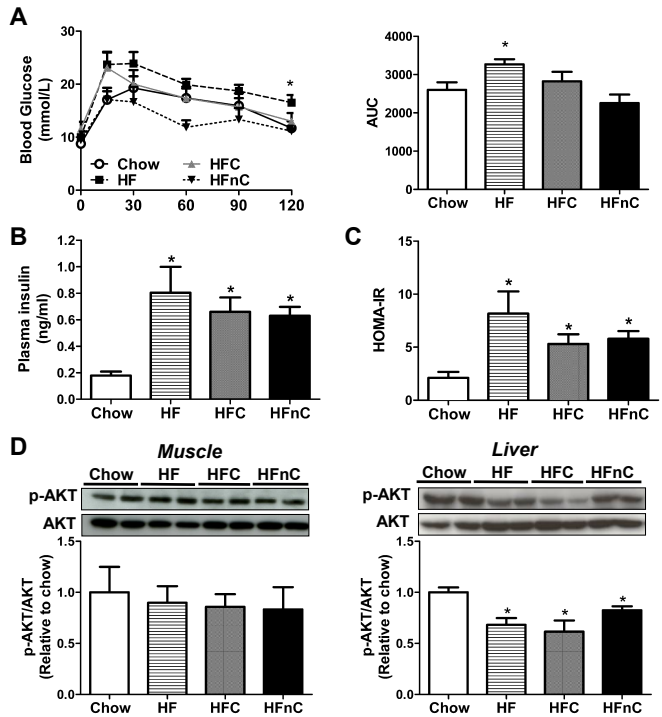

Figure 5. *Hepatic inflammation does not aggravate insulin resistance in obese Ldlr$^{-/-}$ mice. (**A**) Blood glucose levels during an oral glucose tolerance test and AUC for the glucose tolerance test in Ldlr$^{-/-}$ mice at 15 weeks on a chow, HF, HFC or HFnC diet (n = 6 in each group). (**B**) Plasma insulin levels (n = 6 in each group). (**C**) HOMA-IR (n = 6 in each group). (**D**) Representative western blot analysis of phosphorylated and total AKT in skeletal muscle and liver after an insulin injection (n = 8 in each group). * P<0.05 vs chow-fed mice (Mann-Whitney U Test). Data are expressed as means ± SEM.*

Discussion

In this study, we have explored the role of hepatic inflammation as a possible driver of insulin resistance in the onset and presence of obesity. We show that *Ldlr*$^{-/-}$ mice with pronounced hepatic inflammation, induced by a 2-week HFC-diet, do not exhibit signs of insulin resistance in comparison to mice fed a HFnC-diet (Fig. 4). We also show that insulin resistance is not aggravated in obese *Ldlr*$^{-/-}$ mice with sustained hepatic inflammation induced by a 15-week HFC-diet (Fig. 5) compared to mice fed a HFnC-diet. Moreover, we did not find any correlation between the level of hepatic inflammation, insulin resistance and/or obesity in these mice (Supplemental Table 3). Therefore, our data show that HFC-induced hepatic inflammation per sé does not cause insulin resistance in *Ldlr*$^{-/-}$ mice.

Although previous studies have elegantly shown that insulin resistance is causally related to hepatic inflammation (3,5), our data do not support these findings. The reason for this is unclear; however, it may be related to the experimental model used to assess the causality of this association. In this study, we used a Kupffer cell-based approach to drive hepatic inflammation, whereas hepatic inflammation in LIKK mice (3) and Ikbkb$^{\Delta hep}$ mice (5) is hepatocyte-driven. This raises the question whether hepatocyte-driven inflammation is functionally different from Kupffer cell-driven inflammation and whether or not there is a distinctive role in their control of insulin resistance. Nonetheless, it should be noted that Ikbkb$^{\Delta hep}$ mice retain liver insulin responsiveness in response to a high-fat diet, obesity and aging, but continue to develop peripheral insulin resistance in muscle and fat (5). By contrast, LIKK mice expressing constitutively active (IKKβ) in hepatocytes exhibit insulin resistance both locally in liver and systemically (3). Therefore, the possibility arises that a causal relationship between hepatic inflammation and insulin resistance may *only* exist in the liver and not systemically. In addition, deletion of *Ikbkb* in myeloid cells was reported to lead to a global improvement in insulin sensitivity in Ikbkb$^{\Delta mye}$ mice (5) but this effect may not be attributed to Kupffer cells in the liver as the LysM promotor used to generate these mice is not active in Kupffer cells (27). However, Kupffer cell depletion studies have shown conflicting results, and have both been associated with improvement (13-15) and deterioration of hepatic insulin resistance (8), thereby questioning a role of Kupffer cells in control of hepatic and global insulin sensitivity.

In this study we have assessed parameters on two different scales, i.e. inflammation and insulin resistance. On these two scales, changes may not be in the same magnitude. Therefore, we cannot exclude that the absence of insulin resistance at week 2 of HFC-feeding may in fact reflect a temporal delay of onset of insulin resistance induced by hepatic inflammation. Nevertheless, several other reports have also raised doubts on the current concept that hepatic inflammation causes insulin resistance in mice. Mice lacking the TNF receptors, p55 and p75, do not show improvement of insulin resistance despite reduced levels of hepatic inflammation (11). Consistent with this, mice deficient for Myd88, an adaptor protein for TLR/IL-1 receptor signaling, are more prone to develop metabolic disease in response to HF feeding despite lower levels of inflammation (9). Furthermore, hepatic insulin resistance is not always associated with the presence of inflammation in the liver as

Liv-diacylglycerol O-acyltransferase 2 (DGAT2) mice fed a chow diet show hepatic insulin resistance in the absence of liver inflammation (10). In addition, we have recently shown that hepatic inflammation is not associated with insulin resistance in TNFR1 non-sheddable mice with a gain of function mutation in the TNFR1 resulting in chronic low-grade inflammation in the liver (7). Moreover, mice with the non-shedding mutation fed a chow diet for one year were not prone to developing insulin resistance, nor did 12 weeks of HF feeding at the age of one year accelerate the onset of insulin resistance in these mice (7). Therefore, our data and the above-discussed studies all show, using different experimental approaches (genetically engineered mouse models, Kupffer cell depletion, and dietary intervention), a disconnection between hepatic inflammation and the existence of insulin resistance. A similar dissociation has also been observed between hepatic steatosis and insulin resistance in various genetically and pharmacologically manipulated mouse models (28-31) and warrants further study.

Our data also suggest that other obesity-associated factors may be responsible for the development of insulin resistance in our mice. Obesity is known to promote insulin resistance and adiposity was significantly increased in all HF diet groups following 15 weeks of HF feeding (Fig. 3) whereas inflammatory gene expression in the liver did not increase above the 2-week time point (Fig. 2). Moreover, systemic and hepatic insulin resistance only became apparent with increasing adiposity in *Ldlr*$^{-/-}$ mice suggesting that signals originating from the adipose tissue rather than the liver may have interfered with proper insulin signalling in the *Ldlr*$^{-/-}$ mice. This is consistent with recent data showing that increased inflammation in both liver and muscle only became apparent after establishment of obesity (4). Our studies cannot answer the question whether total adiposity may be the driving force behind the development of insulin resistance in our model or whether site-specific fat depots (visceral or subcutaneous adipose tissue), a reduced capacity to store excess nutrients, and/or an altered secretion of adipokines may be involved.

In summary, our results demonstrate that the level of Kupffer cell-mediated hepatic inflammation is not directly correlated to the development of insulin resistance in male *Ldlr*$^{-/-}$ mice. Similar to the dissociation between hepatic steatosis and insulin resistance, we show dissociation between hepatic inflammation and the development of insulin resistance in mice. Therefore, our data provides evidence to question a possible role of Kupffer cell-driven hepatic inflammation in insulin resistance in mice.

References

1. Gregor MF, Hotamisligil GS (2011) Inflammatory mechanisms in obesity. Annu Rev Immunol 29: 415-445
2. Tilg H, Moschen AR (2008) Insulin resistance, inflammation, and non-alcoholic fatty liver disease. Trends Endocrinol Metab 19: 371-379
3. Cai D, Yuan M, Frantz DF, et al (2005) Local and systemic insulin resistance resulting from hepatic activation of IKK-beta and NF-kappaB. Nat Med 11: 183-190
4. Lee YS, Li P, Huh JY, et al (2011) Inflammation is necessary for long-term but not short-term high-fat diet-induced insulin resistance. Diabetes 60: 2474-2483
5. Arkan MC, Hevener AL, Greten FR, et al (2005) IKK-beta links inflammation to obesity-induced insulin resistance. Nat Med 11: 191-198
6. Odegaard JI, Ricardo-Gonzalez RR, Red EA, et al (2008) Alternative M2 activation of Kupffer cells by PPARdelta ameliorates obesity-induced insulin resistance. Cell Metab 7: 496-507
7. Aparicio-Vergara M, Hommelberg PP, Schreurs M, et al (2012) TNF receptor 1 gain-of-function mutation aggravates non-alcoholic fatty liver disease but does not cause insulin resistance in mice. Hepatology: e26046
8. Clementi AH, Gaudy AM, van RN, Pierce RH, Mooney RA (2009) Loss of Kupffer cells in diet-induced obesity is associated with increased hepatic steatosis, STAT3 signaling, and further decreases in insulin signaling. Biochim Biophys Acta 1792: 1062-1072
9. Hosoi T, Yokoyama S, Matsuo S, Akira S, Ozawa K (2010) Myeloid differentiation factor 88 (MyD88)-deficiency increases risk of diabetes in mice. PLoS ONE 5: e12537
10. Jornayvaz FR, Birkenfeld AL, Jurczak MJ, et al (2011) Hepatic insulin resistance in mice with hepatic overexpression of diacylglycerol acyltransferase 2. Proc Natl Acad Sci U S A 108: 5748-5752
11. Schreyer SA, Chua SC, Jr., LeBoeuf RC (1998) Obesity and diabetes in TNF-alpha receptor- deficient mice. J Clin Invest 102: 402-411
12. Olefsky JM, Glass CK (2010) Macrophages, inflammation, and insulin resistance. Annu Rev Physiol 72: 219-246
13. Huang W, Metlakunta A, Dedousis N, et al (2010) Depletion of liver Kupffer cells prevents the development of diet-induced hepatic steatosis and insulin resistance. Diabetes 59: 347-357
14. Neyrinck AM, Cani PD, Dewulf EM, De BF, Bindels LB, Delzenne NM (2009) Critical role of Kupffer cells in the management of diet-induced diabetes and obesity. Biochem Biophys Res Commun 385: 351-356
15. Stienstra R, Saudale F, Duval C, et al (2010) Kupffer cells promote hepatic steatosis via interleukin-1beta-dependent suppression of peroxisome proliferator-activated receptor alpha activity. Hepatology 51: 511-522
16. Ishibashi S, Brown MS, Goldstein JL, Gerard RD, Hammer RE, Herz J (1993) Hypercholesterolemia in low density lipoprotein receptor knockout mice and its reversal by adenovirus-mediated gene delivery. J Clin Invest 92: 883-893
17. Schreyer SA, Vick C, Lystig TC, Mystkowski P, LeBoeuf RC (2002) LDL receptor but not apolipoprotein E deficiency increases diet-induced obesity and diabetes in mice. Am J Physiol Endocrinol Metab 282: E207-E214
18. Subramanian S, Han CY, Chiba T, et al (2008) Dietary cholesterol worsens adipose tissue macrophage accumulation and atherosclerosis in obese LDL receptor-deficient mice. Arterioscler Thromb Vasc Biol 28: 685-691
19. Bieghs V, van Gorp PJ, Wouters K, et al (2012) LDL receptor knock-out mice are a physiological model particularly vulnerable to study the onset of inflammation in non-

alcoholic fatty liver disease. PLoS ONE 7: e30668
20. Subramanian S, Goodspeed L, Wang S, et al (2011) Dietary cholesterol exacerbates hepatic steatosis and inflammation in obese LDL receptor-deficient mice. J Lipid Res 52: 1626-1635
21. Wouters K, van Gorp PJ, Bieghs V, et al (2008) Dietary cholesterol, rather than liver steatosis, leads to hepatic inflammation in hyperlipidemic mouse models of nonalcoholic steatohepatitis. Hepatology 48: 474-486
22. Collins S, Martin TL, Surwit RS, Robidoux J (2004) Genetic vulnerability to diet-induced obesity in the C57BL/6J mouse: physiological and molecular characteristics. Physiol Behav 81: 243-248
23. Bligh EG, Dyer WJ (1959) A rapid method of total lipid extraction and purification. Can J Biochem Physiol 37: 911-917
24. Kinoshita M, Uchida T, Sato A, et al (2010) Characterization of two F4/80-positive Kupffer cell subsets by their function and phenotype in mice. J Hepatol 53: 903-910
25. Koonen DP, Sung MM, Kao CK, et al (2010) Alterations in skeletal muscle fatty acid handling predisposes middle-aged mice to diet-induced insulin resistance. Diabetes 59: 1366-1375
26. Zabel BA, Ohyama T, Zuniga L, et al (2006) Chemokine-like receptor 1 expression by macrophages in vivo: regulation by TGF-beta and TLR ligands. Exp Hematol 34: 1106-1114
27. Maeda S, Kamata H, Luo JL, Leffert H, Karin M (2005) IKKbeta couples hepatocyte death to cytokine-driven compensatory proliferation that promotes chemical hepatocarcinogenesis. Cell 121: 977-990
28. Brown JM, Betters JL, Lord C, et al (2010) CGI-58 knockdown in mice causes hepatic steatosis but prevents diet-induced obesity and glucose intolerance. J Lipid Res 51: 3306-3315
29. Kozlitina J, Boerwinkle E, Cohen JC, Hobbs HH (2011) Dissociation between APOC3 variants, hepatic triglyceride content and insulin resistance. Hepatology 53: 467-474
30. Minehira K, Young SG, Villanueva CJ, et al (2008) Blocking VLDL secretion causes hepatic steatosis but does not affect peripheral lipid stores or insulin sensitivity in mice. J Lipid Res 49: 2038-2044
31. Monetti M, Levin MC, Watt MJ, et al (2007) Dissociation of hepatic steatosis and insulin resistance in mice overexpressing DGAT in the liver. Cell Metab 6: 69-78

Supplemental tables and figures

Supplemental Table 1. *Plasma and liver lipids of 2 week-fed Ldlr$^{-/-}$ mice.*

	Chow	HF	HFC	HFnC
Plasma TC (mmol/L)	6.01 ± 0.25	17.25 ± 0.84	30.16 ± 1.01*#$	22.49 ± 1.67*#
Plasma TG (mmol/L)	4.03 ± 0.11	9.20 ± 0.31	9.08 ± 0.37*	10.03 ± 1.15*
Plasma NEFA (mmol/L)	0.35 ± 0.01	0.72 ± 0.03	0.65 ± 0.04*	0.63 ± 0.07*
Hepatic TC (µmol/g liver)	11.55 ± 0.46	13.55 ± 0.30*	36.91 ± 2.89*#$	19.03 ± 1.48*#
Hepatic TG (µmol/g liver)	11.34 ± 2.62	40.03 ± 2.38	27.53 ± 2.68*#$	35.60 ± 3.39*

*Ldlr$^{-/-}$ mice were fed a chow, HF, HFC or HFnC diet for 2 weeks (n = 6 in each group). Plasma samples were analyzed for total cholesterol (TC), triglycerides (TG) and NEFA. Liver samples were analyzed for TC and TG. Data are expressed as means ± SEM. * P<0.05 vs chow-fed mice; # P<0.05 vs HF-fed mice and $ P<0.05 vs HFnC (Mann-Whitney U Test).*

Supplemental Table 2. *Plasma and liver lipids of 15 week-fed Ldlr$^{-/-}$ mice.*

	Chow	HF	HFC	HFnC
Plasma TC (mmol/L)	9.88 ± 0.25	23.65 ± 1.70*	51.23 ± 3.08*#$	25.96 ± 2.29*
Plasma TG (mmol/L)	1.35 ± 0.19	4.35 ± 0.32*	5.69 ± 1.05*	4.36 ± 0.71*
Plasma NEFA (mmol/L)	0.63 ± 0.05	0.80 ± 0.19	0.68 ± 0.11#$	0.60 ± 0.07#
Hepatic TC (µmol/g liver)	14.33 ± 0.55	21.31 ± 0.68*	61.04 ± 3.30*#$	32.52 ± 3.42*#
Hepatic TG (µmol/g liver)	24.43 ± 8.54	33.00 ± 2.85	28.17 ± 2.55	22.60 ± 2.68#

*Ldlr$^{-/-}$ mice were fed a chow, HF, HFC or HFnC diet for 15 weeks (n = 6 in each group). Plasma samples were analyzed for total cholesterol (TC), triglycerides (TG) and NEFA. Liver samples were analyzed for TC and TG. Data are expressed as means ± SEM. * P<0.05 vs chow-fed mice; # P<0.05 vs HF-fed mice and $ P<0.05 vs HFnC (Mann-Whitney U Test).*

Supplemental Table 3. *Dissociation of hepatic inflammation and insulin resistance.*

	2 weeks			15 weeks		
	Inflammation	Insulin Resistance	Obesity	Inflammation	Insulin Resistance	Obesity
Chow	-	-	-	-	-	
HF	-	-	-	+	√	-√
HFC	+++	-	-	+++	√	√
HFnC	-	-	-	+	√	√

Overview of the level of hepatic inflammation, the occurrence of insulin resistance and obesity in Ldlr$^{-/-}$ mice fed a chow, HF, HFC or HFnC diet for 2 and 15 weeks. (-) = absent, (√) = present, (+) = mild inflammation, and (+++) = strong inflammation.

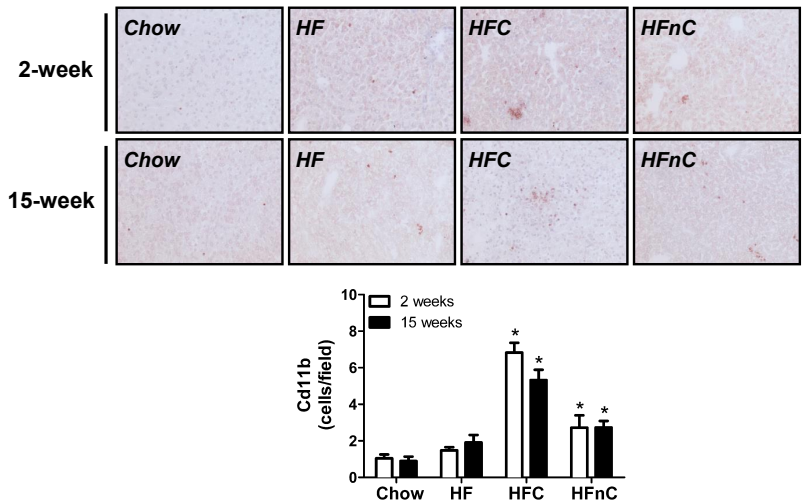

Supplemental Figure 1. *Increased Cd11b+ macrophages in HFC-fed Ldlr$^{-/-}$ mice. (**A**) Representative pictures of Cd11b staining and morphometric analysis of Cd11b stained liver sections from Ldlr$^{-/-}$ mice fed a chow, HF, HFC or HFnC diet for 2 and 15 weeks. Data are expressed as means ± SEM, n = 6 in each group. * P<0.05 vs chow-fed mice (Mann-Whitney U Test); # P<0.05 2- vs 15-week diet period (two-way ANOVA).*

Chapter 3

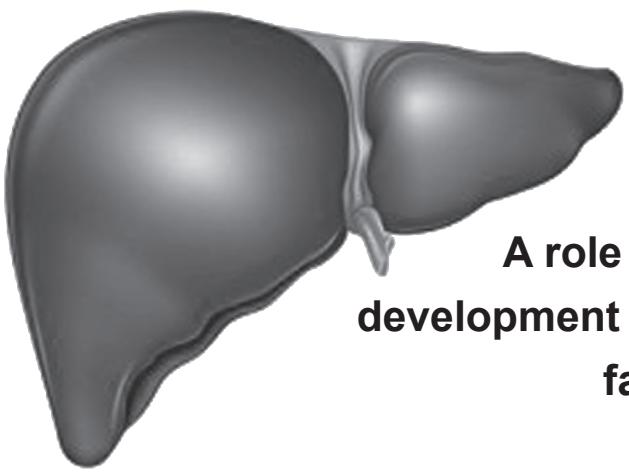

A role for Myd88 in the development of non-alcoholic fatty liver disease

Anouk Funke, Marcela Aparicio-Vergara, Marcel G.M. Wolfs, Marijke Schreurs, Niels J. Kloosterhuis, Henk van der Molen, Sander S. Rensen, Jan Willem M. Greve, Wim A. Buurman, Ludger Scheja, Ronit Shiri-Sverdlov, Jingyuan Fu, Bart van de Sluis, Debby P.Y. Koonen, Marten H. Hofker

In preparation

Abstract

Objective Chronic inflammation plays an important role in the etiology of non-alcoholic fatty liver disease (NAFLD) and insulin resistance. The toll-like receptor (TLR) and interleukin 1 (IL-1) signaling pathways converge on myeloid differentiation primary response gene 88 (MYD88) to initiate nuclear factor-kappa B (NF-κB)-mediated transcription of pro-inflammatory genes. To evaluate the role of Myd88 in the pathogenesis of NAFLD, we assessed the role of Myd88 in mouse models.

Methods To this end, male WT and *Myd88*$^{-/-}$ mice were fed chow or high-fat cholesterol diet for 10 weeks.

Results Myd88 deficiency leads to markedly decreased hepatic inflammation as judged by reduced expression of inflammatory genes. Also, hepatic triglyceride levels were reduced. Overall, this indicates a reduced susceptibility to develop steatohepatitis in *Myd88*$^{-/-}$ mice. Next, we assessed the role of Myd88 in macrophages in a model of non-alcoholic steatohepatitis (NASH) by studying the effects of hematopoietic deficiency of Myd88 on a low-density lipoprotein receptor (*Ldlr*) knockout background. Similarly, we found a strong reduction in hepatic inflammatory genes and a lowering of hepatic triglycerides by ~55%, indicating reduced steatohepatitis. In addition, the *Ldlr*$^{-/-}$ model is susceptible to develop diet-induced insulin resistance, which was protected by hematopoietic Myd88 deficiency as observed by ~35% reduction in HOMA-IR. To further explore the role of MYD88 in metabolic disease in humans, we determined hepatic *MYD88* expression in obese subjects with different stages of NAFLD. Increased *MYD88* expression in the liver positively correlates with increased levels of C-reactive protein (CRP), aspartate aminotransferase (ASAT) and a higher Kleiner score for steatosis ($p<0.001$, $p<0.01$ and $p<0.01$, respectively).

Conclusion Our data strongly suggest that MYD88 plays a role in the development of NAFLD, by impacting on steatosis and inflammation.

Introduction

Non-alcoholic fatty liver disease (NAFLD) is the most common form of chronic liver disease in Western countries. NAFLD is considered to be the hepatic manifestation of the metabolic syndrome (1) and covers a broad spectrum of liver manifestations, from simple steatosis to non-alcoholic steatohepatitis (NASH), which can further progress to liver cirrhosis and end-stage liver disease (2). The frequency of NASH has risen dramatically, as it parallels the growing number of individuals with obesity. Due to the irreversible character of NASH, it leads to liver failure and has become the most important reason for liver transplantation (2). In particular, inflammatory signaling through nuclear factor-κB (NF-κB) plays a central role in the progression of NASH (3) and the development of hepatic insulin resistance. The latter was demonstrated by a mouse model with hepatocyte specific expression of a constitutively active form of inhibitor of κB kinase 2 (IKK2) showing hepatic and systemic insulin resistance (4). Conversely, IKK2 deficiency protects against diet-induced insulin resistance (5). Two signaling pathways are known to activate the IKK complex and drive NF-κB-mediated transcription of inflammatory genes. First, IKK can be activated through the tumor necrosis factor (TNF) signaling pathway. Although the TNF pathway is important in NASH (6-8), it remains doubtful if low-grade TNF signaling can also cause insulin resistance (6,9). Second, the toll-like receptor (TLR) and interleukin-1 (IL-1) pathways converge on myeloid differentiation primary response gene 88 (Myd88) and subsequently activate the IKK complex (10).

There is considerable evidence that TLRs contribute to NASH and insulin resistance, in particular in the obese state (11-13). TLRs are the major cell surface receptors responding to a broad spectrum of inflammatory microbial components and lipids (14). Mice deficient in Tlr4 signaling are protected from diet-induced NASH (12). Moreover, Tlr9 deficient mice showed less steatohepatitis compared to WT mice on a choline deficient diet and demonstrated reduced insulin resistance (11). The role of TLRs has recently gained even more interest, after the discovery that products of the gut microbiota can cause hepatic inflammation by activating TLRs (15). The other activation route of the MYD88/NF-κB pathway is mediated by IL-1/IL-1R. Obese individuals exhibit elevated levels of pro-inflammatory cytokine IL-1β, and elevated levels of IL-1β are predictive of type 2 diabetes (T2D) (16). Moreover, interleukin-1 receptor (IL-1R) knockout mice have lower plasma glucose and insulin levels, and improved insulin sensitivity compared with control mice (17). In addition, serum concentrations of IL-1 receptor antagonist (IL-1Ra) are elevated in obesity and pre-diabetes (18). In line with this, *IL1Ra*$^{-/-}$ mice have lower fasting glucose and insulin levels and improved insulin sensitivity compared with WT controls (19).

Because TLR and IL-1 signaling activate NF-κB via Myd88, which is non-redundant, Myd88 is likely to play a central role in the pathogenesis of NAFLD. We therefore reasoned that Myd88 deficiency would attenuate hepatic inflammation, thereby protecting against NAFLD and insulin resistance. Understanding the role of Myd88 is likely to further strengthen the importance of the proposed pathway and its relevance as a therapeutic target.

However, at present, work in *Myd88*$^{-/-}$ mice does not support its proposed role in disease, because Myd88 deficient mice fed a high-fat diet show a paradoxical insulin resistant phenotype (20,21), which is in contrast to what is expected based on TLR and IL-1 knockout studies. To better understand the role of Myd88 in the pathogenesis of NAFLD, we used Myd88 deficient mice and exposed these mice to a high fat diet with cholesterol to induce hepatic inflammation. Our results reveal that *Myd88*$^{-/-}$ mice have reduced hepatic inflammatory gene expression levels and steatosis, but are not protected from the development of insulin resistance. Subsequently, we focused our study on the role of macrophage Myd88 in NASH and insulin resistance and therefore we made use of the cholesterol-fed low-density lipoprotein receptor knockout (*Ldlr*$^{-/-}$) mouse, recently developed as a model for NASH (22). In this model, NASH is driven by oxidized lipids activating the macrophages and Kupffer cells (23,24). We studied *Ldlr*$^{-/-}$ mice deficient in Myd88 in their hematopoietic compartment using bone marrow transplantation. These mice show a marked reduction in hepatic inflammatory gene expression and steatosis and are protected from the development of insulin resistance. To validate the role of MYD88 in humans, we examined whether the level of *MYD88* expression in livers from obese subjects correlated with different indices of NAFLD. Here, we found that *MYD88* expression in the liver positively correlates with disease progression, supporting a role for Myd88 in the development of NAFLD.

Materials and methods

Mice and Diet intervention. All experiments were performed according to Dutch law and approved by the Ethical Committee for Animal Experiments, University of Groningen, the Netherlands. Experiments were carried out on male *Myd88*$^{-/-}$ mice and their wildtype littermates (*Myd88*$^{+/+}$ referred to as WT mice) and maintained on a C57BL/6J background. These mice were generously provided by Dr. Akira (Osaka University, Japan). For the bone marrow transplantation *Ldlr*$^{-/-}$ mice (Jackson Laboratory, Bar Harbor, USA, ME) were used as recipients and *Myd88*$^{-/-}$ and GFP (WT) mice (Jackson Laboratory, Bar Harbor, USA, ME) were used as donors. The mice were housed individually in a temperature-and light-controlled facility with *ad libitum* access to food and water.

At the age of 8-10 weeks, mice were split into 2 groups and diet was either maintained in the case of standard chow (2181, RMH-B, Hope Farms, Woerden, the Netherlands) or switched to a high-fat cholesterol diet containing 21% milk butter and 0.2% cholesterol (HFC; diet 0035, Scientific Animal Food and Engineering, Villemoisson-sur-Orge, France). Mice were kept on these diets for 10 weeks.
Myd88$^{-/-}$ mice are susceptible to infections and therefore all the mice were treated with 0.35% Neomycin (Spryt-Hillen, Utrecht, the Netherlands) added to the drinking water.

Bone marrow transplantation. Chimeric mice with a deletion of the Myd88 gene in hematopoietic cells, including Kupffer cells, were generated using the bone marrow transplantation approach as described previously (25). Briefly, at 8-10 weeks of age *Ldlr*$^{-/-}$ recipient mice were exposed to a single dose of 9.5 Gy of total body irradiation,

using ^{137}Cs γ- rays, (IBL 637, CIS Biointernational, Gif-sur Yvette, Cedex, France). Irradiated mice were transplanted by intravenous injection of 10^7 bone marrow cells, isolated from GFP (WT) or *Myd88*$^{-/-}$ donor mice. After bone marrow injections, the radiation chimeras, from now on referred to as WT-tp and *Myd88*$^{-/-}$-tp mice, were maintained on a regular chow diet for 10 weeks to allow the reconstitution of bone marrow derived cells, including Kupffer cells. After reconstitution, chimeric mice were placed on a HFC diet for 10 weeks.

Determination of chimerism. Genomic DNA was isolated from blood with the QIAamp DNA Blood Mini Kit (QIAGEN, Venlo, the Netherlands) according to manufacturer's instructions and a PCR using PCR plates from Greiner Bio-One B.V. (Alphen a/d Rijn, the Netherlands) was performed to genotype the WT and Myd88 knockout allele. Myd88 primer a: 5'-AGACAGGCTGAGTGCAAACTTGTGCTG-3'; primer b: 5'-AGCCTCTACACCCTTCTCTTCTCCACA-3'; primer c: 5'-ATCCCCTTCTATCGCCTTCTTGACGAG-3'. For detection of the WT allele; we used primers "a" and "b" and for the Myd88 mutated allele; we use primers "b" and "c".

Glucose Tolerance and Insulin Tolerance Test. Mice were fasted for 9 hours after which either a glucose bolus (2g/kg of a 20% glucose solution) was given by oral gavage (glucose tolerance test) or human recombinant insulin (Actrapid, Novo Nordisk Canada Inc, Ontario, Canada) was injected intraperitoneally (0.5U/kg body weight; insulin tolerance test). Glucose levels were measured with an OneTouch Ultra glucometer (Lifescan Benelux, Beerse, Belgium) before and 15, 30, 60, 90, and 120 minutes after the gavage or injection.

Analysis of plasma parameters. Insulin was determined in plasma from overnight fasted mice using an enzyme-linked immunosorbent assay kit (Insulin (mouse) Ultrasensitive EIA, Alpco Diagnostics, Salem, USA). Free fatty acids (FFA), triglycerides (TG), total cholesterol (TC), alanine aminotransferase (ALT) and aspartate aminotransferase (AST) were determined by commercially available kits, according to the manufacturer's instructions (FFA: NEFA-HR, Wako Chemicals GmbH, Neuss, Germany; TG: Hitachi, Roche, Woerden, the Netherlands; TC: cholesterol CHOD-PAP, Roche, Woerden, the Netherlands; ALT and AST: Spinreact, Santa Coloma, Spain).

Liver lipids. Total liver lipids were extracted from the liver according to Bligh and Dyer (26). Hepatic free and total cholesterol (respectively FC and TC) and triglycerides (TG) were quantified using commercially available kits (FC: DiaSys Diagnostic Systems GmbH, Holzheim, Germany; TC: cholesterol CHOD-PAP, Roche, Woerden, the Netherlands; TG: Hitachi, Roche, Woerden, the Netherlands).

Liver Histology. Liver tissues were isolated, fixated in 4% paraformaldehyde and embedded in paraffin. Paraffin embedded sections of the liver (4 μm) were stained with Hematoxylin & Eosin (H&E) for morphological examination. Liver sections (5 μm) were snap-frozen in liquid nitrogen and stained with Oil Red O and Cd68 antibody (FA11, Abcam, Cambridge, UK). Microscopy was performed with a LEICA

DM 3000 microscope with a DFC420 camera (Leica Microsystems, Rijswijk, the Netherlands). The slides were scanned with the NanoZoomer 2.0-HT slide scanner from Hamamatsu, Herrsching am Ammersee, Germany) and analyzed using Imagescope software from Aperio (Vista, USA).

Real-time polymerase chain reaction (RT-PCR), Total RNA was isolated from the liver with QIAzol reagent (QIAGEN, Venlo, the Netherlands) according to the manufacturer's instructions. Total RNA (1 µg) from each individual mouse was converted into cDNA with Quantitect Reverse Transcription kit (QIAGEN, Venlo, the Netherlands) according to manufacturer's instructions. RT-PCR was performed using a 7900HT system (Applied Biosystems, Warrington, UK) by using Power SYBR Green Master Mix (Biorad, Veenendaal, the Netherlands). For each gene, a standard curve was generated with a serial dilution of pooled cDNA pool of all the mice. Values were corrected using the housekeeping gene Cyclophillin A (*Ppia*). Primer sequences are listed in Supplemental Table 1.

Human study population. Wedge biopsies of liver, visceral adipose tissue (VAT, *omentum majus*), subcutaneous adipose tissue (SAT, abdominal), and muscle (*musculus rectus abdominis*) were obtained from 93 severely obese (BMI>35) subjects undergoing elective bariatric surgery at the Maastricht University Medical Centre. Subject characteristics are presented in Supplemental Table 2. None of the subjects reported excessive alcohol intake (>10g/day) or suffered from autoimmune diseases or viral hepatitis. The study was approved by the local Medical Ethics Committee and conducted according to the revised version of the Declaration of Helsinki (October 2008, Seoul). Written informed consent was obtained from every patient before study participation. NASH severity was assessed by an independent pathologist in the field of hepatology according to the NAFLD Activity Score (NAS score) (27) and according to the Brunt classification (28). The study population comprised severely obese subjects displaying the full spectrum of NAFLD (Supplemental Table 3).

RNA profiling in four tissues and MYD88 co-expression with liver histology. RNA was isolated from liver, VAT, SAT and muscle using the QIAGEN Lipid Tissue Mini Kit (QIAGEN, Crawley, West Sussex, UK, 74804). Assessment of RNA quality and concentration was done with an Agilent Bioanalyzer (Agilent Technologies, Santa Clara, USA). Starting with 200 ng of RNA, the Ambion Illumina TotalPrep Amplification Kit was used for anti-sense RNA synthesis, amplification, and purification according to the protocol provided by the manufacturer (Ambion, Austin, USA). 750 ng of complementary RNA was hybridized to Illumina HumanHT12 BeadChips and scanned on the Illumina BeadArray Reader. Raw probe intensity data for these samples was extracted using Illumina's BeadStudio Gene expression module v3.2.

Statistical analysis. For the mouse studies, data were expressed as mean ± SEM. Data were statistically analyzed by performing a non-parametric Mann-Whitney *U* Test using GraphPad Prism to compare experimental groups (version 5.00 for Windows, GraphPad Software, San Diego, CA, USA). The level of significance was set at $P < 0.05$. For the human studies, the raw expression intensities from four

tissues were jointly quantile normalized and $\log_2$ transformed. Expression data has been deposited in GEO with accession numbers GSE22070. The correlation between *MYD88* expression in four tissues and NAFLD were calculated using Spearman correlation. The significance was controlled at $P < 0.01$. Some patients were scored with a 1-2 for steatosis according to the Kleiner system, for these patients 1.5 is used for the Kleiner score for steatosis. Correlations of *MYD88* expression in four different tissues with features of the metabolic syndrome in subjects with NAFLD are listed in Supplemental Table 3.

Results

Hepatic inflammation in Myd88 deficient mice.

In order to explore the role of Myd88 in liver disease, *Myd88*$^{-/-}$ mice and their WT littermates were fed a chow or high-fat cholesterol (HFC) diet for 10 weeks. Hepatic inflammation was investigated by establishing the mRNA expression levels of inflammatory genes and macrophage markers. *Myd88*$^{-/-}$ mice showed reduced mRNA expression levels of cluster of differentiation 68 (*Cd68*), monocyte chemoattractant protein 1 (*Mcp1*), tumor necrosis factor α (*Tnfα*) and interleukin-1β (*Il-1β*) in the liver (Fig. 1A). To investigate whether reduced hepatic inflammation was due to decreased number of macrophages, we counted Cd68-positive cells in the liver. In contrast to the markedly reduced gene expression level of inflammatory markers, the number of macrophages was not different between WT and *Myd88*$^{-/-}$ mice (Fig. 1B, 1C). Moreover, the levels of alanine aminotransferase (ALT) and aspartate aminotransferase (AST), surrogate markers of liver damage, were not affected by the diet (Table 1). Thus, Myd88 deficiency leads to a marked reduction in HFC-induced hepatic inflammatory gene expression.

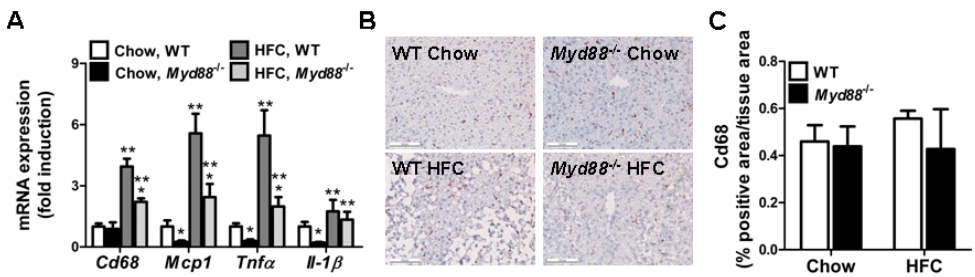

Figure 1. *Hepatic inflammation in Myd88 deficient mice. Real-time polymerase chain reaction (RT-PCR) analysis was performed to measure mRNA expression levels of hepatic inflammatory genes Cd68, and monocyte chemoattractant protein 1 (Mcp1), and the cytokines tumor necrosis factor α (Tnfα) and interleukin-1β (Il-1β) (**A**). (□) = WT mice on chow diet, (■) = Myd88*$^{-/-}$ *on chow diet, (■) = WT mice on high-fat cholesterol (HFC) diet and (■) = Myd88*$^{-/-}$ *mice on HFC diet. Representative pictures of the immunohistochemical staining of Cd68 on liver sections (**B**) and quantification of the Cd68 staining (**C**). (□) = WT mice, (■) = Myd88*$^{-/-}$ *mice. Data are expressed as mean ± SEM, n = 6. The mRNA data is expressed as fold induction versus chow-fed WT mice and the levels are normalized for Cyclophillin A (Ppia). * P < 0.05 versus WT mice (Mann-Whitney U Test); ** P < 0.05 versus chow diet (two-way ANOVA test).*

Plasma and hepatic lipid levels in Myd88 deficient mice.

Body weight was unaltered in *Myd88*$^{-/-}$ mice compared to WT controls (Table 1). Plasma cholesterol and triglycerides were not different between WT and *Myd88*$^{-/-}$ mice (Table 1). However, plasma cholesterol levels were increased upon HFC feeding (Table 1). Of note, whereas plasma free fatty acid (FFA) levels were significantly reduced in chow-fed *Myd88*$^{-/-}$ mice compared to WT mice, no differences in plasma FFA levels on a HFC diet (Table 1). No difference in hepatic cholesterol levels between WT and *Myd88*$^{-/-}$ mice on either diet, however hepatic cholesterol levels were increased upon HFC feeding (Fig. 2A). In addition, hepatic triglyceride (TG) content was reduced in chow-fed and HFC-fed *Myd88*$^{-/-}$ mice (Fig. 2B). This was confirmed by histological

Table 1. *Plasma and liver parameters of WT and Myd88$^{-/-}$ mice on a chow and HFC diet for 10 weeks.*

	Chow		HFC	
	WT	***Myd88$^{-/-}$***	**WT**	***Myd88$^{-/-}$***
Body weight (g)	29.5 ± 0.8	28.2 ± 1.6	42.2 ± 2.3	40.3 ± 3.8
Liver weight (g)	1.53 ± 0.05	1.09 ± 0.03*	2.69 ± 0.20	1.85 ± 0.11*
Liver/body weight ratio (%)	5.19 ± 0.17	3.91 ± 0.19*	6.41 ± 0.45	4.78 ± 0.54*
Plasma glucose (mmol/L)	6.22 ± 0.28	6.88 ± 0.52	8.20 ± 0.40	6.68 ± 0.63
Plasma cholesterol (mmol/L)	2.13 ± 0.21	2.32 ± 0.27	6.22 ± 0.14	5.54 ± 0.41
Plasma free fatty acids (µmol/L)	619.60 ± 34.69	425.71 ± 16.97*	684.07 ± 35.96	603.69 ± 30.37
Plasma triglycerides (mmol/L)	0.87 ± 0.13	0.86 ± 0.08	0.56 ± 0.07	0.74 ± 0.10
Plasma ALT (U/L)	18.71 ± 0.43	19.61 ± 0.84	20.03 ± 0.75	18.92 ± 0.55
Plasma AST (U/L)	4.13 ± 0.22	4.46 ± 0.50	3.92 ± 0.31	4.14 ± 0.30

*Myd88$^{-/-}$ and WT mice were fed a chow or high-fat cholesterol (HFC) diet for 10 weeks. Body weight, liver weight and liver/body weight ratio were assessed. Fasted glucose levels were determined and plasma samples were analyzed for cholesterol (TC), free fatty acids (FFA), triglycerides (TG), alanine aminotransferase (ALT) and aspartate aminotransferase (AST). Data are expressed as mean ± SEM, n = 6 per group. * P < 0.05 versus WT (Mann-Whitney U Test).*

analysis of hematoxylin and eosin (H&E) and Oil red O (ORO) stainings in the livers of these mice (Fig. 2C, 2D). In line with reduced hepatic TG levels, liver weight and liver/body weight ratios were lower in *Myd88$^{-/-}$* mice compared to WT mice, irrespective of the diet (Table 1). Thus, Myd88 deficiency leads to a marked reduction in hepatic TG, which is mirrored by a lower liver weight.

HFC-fed Myd88$^{-/-}$ mice are not protected from the development of insulin resistance.

Since hepatic inflammation has been linked to systemic insulin resistance (4), we evaluated the development of insulin resistance in *Myd88$^{-/-}$* mice. Fasted plasma glucose levels were not significantly altered between chow- or HFC-fed WT and *Myd88$^{-/-}$* mice (Table 1). However, HFC feeding increased plasma insulin levels (Supplemental Fig. 1A) and homeostasis model of assessment-insulin resistance (HOMA-IR) (Supplemental Fig. 1B) in WT mice and lead to a further increase in *Myd88$^{-/-}$* mice. In line with the normal glucose values (Table 1), the response to an oral glucose tolerance test did not differ upon HFC feeding and was unaffected by the genotype (Supplemental Fig. 1C, 1D). The HFC lead to a mild decrease in the response to insulin in an insulin tolerance tests (ITT), but *Myd88$^{-/-}$* mice showed no significant improvement (Supplemental Fig. 1E, 1F). Taken together, these results demonstrate that *Myd88$^{-/-}$* mice are not protected from the development of insulin resistance in response to a HFC diet and even show a mild increase in insulin resistance as indicated by increased insulin levels and a higher HOMA-IR index.

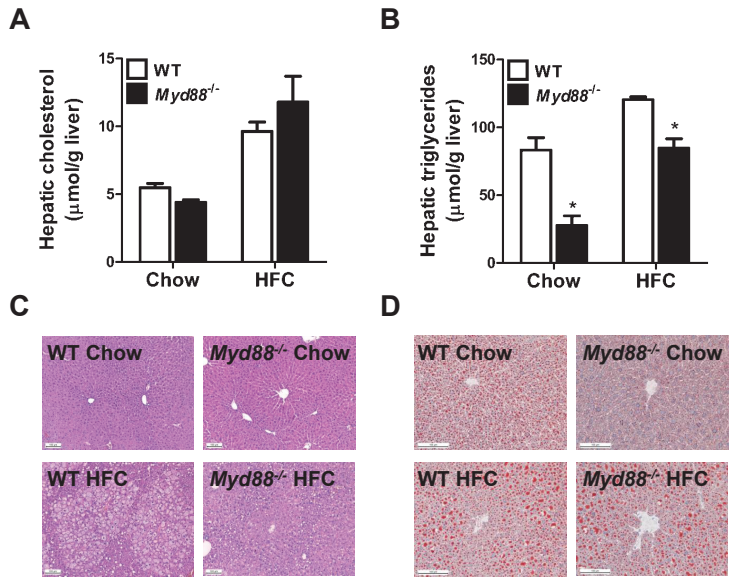

Figure 2. *Plasma and hepatic lipid levels in Myd88 deficient mice. Quantitative measurement of hepatic total cholesterol levels (**A**) and triglyceride levels (**B**). Representative pictures of immunohistochemical stainings of Hematoxylin & Eosin (H&E) (**C**) and Oil red O (ORO) on liver sections (**D**). Data are expressed as mean ± SEM, n = 6. (□) = WT mice, (■) = Myd88$^{-/-}$ mice.* P < 0.05 versus WT mice (Mann-Whitney U Test).*

Hematopoietic deficiency of Myd88 reduces hepatic inflammatory genes and steatosis in the Ldlr$^{-/-}$ mouse.

Because the leukocytes are the primary inflammatory cells of the body, we would like to address if our findings could be replicated studying hematopoietic Myd88 deficiency by generating bone marrow chimeras. As a host, we made use of the low density lipoprotein receptor knockout (*Ldlr*$^{-/-}$) mouse strain because this mouse shows increased susceptibility to HFC-induced hepatic inflammation through activation of hepatic macrophages and Kupffer cells (22,23). Hence, WT or *Myd88*$^{-/-}$ bone marrow cells were transplanted into lethally irradiated *Ldlr*$^{-/-}$ mice generating respectively WT-tp and *Myd88*$^{-/-}$-tp mice. Transplantation efficacy was assessed by genotyping genomic DNA isolated from blood leukocytes using PCR analysis. Since no residual host bands were observed, a near 100% of engraftment of transplanted cells into the recipient mice was achieved (Supplemental Fig. 2A). The inflammatory profile of the liver was determined by gene expression analysis of inflammatory genes and macrophage markers. The expression levels of *Cd68*, *Mcp1*, *Tnfα* and *Il-1β* were significantly reduced in *Myd88*$^{-/-}$-tp mice compared to WT-tp controls (Fig. 3A). However, immunostaining of Cd68 positive cells showed no difference in the number of macrophages between *Myd88*$^{-/-}$-tp mice and WT-tp mice (Fig. 3B). We next investigated whether lipid metabolism was altered in *Myd88*$^{-/-}$-tp mice. Strikingly, *Myd88*$^{-/-}$-tp mice displayed significantly increased plasma TG and TC levels compared to WT-tp mice (Table 2). In addition, hepatic triglyceride accumulation was reduced in the livers of *Myd88*$^{-/-}$-tp mice compared

to WT-tp mice (Fig. 3C). This was confirmed by histological analysis of hematoxylin and eosin (H&E) and Oil red O (ORO) stainings in the livers of these mice (Fig. 3D). *Myd88*$^{-/-}$-tp mice showed reduced expression of the fibrotic genes (data not shown), but fibrosis was not observed in WT-tp and *Myd88*$^{-/-}$-tp mice after 10 weeks of HFC feeding. Taken together, deletion of Myd88 from the hematopoietic compartment leads to reduction of hepatic inflammatory genes and steatosis. The lack of steatosis is remarkable, in view of the increased levels of plasma lipids in the *Myd88*$^{-/-}$-tp mice.

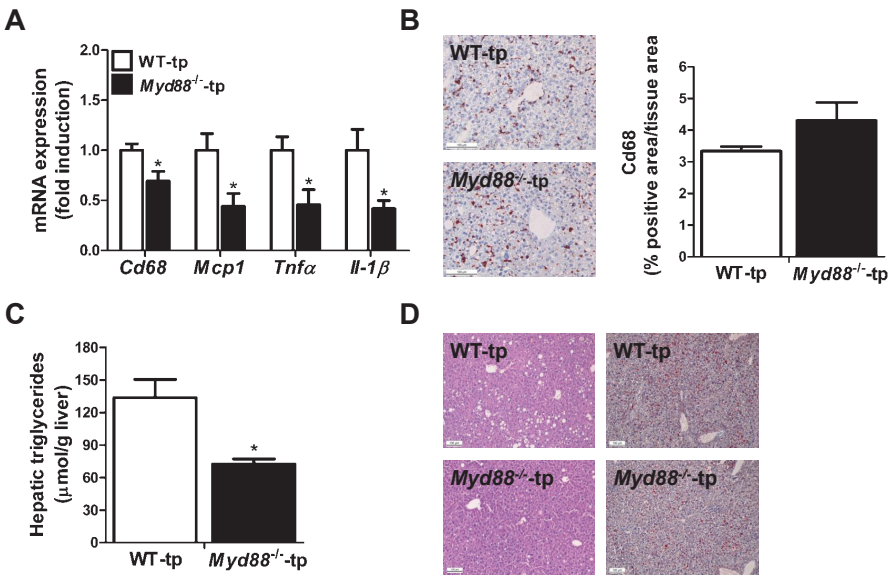

Figure 3. *Hematopoietic deficiency of Myd88 reduces hepatic inflammatory genes and steatosis in the Ldlr*$^{-/-}$ *mouse. Real-time polymerase chain reaction (RT-PCR) analysis was performed to measure mRNA expression levels of hepatic inflammatory genes Cd68, and monocyte chemoattractant protein 1 (Mcp1), and the cytokines tumor necrosis factor α (Tnfα) and interleukin-1β (Il-1β) (**A**). Representative pictures of the immunohistochemical staining of Cd68 on liver sections and the quantification of Cd68 positive cells (**B**). Quantitative measurement of hepatic triglyceride levels (**C**). Representative pictures of Hematoxylin & Eosin (H&E) and Oil red O (ORO) staining (**D**). Data are expressed as mean ± SEM, n = 8 per group. The mRNA data is expressed as fold induction versus HFC-fed WT-tp mice and the levels are normalized for Cyclophillin A (Ppia). (□) = low-density lipoprotein receptor knockout (Ldlr*$^{-/-}$*) mice transplanted with WT bone marrow cells, (■) = Ldlr*$^{-/-}$ *mice transplanted with myeloid differentiation primary response gene 88 (Myd88)*$^{-/-}$ *bone marrow cells. * P < 0.05 versus WT-tp mice (Mann-Whitney U Test).*

Hematopoietic deficiency of Myd88 improves insulin sensitivity in the Ldlr$^{-/-}$ *mouse.*

In view of the reduced inflammation, *Myd88*$^{-/-}$-tp mice were predicted to be protected from the development of insulin resistance. No differences were observed in body weight between *Myd88*$^{-/-}$-tp and WT-tp mice (Fig. 4A). Glucose tolerance was significantly improved in HFC-fed *Myd88*$^{-/-}$-tp mice compared to WT-tp mice (Fig. 4B and 4C). Moreover, fasting plasma glucose (Fig. 4D) and insulin levels (Fig. 4E) were significantly reduced in *Myd88*$^{-/-}$-tp mice compared to WT-tp mice. In line with

Table 2. *Plasma and liver parameters of WT-tp and Myd88$^{-/-}$-tp mice on a HFC diet for 10 weeks.*

	HFC	
	WT-tp	***Myd88*$^{-/-}$-tp**
Liver weight (g)	1.09 ± 0.06	0.90 ± 0.03*
Liver/body weight ratio (%)	4.45 ± 0.15	3.79 ± 0.11*
Plasma cholesterol (mmol/L)	29.25 ± 2.10	37.80 ± 3.62*
Plasma triglycerides (mmol/L)	4.50 ± 0.70	13.66 ± 1.06*
Liver free cholesterol (µmol/g liver)	6.10 ± 0.29	3.82 ± 0.21*
Liver cholesterol (µmol/g liver)	17.06 ± 1.66	14.31 ± 1.71
Liver cholesterol esters (µmol/g liver)	10.96 ± 1.43	10.49 ± 1.53

*Myd88$^{-/-}$-tp and WT-tp mice were fed a HFC diet for 10 weeks. Liver weight and liver/body weight ratio were assessed. Fasted plasma samples were analyzed for cholesterol (TC) and triglycerides (TG). Liver free and total cholesterol (FC and TC respectively), and cholesterol esters (CE) were biochemically determined. Data are expressed as mean ± SEM, n = 8 per group. * P < 0.05 versus WT-tp (Mann-Whitney U Test).*

these data, HOMA-IR was markedly lower in *Myd88$^{-/-}$*-tp mice compared to WT-tp mice (Fig. 4F). These data show an overall improvement in insulin sensitivity as a result of Myd88 deficiency in the hematopoietic cell compartment.

MYD88 expression in humans with NAFLD.

After exploring the relationship between Myd88, NAFLD and insulin resistance in rodents, we assessed if hepatic *MYD88* expression could play a role in the disease progression in humans. Therefore, using Illumina HT12 Beadchips the level of hepatic *MYD88* expression was determined in 93 biopsied subjects showing different stages of NAFLD (Supplemental Table 3). The hepatic expression levels of *MYD88* were positively associated with the degree of steatosis as evaluated according to Kleiner (27). Subjects expressing the highest levels of *MYD88* showed the higher, less favorable, Kleiner score for steatosis (Fig. 5; Table 3; rs=0.31, p<0.01). Furthermore, plasma levels of ASAT, known to increase with liver injury, were also positively associated with increased levels of hepatic *MYD88* expression (Fig. 5; Table 3; rs=0.30, p<0.01). An even stronger correlation (rs=0.42, p<0.001) was observed between *MYD88* expression in the liver and plasma levels of C-reactive protein (CRP; Fig. 5; Table 3), a marker of systemic inflammation that is known to be increased in subjects with NAFLD and T2D (29). However, no correlation was found between hepatic *MYD88* expression and plasma glucose (rs=-0.16, p=0.159), plasma insulin (rs=0.05, p=0.694) or HbA1c levels (Table 4; rs=-0.02, p=0.834), as measurements of insulin resistance and T2D. These data show that increased expression of *MYD88* is associated with an unfavorable hepatic phenotype in the human population.

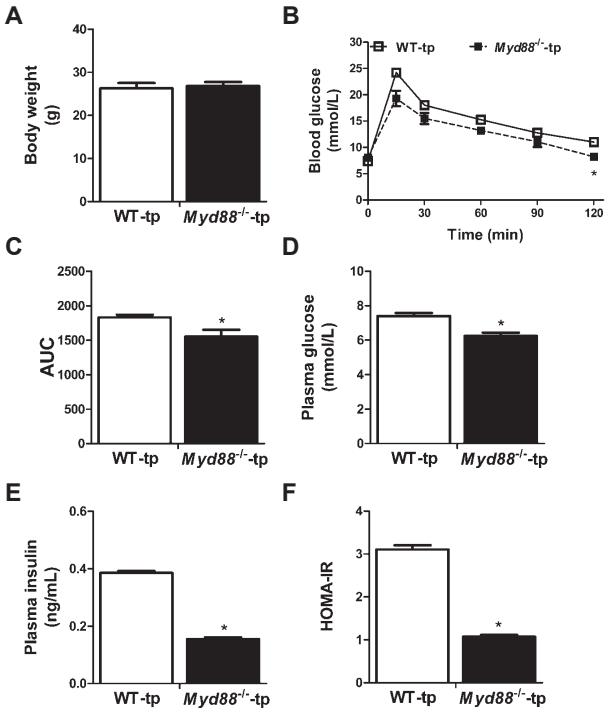

Figure 4. *Hematopoietic deficiency of Myd88 improves insulin sensitivity in the Ldlr$^{-/-}$ mouse. Body weight was measured (**A**). Blood glucose levels during an oral glucose tolerance test (OGTT) (**B**). Area under the curve (AUC) was calculated for the glucose tolerance test (**C**). Glucose (**D**) and insulin levels (**E**) following a 9-hr fast in plasma. Homeostasis model of assessment- insulin resistance (HOMA-IR) was assessed as a surrogate marker of insulin resistance (**F**). Data are expressed as mean ± SEM, n = 8 per group. (□) = low-density lipoprotein receptor knockout (Ldlr$^{-/-}$) mice transplanted with WT bone marrow cells, (■) = Ldlr$^{-/-}$ mice transplanted with myeloid differentiation primary response gene 88 (Myd88)$^{-/-}$ bone marrow cells. * P < 0.05 versus WT-tp mice (Mann-Whitney U Test).*

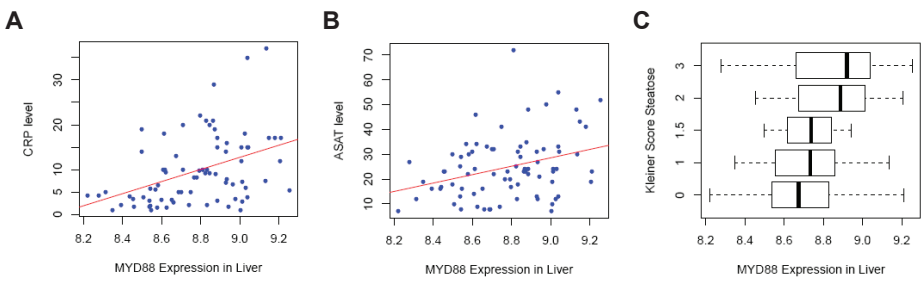

Figure 5. *Correlation between MYD88 expression and CRP, ASAT and Kleiner score for steatosis. The graphs show the correlation between hepatic MYD88 expression and CRP (**A**), ASAT (**B**) and Kleiner score for steatosis (**C**). CRP, C-reactive protein; ASAT, aspartate aminotransaminase.*

Table 3. *Hepatic MYD88 expression correlates with features of the metabolic syndrome in severly obese subjects.*

Phenotype	Spearman Correlation R	Spearman P value
CRP	0.42	1.29x10-4
KLeiner score steatosis	0.312	0.0043
ASAT	0.301	0.0069
Glucose	-0.159	0.1586
Insulin	0.046	0.6943
HbA1c	-0.024	0.8338

CRP, C-reactive protein; ASAT, aspartate aminotransaminase.

Discussion

TLR and IL-1 signaling pathways have been established to play a role in NAFLD and insulin resistance (11-13,17,19). The signals of both TLR and IL-1 pathways converge on MYD88, subsequently leading to the activation of NF-κB-mediated inflammation. Therefore, silencing MYD88 is a promising target to reduce inflammation, and protect against NAFLD and insulin resistance. Here, we provide evidence for a role for Myd88 in the pathogenesis of NAFLD using complementary approaches. First, the two mouse models, i.e., *Myd88*$^{-/-}$ and *Myd88*$^{-/-}$-tp mice, show that Myd88 is involved in inflammation during NAFLD. Second, we show that these mouse models with Myd88 deficiency show decreased hepatic triglyceride levels. This role of Myd88 is mirrored in humans, where increased *MYD88* expression is associated with a higher Kleiner score for steatosis. In addition, the *Ldlr*$^{-/-}$ model with hematopoietic Myd88 deficiency showed that the decreased hepatic inflammation and lipid accumulation is accompanied by improved systemic insulin sensitivity.

Myd88 deficiency leads to reduced inflammation in chow- and HFC-fed C57BL6/J mice, as well as in the *Myd88*$^{-/-}$-tp mice on the *Ldlr*$^{-/-}$ background. It is well established that the HFC causes low-grade inflammation in C57BL6/J mice (30). In particular the cholesterol in the HFC diet is a cause of inflammation (31). However, the mechanisms of the inflammation have remained unclear. Here we show, that in the absence of Myd88, inflammation is attenuated in C57BL6/J mice, indicating that the HFC diet may provide ligands for TLRs or the inflammasome. Recently, we have delineated the mechanism of HFC-induced inflammation in more detail in cholesterol-fed *Ldlr*$^{-/-}$ mice as a model to understand the etiology of NASH (22,23). We found that the susceptibility to develop inflammation in this mouse model originates from the high levels of oxidized LDL in the plasma (24). This oxidized LDL is cleared from the circulation by the Kupffer cells and hepatic macrophages. Because oxidized LDL remains trapped in the lysosomes, it induces inflammation (32). An important step in the induction of the inflammation is the activation of the inflammasome. Interestingly, we noted that the cholesterol diet induced the formation of cholesterol crystals, which are capable of activating the inflammasome (33). As the inflammasome activates the IL-1-MYD88 pathway to activate the IKK complex (34), we reasoned that Kupffer cell/macrophage Myd88 deficiency could interrupt this inflammatory pathway and attenuate hepatic inflammation and possibly improve insulin sensitivity. Our current data strongly supports this model.

Interestingly, both the mice with a complete knockout of Myd88 as well as the mice with hematopoietic Myd88 deficiency show a decrease in hepatic steatosis. These latter finding strongly argues for a crucial role of hepatic macrophages and Kupffer cells controlling hepatic lipid levels. This is in agreement with earlier studies using intraperitoneal injections with clodronate-encapsulated liposomes showing that Kupffer cell depletion leads to reduced hepatic lipid levels (35,36). Interestingly, it was found that ablation of Kupffer cells leads to decreased IL-1β suppression of peroxisome proliferator activated receptor alpha (PPARα,), sustained fatty acid oxidation and a reduction in hepatic lipid content (35). In both of our models, we find a reduction in *IL-1β* expression, indicating that Myd88 deficiency may lead to a

similar mechanism where decreased IL-1β signaling leads to a lower hepatic lipid accumulation.

We have shown that *Myd88*$^{-/-}$ mice are not protected against the development of insulin resistance. Similarly, others have also shown that *Myd88*$^{-/-}$ mice fed a high-fat diet developed a diabetic phenotype, characterized by glucose intolerance and increased blood glucose and insulin levels (20,37). This is in contrast with data obtained from *Tlr4*$^{-/-}$ or *IL1R*$^{-/-}$ mice showing that these mice are protected against the development of insulin resistance (12,13,17,19). It has been demonstrated that stearoyl-Coenzyme A desaturase 1 (*Scd1*) is up regulated in *Myd88*$^{-/-}$ mice (37). Moreover, it has been suggested that SCD1 is a key factor in the pathogenesis of lipid-induced insulin resistance (38). Since it has been shown that the circulating levels of free and esterified cholesterol are increased in *Myd88*$^{-/-}$ mice fed a high-fat diet (20) and the production of cholesterol esters from monounsaturated fatty acids in the mouse liver is highly dependent on Scd1 (39), it has been suggested that the high levels of *Scd1* in *Myd88*$^{-/-}$ mice fed a high-fat diet contribute to the production of cholesterol esters, leading to the abnormal cholesterol homeostasis or lipid metabolism which results in insulin resistance. This finding corroborated studies with *Scd1*$^{-/-}$ mice (40) and could explain the paradoxical insulin resistant phenotype of *Myd88*$^{-/-}$ mice.

To focus more on the role of Myd88 in hematopoietic cells, we carried out bone marrow transplantation experiments. Strikingly, *Myd88*$^{-/-}$-tp mice are protected from HFC-induced hyperinsulinemia, hyperglycemia and whole-body insulin resistance. These results are in line with recent studies in which hematopoietic deficiency of Tlr4 resulted in the protection against HFD-induced hyperinsulinemia and insulin tolerance (41). Tlr4 deletion in the hematopoietic compartment did not affect obesity nor adiposity, but markedly reduced hepatic inflammation (41). Altogether, these data show that deletion of Myd88 in the hematopoietic compartment specifically protects against high-fat diet mediated-insulin resistance. It is of interest that both of our models showed a decrease in inflammation and steatosis, but have contrasting phenotypes for glucose metabolism.

In summary, we have demonstrated that Myd88 deficiency leads to decreased steatohepatitis in mouse models. In addition, we show that *MYD88* expression in the livers of subjects with different stages of NAFLD correlates with the levels of CRP, ASAT and Kleiner score for steatosis. Altogether, these data indicate an important role for Myd88 in the development of NAFLD.

References

1. Marchesini G, Brizi M, Bianchi G, Tomassetti S, Bugianesi E, Lenzi M, et al. Nonalcoholic fatty liver disease: a feature of the metabolic syndrome. Diabetes 2001;50(8):1844-1850.
2. Marchesini G, Forlani G. NASH: from liver diseases to metabolic disorders and back to clinical hepatology. Hepatology 2002;35(2):497-499.
3. Dela PA, Leclercq I, Field J, George J, Jones B, Farrell G. NF-kappaB activation, rather than TNF, mediates hepatic inflammation in a murine dietary model of steatohepatitis. Gastroenterology 2005;129(5):1663-1674.
4. Cai D, Yuan M, Frantz DF, Melendez PA, Hansen L, Lee J, et al. Local and systemic insulin resistance resulting from hepatic activation of IKK-beta and NF-kappaB. Nat Med 2005;11(2):183-190.
5. Yuan M, Konstantopoulos N, Lee J, Hansen L, Li ZW, Karin M, et al. Reversal of obesity- and diet-induced insulin resistance with salicylates or targeted disruption of Ikkbeta. Science 2001;293(5535):1673-1677.
6. Aparicio-Vergara M, Hommelberg PP, Schreurs M, Gruben N, Stienstra R, Shiri-Sverdlov R, et al. Tumor necrosis factor receptor 1 gain-of-function mutation aggravates nonalcoholic fatty liver disease but does not cause insulin resistance in a murine model. Hepatology 2013;57(2):566-576.
7. Abiru S, Migita K, Maeda Y, Daikoku M, Ito M, Ohata K, et al. Serum cytokine and soluble cytokine receptor levels in patients with non-alcoholic steatohepatitis. Liver Int 2006;26(1):39-45.
8. Crespo J, Cayon A, Fernandez-Gil P, Hernandez-Guerra M, Mayorga M, Dominguez-Diez A, et al. Gene expression of tumor necrosis factor alpha and TNF-receptors, p55 and p75, in nonalcoholic steatohepatitis patients. Hepatology 2001;34(6):1158-1163.
9. Schreyer SA, Chua SC, Jr., LeBoeuf RC. Obesity and diabetes in TNF-alpha receptor- deficient mice. J Clin Invest 1998;102(2):402-411.
10. Hultmark D. Macrophage differentiation marker MyD88 is a member of the Toll/IL-1 receptor family. Biochem Biophys Res Commun 1994;199(1):144-146.
11. Miura K, Kodama Y, Inokuchi S, Schnabl B, Aoyama T, Ohnishi H, et al. Toll-like receptor 9 promotes steatohepatitis by induction of interleukin-1beta in mice. Gastroenterology 2010;139(1):323-334.
12. Rivera CA, Adegboyega P, van Rooijen N, Tagalicud A, Allman M, Wallace M. Toll-like receptor-4 signaling and Kupffer cells play pivotal roles in the pathogenesis of non-alcoholic steatohepatitis. J Hepatol 2007;47(4):571-579.
13. Tsukumo DM, Carvalho-Filho MA, Carvalheira JB, Prada PO, Hirabara SM, Schenka AA, et al. Loss-of-function mutation in Toll-like receptor 4 prevents diet-induced obesity and insulin resistance. Diabetes 2007;56(8):1986-1998.
14. Akira S, Uematsu S, Takeuchi O. Pathogen recognition and innate immunity. Cell 2006;124(4):783-801.
15. Henao-Mejia J, Elinav E, Jin C, Hao L, Mehal WZ, Strowig T, et al. Inflammasome-mediated dysbiosis regulates progression of NAFLD and obesity. Nature 2012;482(7384):179-185.
16. Spranger J, Kroke A, Mohlig M, Hoffmann K, Bergmann MM, Ristow M, et al. Inflammatory cytokines and the risk to develop type 2 diabetes: results of the prospective population-based European Prospective Investigation into Cancer and Nutrition (EPIC)-Potsdam Study. Diabetes 2003;52(3):812-817.
17. de Roos B, Rungapamestry V, Ross K, Rucklidge G, Reid M, Duncan G, et al. Attenuation of inflammation and cellular stress-related pathways maintains insulin sensitivity in obese type I interleukin-1 receptor knockout mice on a high-fat diet. Proteomics 2009;9(12):3244-3256.

18. Meier CA, Bobbioni E, Gabay C, Assimacopoulos-Jeannet F, Golay A, Dayer JM. IL-1 receptor antagonist serum levels are increased in human obesity: a possible link to the resistance to leptin? J Clin Endocrinol Metab 2002;87(3):1184-1188.
19. Matsuki T, Horai R, Sudo K, Iwakura Y. IL-1 plays an important role in lipid metabolism by regulating insulin levels under physiological conditions. J Exp Med 2003;198(6):877-888.
20. Hosoi T, Yokoyama S, Matsuo S, Akira S, Ozawa K. Myeloid differentiation factor 88 (MyD88)-deficiency increases risk of diabetes in mice. PLoS One 2010;5(9): e12537
21. Kennedy DJ, Kuchibhotla S, Westfall KM, Silverstein RL, Morton RE, Febbraio M. A CD36-dependent pathway enhances macrophage and adipose tissue inflammation and impairs insulin signalling. Cardiovasc Res 2011;89(3):604-613.
22. Wouters K, van Gorp PJ, Bieghs V, Gijbels MJ, Duimel H, Lutjohann D, et al. Dietary cholesterol, rather than liver steatosis, leads to hepatic inflammation in hyperlipidemic mouse models of nonalcoholic steatohepatitis. Hepatology 2008;48(2):474-486.
23. Bieghs V, van Gorp PJ, Wouters K, Hendrikx T, Gijbels MJ, van Bilsen M, et al. LDL receptor knock-out mice are a physiological model particularly vulnerable to study the onset of inflammation in non-alcoholic fatty liver disease. PLoS One 2012;7(1):e30668.
24. Bieghs V, van Gorp PJ, Walenbergh SM, Gijbels MJ, Verheyen F, Buurman WA, et al. Specific immunization strategies against oxidized low-density lipoprotein: a novel way to reduce nonalcoholic steatohepatitis in mice. Hepatology 2012;56(3):894-903.
25. Aparicio-Vergara M, Shiri-Sverdlov R, de Haan G, Hofker MH. Bone marrow transplantation in mice as a tool for studying the role of hematopoietic cells in metabolic and cardiovascular diseases. Atherosclerosis 2010;213(2):335-344.
26. Bligh EG, Dyer WJ. A rapid method of total lipid extraction and purification. Can J Biochem Physiol 1959;37(8):911-917.
27. Kleiner DE, Brunt EM, Van Natta M, Behling C, Contos MJ, Cummings OW, et al. Design and validation of a histological scoring system for nonalcoholic fatty liver disease. Hepatology 2005;41(6):1313-1321.
28. Brunt EM, Janney CG, Di Bisceglie AM, Neuschwander-Tetri BA, Bacon BR. Nonalcoholic steatohepatitis: a proposal for grading and staging the histological lesions. Am J Gastroenterol 1999;94(9):2467-2474.
29. Sattar N, Gaw A, Scherbakova O, Ford I, O'Reilly DS, Haffner SM, et al. Metabolic syndrome with and without C-reactive protein as a predictor of coronary heart disease and diabetes in the West of Scotland Coronary Prevention Study. Circulation 2003;108(4):414-419.
30. Liao F, Andalibi A, Qiao JH, Allayee H, Fogelman AM, Lusis AJ. Genetic evidence for a common pathway mediating oxidative stress, inflammatory gene induction, and aortic fatty streak formation in mice. J Clin Invest 1994;94(2):877-884.
31. Vergnes L, Phan J, Strauss M, Tafuri S, Reue K. Cholesterol and cholate components of an atherogenic diet induce distinct stages of hepatic inflammatory gene expression. J Biol Chem 2003;278(44):42774-42784.
32. Bieghs V, Verheyen F, van Gorp PJ, Hendrikx T, Wouters K, Lutjohann D, et al. Internalization of modified lipids by CD36 and SR-A leads to hepatic inflammation and lysosomal cholesterol storage in Kupffer cells. PLoS One 2012;7(3):e34378.
33. Bieghs V, Hendrikx T, van Gorp PJ, Verheyen F, Guichot YD, Walenbergh SM, et al. The cholesterol derivative 27-hydroxycholesterol reduces steatohepatitis in mice. Gastroenterology 2013;144(1):167-178.
34. Stutz A, Golenbock DT, Latz E. Inflammasomes: too big to miss. J Clin Invest 2009;119(12):3502-3511.
35. Stienstra R, Saudale F, Duval C, Keshtkar S, Groener JE, van Rooijen N, et al. Kupffer cells promote hepatic steatosis via interleukin-1beta-dependent

suppression of peroxisome proliferator-activated receptor alpha activity. Hepatology 2010;51(2):511-522.
36. Huang W, Metlakunta A, Dedousis N, Zhang P, Sipula I, Dube JJ, et al. Depletion of liver Kupffer cells prevents the development of diet-induced hepatic steatosis and insulin resistance. Diabetes 2010;59(2):347-357.
37. Yokoyama S, Hosoi T, Ozawa K. Stearoyl-CoA Desaturase 1 (SCD1) is a key factor mediating diabetes in MyD88-deficient mice. Gene 2012;497(2):340-343.
38. Brown JM, Rudel LL. Stearoyl-coenzyme A desaturase 1 inhibition and the metabolic syndrome: considerations for future drug discovery. Curr Opin Lipidol 2010;21(3):192-197.
39. Miyazaki M, Kim YC, Gray-Keller MP, Attie AD, Ntambi JM. The biosynthesis of hepatic cholesterol esters and triglycerides is impaired in mice with a disruption of the gene for stearoyl-CoA desaturase 1. J Biol Chem 2000;275(39):30132-30138.
40. Ntambi JM, Miyazaki M, Stoehr JP, Lan H, Kendziorski CM, Yandell BS, et al. Loss of stearoyl-CoA desaturase-1 function protects mice against adiposity. Proc Natl Acad Sci U S A 2002;99(17):11482-11486.
41. Saberi M, Woods NB, de LC, Schenk S, Lu JC, Bandyopadhyay G, et al. Hematopoietic cell-specific deletion of toll-like receptor 4 ameliorates hepatic and adipose tissue insulin resistance in high-fat-fed mice. Cell Metab 2009;10(5):419-429.

Supplemental tables and figures

Supplemental Table 1. *Primer sequences used for RT-PCR.*

Gene	Forward primer 5'-3'	Reverse primer 5'-3'
Cd68	TGACCTGCTCTCTCTAAGGCTACA	TCACGGTTGCAAGAGAAACATG
Mcp1	GCTGGAGAGCTACAAGAGGATCA	ACAGACCTCTCTCTTGAGCTTGGT
Tnfα	CATCTTCTCAAAATTCGAGTGACAA	TGGGAGTAGACAAGGTACAACCC
Fizz1	TCCCAGTGAATACTGGATGAGA	CCACTCTGGATCTCCCAAGA
Ym1	AGAAGGGAGTTTCAAACCTGGT	GTCTTGCTCATGTGTGTAAGTGA
Il-1β	TGCAGCTGGAGAGTGTGG	TGCTTGTGAGGTGCTGATG
Col1a1	AACCCTGCCCGCACATG	CAGACGGCTGAGTAGGGAACA
Timp1	CGCCTAAGGAACGGAAATTTG	AGGGATAGATAAACAGGGAAACACTGT
Mmp9	CCTGGAACTCACACGACATCTTC	TGGAAACTCACACGCCAGAA
Ppia	TTCCTCCTTTCACAGAATTATTCCA	CCGCCAGTGCCATTATGG

Supplemental Table 2. *Clinical and plasma parameters of the study population.*

	Means ± SD	Minimal/maximal values
Male/Female	26/67	
Age (years)	44.20 ± 9.74	17-67
BMI (kg/m^2)	46.15 ± 9.54	30.7-73.6
Glucose (mmol/L)	6.45 ± 1.98	4.3-14.5
HbA1c (%)	6.54 ± 1.34	5.1-12.1
Insulin (mU/L)	18.95 ± 10.61	3.8-53
Triglycerides (mmol/L)	2.22 ± 1.98	0.63-16.4
NEFA (nmol/L)	0.70 ± 0.70	0.12-6.4
ALAT(U/L)	26.53 ± 16.05	6-124
ASAT (U/L)	24.07 ± 12.44	7-72
C-reactive protein (mg/L)	10.17 ± 8.10	1-37

Data are means ± standard deviation (SD) and the minimal and maximal values for each trait. NEFA, non-esterified fatty acid; ALAT, alanine amintransaminase; ASAT, aspartate aminotransaminase.

Supplemental Table 3. *Summary of liver pathology of the study population*

	Total number of individuals scored	No. of individuals with score			
		0	1	2	3
Steatosis (0-3)	93	25	26	29	13
Fibrosis (0-3)	91	62	15	11	3
Lobular Inflammation	88	36	35	12	5

Data are the number of individuals scored for different grades of hepatic steatosis and features of non-alcoholic steatohepatitis (NASH) as described by Kleiner et al (27). The table also shows the total number of individuals per trait that were scored.

Supplemental Table 4. *Correlation of MYD88 expression in four different tissues with features of the metabolic syndrome in subjects with NAFLD.*

	Spearman Correlation Coefficient with *MYD88* Expression (P value)			
Trait	**Liver**	**SAT**	**VAT**	**Muscle**
Sex	-0.161 (P=0.149)	0.201 (P=0.0575)	0.106 (P=0.338)	0.0423 (P=0.149)
Age	-0.249 (P=0.024)	0.0559 (P=0.601)	0.0771 (P=0.486)	-0.065 (P=0.024)
BMI	0.257 (P=0.0205)	0.199 (P=0.0613)	0.00738 (P=0.947)	-0.042 (P=0.0205)
Waist-hip ratio	-0.0142 (P=0.914)	0.249 (P=0.0527)	0.0159 (P=0.906)	0.0379 (P=0.914)
Glucose	-0.159 (P=0.159)	0.16 (P=0.138)	0.0218 (P=0.846)	-0.0629 (P=0.159)
HbA1c	-0.0241 (P=0.834)	0.197 (P=0.0711)	0.156 (P=0.17)	0.0294 (P=0.834)
Insulin	0.0455 (P=0.694)	0.223 (P=0.0417)	0.0382 (P=0.738)	0.00655 (P=0.694)
Total Cholesterol	-0.092 (P=0.429)	-0.292 (P=0.00771)	-0.0434 (P=0.708)	-0.176 (P=0.429)
High-density lipoprotein	-0.151 (P=0.19)	-0.438 (P=3.51e-05)	-0.0721 (P=0.531)	0.02 (P=0.19)
Low-density lipoprotein	-0.0402 (P=0.729)	-0.196 (P=0.0764)	-0.0109 (P=0.924)	-0.122 (P=0.729)
Triglyceride	-0.0495 (P=0.669)	0.156 (P=0.158)	0.0508 (P=0.658)	-0.00888 (P=0.669)
Free fatty acids	0.148 (P=0.212)	-0.00665 (P=0.953)	-0.171 (P=0.141)	-0.0646 (P=0.212)
C-reactive protein	0.423 (P=0.000129)	0.103 (P=0.356)	-0.103 (P=0.369)	0.00779 (P=0.000129)
Alanine transaminase	-0.00155 (P=0.989)	0.238 (P=0.0295)	0.0288 (P=0.801)	-0.167 (P=0.989)
Aspartate transaminase	0.301 (P=0.00695)	0.195 (P=0.0758)	-0.0204 (P=0.858)	-0.0675 (P=0.00695)
Kleiner score steatose	0.312 (P=0.0043)	0.202 (P=0.0556)	0.0614 (P=0.579)	-0.0479 (P=0.0043)
Fibrose	0.129 (P=0.253)	0.159 (P=0.138)	0.113 (P=0.311)	0.13 (P=0.253)
Lobular inflammation	0.134 (P=0.247)	0.123 (P=0.261)	0.277 (P=0.0136)	-0.0473 (P=0.247)
Large lipogranulomas	0.242 (P=0.0296)	-0.00406 (P=0.97)	0.17 (P=0.124)	0.0815 (P=0.0296)
Portal inflammation	0.0461 (P=0.681)	-0.0329 (P=0.758)	0.157 (P=0.154)	-0.0657 (P=0.681)
Ballooning	0.164 (P=0.143)	0.125 (P=0.243)	0.186 (P=0.0928)	0.0147 (P=0.143)
Glycogenated nuclei	-0.0698 (P=0.541)	0.0536 (P=0.622)	0.023 (P=0.838)	-0.144 (P=0.541)
NAS score	0.154 (P=0.197)	0.162 (P=0.154)	0.0855 (P=0.472)	-0.0134 (P=0.197)

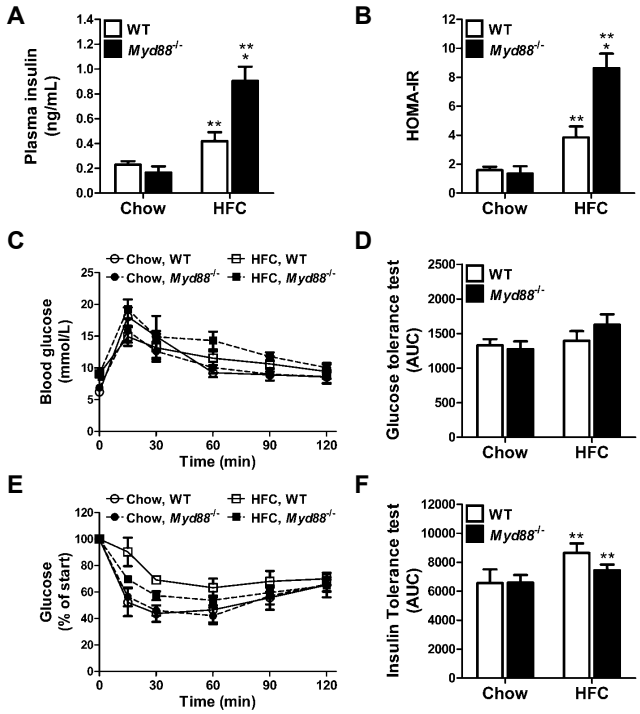

Supplemental Figure 1. *HFC-fed Myd88$^{-/-}$ mice are not protected from the development of insulin resistance. Insulin levels following a 9-hr fast in plasma (**A**). Homeostasis model of assessment-insulin resistance (HOMA-IR) was assessed as a surrogate marker of insulin resistance (**B**). Blood glucose levels during an oral glucose tolerance test (OGTT) (**C**). Area under the curve (AUC) was calculated for the glucose tolerance test (**D**). Blood glucose levels during an insulin tolerance test (ITT) following a 6-h fast (**E**). AUC for the insulin tolerance test (**F**) was calculated. Data are expressed as mean ± SEM, n = 6 per group. (□) = WT mice, (■) = Myd88$^{-/-}$ mice. * P < 0.05 versus WT mice (Mann-Whitney U Test); ** P < 0.05 versus chow diet (two-way ANOVA test).*

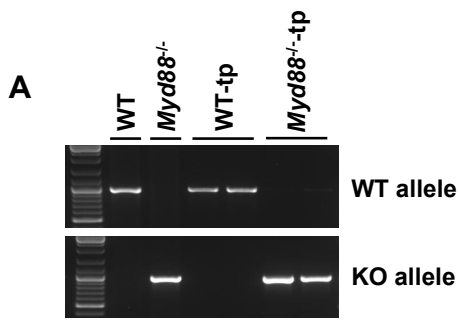

Supplemental Figure 2. *Transplantation efficacy. To confirm transplantation efficacy, whole blood was collected from the transplanted animals at the end of the study and genomic DNA was isolated to perform a PCR to genotype the WT and Myd88 knockout allele. WT and global Myd88$^{-/-}$ DNA serve as a positive control (**A**).*

Chapter 4

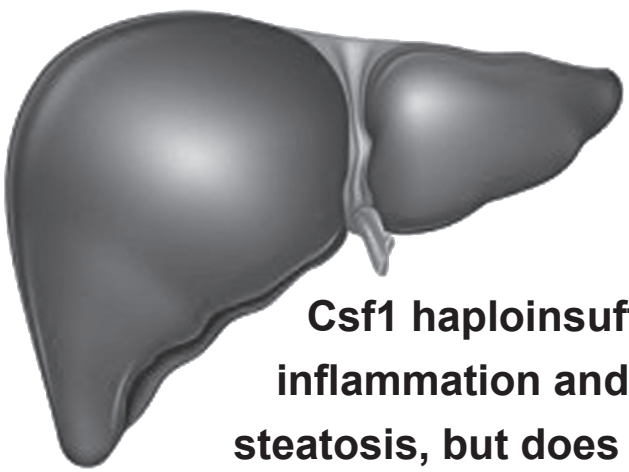

Csf1 haploinsufficiency reduces inflammation and triggers hepatic steatosis, but does not protect from obesity-induced insulin resistance in mice

Anouk Funke, Pascal P.H. Hommelberg, Bastiaan Moesker, Marijke Schreurs, Niels J. Kloosterhuis, Albert Gerding, Theo H. van Dijk, Dirk-Jan Reijngoud, Albert K. Groen, Ronit Shiri-Sverdlov, Bart van de Sluis, Marten H. Hofker, Debby P.Y. Koonen

Submitted

Abstract

Background Macrophages have been implicated in obesity-related pathologies through their role in inflammation. Colony stimulating factor (Csf1) mediates macrophage development and function, thereby playing a key role in inflammation. Mice haploinsufficient for *Csf1* (*Csf1*$^{op/+}$) are protected against atherosclerosis, suggesting that macrophages may contribute to the pathogenesis of obesity-related disorders via Csf1 regulation.

Methods To assess the role of Csf1 in fatty liver disease and insulin resistance, we studied *Csf1*$^{+/+}$ and *Csf1*$^{op/+}$ mice fed a chow or high-fat cholesterol (HFC) diet.

Results Although body weight did not differ between genotypes, *Csf1*$^{op/+}$ mice showed a reduced lean body mass and an increased fat mass compared to controls. In line with a lower lean body mass, indirect calorimetric analysis revealed a lower metabolic rate in *Csf1*$^{op/+}$ mice compared to *Csf1*$^{+/+}$ mice. Hepatic, adipose tissue and systemic inflammation were reduced in *Csf1*$^{op/+}$ compared to *Csf1*$^{+/+}$ mice. Hepatic cell fractionations indicated that the Kupffer cells are responsible for the differences in liver inflammation. Csf1 haploinsufficiency also resulted in increased fasting-induced hepatic lipid accumulation. Whereas no differences were found in *de novo* lipogenesis, VLDL-TG synthesis and secretion were markedly reduced in *Csf1*$^{op/+}$ mice, which might explain the increased hepatic steatosis. Despite reduced inflammation, whole-body glucose tolerance and fasting insulin levels did not differ between the genotypes.

Conclusion As haploinsufficiency of Csf1 affects macrophage function, our results demonstrate that Csf1 does not impact the development of insulin resistance. However, it does protect against the development of hepatic steatosis, suggesting an unexpected beneficial role for Csf1 in hepatic lipid metabolism. Treatment of inflammatory or autoimmune diseases with CSF-blockade or neutralization agents may thus give rise to adverse side-effects in the liver.

Introduction

Obesity and its associated comorbidities are among the most challenging conditions in the 21st century, imposing a major burden on human health worldwide (1,2). Studies in the past two decades have left little doubt about the critical involvement of inflammatory pathways in the mechanisms underlying insulin resistance and type 2 diabetes (T2D) (3,4).

Macrophages, in addition to their established role in innate immunity, are regarded as key players in metabolic homeostasis and in the pathogenesis of diet-induced obesity and insulin resistance (5). Indeed, the production of pro-inflammatory cytokines secreted by activated macrophages has been linked to the induction of insulin resistance in adipose tissue. Moreover, inflammatory cytokines are thought to promote hepatic steatosis and facilitate foam cell and plaque formation in the vessel wall (6). The production of pro-inflammatory cytokines secreted by the resident macrophages in the liver (Kupffer cells) is also linked to disruption of hepatic insulin signaling (7,8). Nonetheless, their role in obesity-related pathologies and the etiology of insulin resistance is still a matter of debate (9).

One essential regulator of macrophage homeostasis *in vivo* is macrophage colony-stimulating factor, or Csf1 (10). Csf1 is a macrophage growth factor, stimulating the survival, proliferation and differentiation of mononuclear phagocytes, in addition to the spreading and motility of macrophages (11). Csf1 not only regulates macrophage survival and proliferation, but also macrophage activation (12). Csf1 has been shown to play an important role in chronic diseases and inflammatory disease states (11-13), providing therapeutic potential for neutralization or blockade of Csf1 in joint pathology, atherosclerosis, and cancer metastasis (13). Csf1 is expressed in liver (14-16), and adipocytes (17), and was shown to actively promote adipose tissue hyperplasia in rabbits and humans (17). Although, it has frequently been suggested that Csf1 contributes to the pathogenesis of obesity-related disorders, including insulin resistance and T2D (11,12,17), it has never been experimentally studied in mice. We decided to investigate the role of Csf1 in the development of liver steatosis and the susceptibility to obesity-induced insulin resistance. For this we used heterozygous mice deficient for CSF-1 (*Csf1*$^{op/+}$) that have plasma levels of CSF-1 of ~65% of those in control mice (*Csf1*$^{+/+}$) (18). In contrast to homozygous (*Csf1*$^{op/op}$, *op/op*) mice, the deficient mice do not exhibit growth or skeletal defects, nor do they lack teeth, so it is possible to perform dietary intervention and obesity studies (19,20).

We demonstrated that haploinsufficiency of Csf1 is associated with reduced hepatic, adipose tissue and systemic inflammation in mice. However, *Csf1*$^{op/+}$ mice showed enhanced hepatic steatosis following an overnight fast, and have increased adiposity associated with the normal development of diet-induced insulin resistance. Our data therefore point towards a beneficial role of Csf1 in the control of lipid metabolism in the liver, but it does not affect the development of systemic insulin resistance in mice.

Research Design and Methods

Mice. All procedures were approved by the University of Groningen Ethics Committee for Animal Experiments, which adheres to the principles and guidelines established by the European Convention for the Protection of Laboratory Animals. Experiments were carried out on male *Csf1*$^{+/+}$ and *Csf1*$^{op/+}$ mice (supplied by Jackson Laboratory, Bar Harbor, ME, USA), back-crossed to C57BL/6J mice for 10 generations.

Mice were individually housed in a temperature-controlled room under a 12 h light-dark cycle, with free access to water and a standard chow diet (6.2% (w/w) fat and 0% (w/w) cholesterol; RMH-B, Hope Farms, Woerden, the Netherlands). At the age of 8-10 weeks, their diet was either maintained or switched to a high-fat cholesterol diet (HFC; 21% milk butter and 0.2% cholesterol; Scientific Animal Food and Engineering, Villemoisson-sur-Orge, France). They were kept on these diets for 10 weeks.

Fractionation of liver cells. Liver cells of chow-fed *Csf1*$^{op/op}$ and *Csf1*$^{op/+}$ mice were fractionated into hepatocytes and Kupffer cells as previously described (21). Briefly, mouse livers were digested by collagenase perfusion (Sigma-Aldrich Chemie BV, Zwijndrecht, the Netherlands) followed by 3-layer discontinuous density gradient centrifugation with 8.2% and 14.5% Nycodenz (Bio-Connect BV, Huissen, the Netherlands) to obtain both cell fractions. To check whether the fractionation resulted in clean hepatocyte and Kupffer cell fractions, *Apoa1* was used as a marker for hepatocytes and *Cd68* for Kupffer cells.

Liver lipids. Total liver lipids were extracted from the liver according to Bligh and Dyer's method (22). Hepatic total cholesterol (TC) and triglycerides (TG) were quantified using commercially available kits (TC: cholesterol CHOD-PAP, Roche, the Netherlands; TG Hitachi, Roche, the Netherlands).

In vivo VLDL-TG production. Mice were injected intraperitoneally with Poloxamer 407 (1g/kg body weight; BASF, Ludwigshaven, Germany) as a 50 mg/mL solution in saline as previously described (23). Blood samples were drawn by retro-orbital bleeding into heparinized tubes at 0, 30, 60, 120, and 240 min after injection. Immediately after the final blood draw, animals were sacrificed by cardiac puncture under isoflurane anesthesia. Plasma TG levels and TG production rates were determined as previously described (23). Nascent VLDL ($d < 1.006$) was isolated from the final plasma sample of each animal using a Optima TM LX tabletop ultracentrifuge (Beckman Instruments Inc., Palo Alto, CA, USA) at 108,000 rpm for 150 minutes.

Determining de novo lipogenesis and chain elongation in vivo. A 2% sodium [1-^{13}C]-acetate (99 atom %, Isotec/Sigma-Aldrich, Chemie BV, Zwijndrecht, the Netherlands) solution was given to the mice in their drinking water for 3 consecutive days. Analysis was performed according to Oosterveer *et al* (24).

Mitochondrial respiration. Mitochondrial respiration was measured in liver

mitochondria freshly isolated from chow-fed *Csf1*$^{+/+}$ and *Csf1*$^{op/+}$ mice using a 2-chamber Oxygraph (Oroboros Instruments, Innsbruck, Austria). Malate, glutamate and pyruvate were used as substrates. State 3 respiration was measured by addition of adenosine diphosphate (ADP) to the mitochondria in suspension, and oligomycin was used to block adenosine triphosphate (ATP) synthase activity to reflect respiration not coupled to ATP synthesis (state 4o). The maximal oxygen uptake rate (state uncoupled) was obtained by titration of the chemical uncoupler. Oxygen concentrations were recorded, and the first derivative of the oxygen tension changes in time was displayed as oxygen flux. Respiratory control rates were calculated as the ratio between state 3 and state 4 in order to determine the coupling of mitochondrial respiration.

Statistical analysis. Data are expressed as mean ± SEM. Comparisons between groups were performed using unpaired Student's two-tailed *t* tests. The level of significance was set at $P < 0.05$.

Results

Csf1 haploinsufficiency leads to fasting-induced hepatic steatosis.
As macrophages are key players in metabolic homeostasis (6), we first investigated the effects of Csf1 haploinsufficiency on plasma and liver lipid metabolism in both *Csf1*$^{+/+}$ and *Csf1*$^{op/+}$ mice fed a chow and a high-fat diet supplemented with 0.2% cholesterol (HFC) for 10 weeks. Plasma triglyceride (TG; Fig. 1A) and cholesterol (Fig. 1B) levels were lower in chow-fed *Csf1*$^{op/+}$ mice than *Csf1*$^{+/+}$ mice. However, this was not observed when *Csf1*$^{op/+}$ mice were fed a HFC diet (Fig. 1A, 1B). In addition, we saw no difference in plasma free fatty acids (Supplemental Fig. 1A) and hepatic cholesterol levels (Supplemental Fig. 1B) between *Csf1*$^{+/+}$ and *Csf1*$^{op/+}$ mice fed either diet. However, hepatic triglyceride content was significantly increased in fasted chow- and HFC-fed *Csf1*$^{op/+}$ mice compared to *Csf1*$^{+/+}$ controls (Fig. 1C). This was confirmed by histological analysis of hematoxylin and eosin (H&E) and Oil red O (ORO) stainings in the livers of these mice, and highlights a predominant periportal steatosis in liver sections of *Csf1*$^{op/+}$ mice fed a HFC diet (Fig. 1D). Of note, this 2-fold increase in hepatic TG accumulation seen under fasting conditions was not observed in the fed state (Fig. 1E), suggesting an exaggerated fasting response in *Csf1*$^{op/+}$ mice.

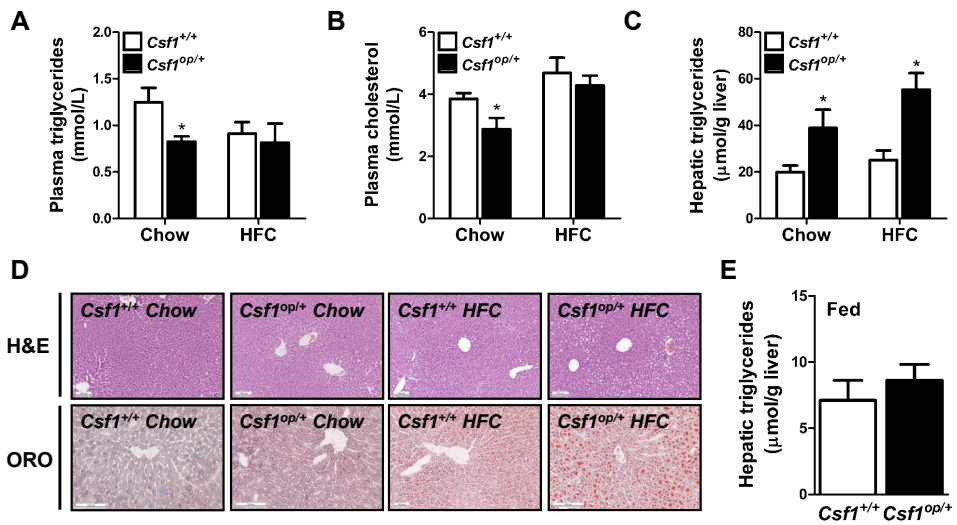

Figure 1. *Csf1 haploinsufficiency leads to fasting-induced hepatic steatosis. Plasma triglycerides (**A**), cholesterol (**B**) and hepatic triglyceride (**C**) levels were determined biochemically in chow- and high-fat cholesterol (HFC)-fed Csf1*$^{+/+}$ *and Csf1*$^{op/+}$ *mice. Representative pictures of hematoxylin & eosin (H&E) and Oil red O (ORO) stained liver sections taken from chow- and HFC-fed Csf1*$^{+/+}$ *and Csf1*$^{op/+}$ *mice (**D**). Hepatic triglyceride content in the fed state in chow-fed Csf1*$^{+/+}$ *and Csf1*$^{op/+}$ *mice (**E**). (□) = Csf1*$^{+/+}$ *mice and (■) = Csf1*$^{op/+}$ *mice. Data are expressed as mean ± SEM, n = 6 per group. * P < 0.05 versus Csf1*$^{+/+}$ *mice (Mann-Whitney U Test).*

Downregulation of inflammatory mediators in the livers of Csf1$^{op/+}$ ***mice.***
As Kupffer cells facilitate the metabolic adaptations of hepatocytes during increased caloric intake (25) and co-culture studies have suggested a role for Kupffer cell-derived

factors in the maintenance of hepatic lipid homeostasis (26,27), we next investigated whether haploinsufficiency of Csf1 affects the level of hepatic inflammation in Csf1$^{op/+}$ mice. Hepatic inflammation was reduced in *Csf1*$^{op/+}$ mice as shown by reduced mRNA levels of *Cd68*, *Mcp1* and *Cd11b* on both chow and HFC diet compared to *Csf1*$^{+/+}$ mice (Fig. 2A). Similarly, the mRNA expression of the cytokines *Tnfα*, *Il-1β* and *Il-6* was lower in *Csf1*$^{op/+}$ mice (Fig. 2B). To assess the contribution of Kupffer cells in our experimental model, we isolated the hepatocyte and Kupffer cell populations from the livers of chow-fed *Csf1*$^{+/+}$ and *Csf1*$^{op/+}$ mice. The expression of *Csf1*, *Cd68*, *Tnfα*, *Il-6* and the M2 markers *Fizz1* and *Ym1* (Fig. 2D) were significantly reduced in the Kupffer cell fraction of *Csf1*$^{op/+}$ mice compared to *Csf1*$^{+/+}$ mice. As the expression of these genes was not changed in the hepatocyte fraction (Fig. 2C), this suggests that Kupffer cells are the main drivers of the inflammatory tone in the liver. We next determined Cd68 levels in stained liver sections to investigate whether reduced hepatic inflammation was due to decreased activation of macrophages in *Csf1*$^{op/+}$ mice. However, there was no difference in the number of activated macrophages in the liver, as determined by Cd68 staining (Fig. 2D, 2E). Therefore, our data suggest that fasting-induced hepatic steatosis is associated with reduced Kupffer cell-driven inflammation in *Csf1*$^{op/+}$ mice.

Fasting triggers β-oxidation in Csf1$^{op/+}$ mice.

As efficient hepatic fatty acid oxidation is obligatory to the metabolic response to fasting (28), we next examined whether fatty acid oxidation was affected in *Csf1*$^{op/+}$ mice fed a chow diet. As a first indication as to whether fatty acid oxidation is affected, we investigated the levels of β-hydroxybutyrate in the plasma of chow-fed *Csf1*$^{+/+}$ and *Csf1*$^{op/+}$ mice. β-hydroxybutyrate levels were increased in fasted *Csf1*$^{op/+}$ mice compared to *Csf1*$^{+/+}$ mice (Fig. 3A). To assess mitochondrial function, mitochondria were isolated from fasted chow-fed *Csf1*$^{+/+}$ and *Csf1*$^{op/+}$ mice and subjected to respiratory measurements using an Oroboros Oxygraph. When malate was used as a substrate, absolute state 3 was elevated in the mitochondria from *Csf1*$^{op/+}$ mice, whereas no differences were observed in state 4o respiration (Fig. 3B). Furthermore, the respiratory control ratio (RCR), representing the degree of uncoupling or efficiency of electron transport chain activity, was increased in *Csf1*$^{op/+}$-derived liver mitochondria compared to *Csf1*$^{+/+}$ controls (Fig. 3C), indicating that liver mitochondria of *Csf1*$^{op/+}$ mice use their oxygen more efficiently than *Csf1*$^{+/+}$ mice. This suggests that β-oxidation is, in fact, enhanced in livers of *Csf1*$^{op/+}$ mice, which is likely a secondary effect to enhanced lipid storage in these mice.

Reduced VLDL-TG synthesis contributes to hepatic steatosis in Csf1$^{op/+}$ mice.

To further trace the underlying mechanisms for the fasting-induced hepatic steatosis in *Csf1*$^{op/+}$ mice, we examined the processes of very-low density lipoprotein (VLDL)-TG secretion and *de novo* lipogenesis (DNL) in *Csf1*$^{+/+}$ and *Csf1*$^{op/+}$ mice fed a chow diet. To assess whether hepatic lipid secretion is changed in *Csf1*$^{op/+}$ mice, we first determined VLDL-TG production rates. Plasma TG levels were reduced in *Csf1*$^{op/+}$ mice following an intraperitoneal injection with Poloxamer-407 (Fig. 4A). Consistent with this, hepatic VLDL-TG production was reduced in *Csf1*$^{op/+}$ mice compared to *Csf1*$^{+/+}$ mice (Fig. 4B). In addition, plasma VLDL composition was altered and contained a lower amount of TG in *Csf1*$^{op/+}$ mice compared to plasma from *Csf1*$^{+/+}$

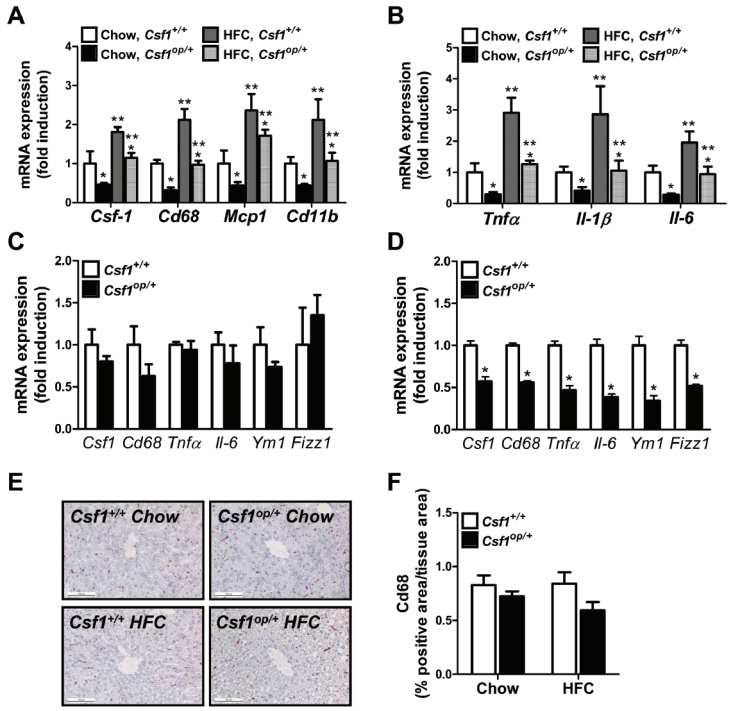

Figure 2. *Downregulation of inflammatory mediators in livers of Csf1$^{op/+}$ mice. Real-time polymerase chain reaction (RT-PCR) analysis was performed to measure hepatic mRNA expression levels of colony stimulating factor (Csf-1), inflammatory genes cluster of differentiation 68 (Cd68), monocyte chemoattractant protein 1 (Mcp1), integrin, alpha M (Cd11b) (**A**), and cytokines tumor necrosis factor α (Tnfα), interleukin-1β (Il-1β) and Il-6 (**B**) in chow- and high-fat cholesterol (HFC)-fed Csf1$^{+/+}$ and Csf1$^{op/+}$ mice; (□) = Csf1$^{+/+}$ mice on chow diet, (■) = Csf1$^{op/+}$ mice on chow diet, (■) = Csf1$^{+/+}$ mice on HFC diet and (■) = Csf1$^{op/+}$ mice on HFC diet. Liver cells were fractionated into hepatocytes and Kupffer cells by 3-layer discontinuous density gradient centrifugation and mRNA expression of Csf-1, Cd68, Tnfα, Il-6, Fizz1 and Ym1 were determined in the hepatocyte (**C**) and Kupffer cell fraction (**D**) in chow-fed Csf1$^{+/+}$ and Csf1$^{op/+}$ mice. Representative pictures of immunohistochemical staining of Cd68 on liver sections (**E**) and quantification of Cd68 staining (**F**) in chow- and HFC-fed Csf1$^{+/+}$ and Csf1$^{op/+}$ mice. (□) = Csf1$^{+/+}$ mice and (■) = Csf1$^{op/+}$ mice. Data are expressed as mean ± SEM, n = 6 per group. The mRNA expression levels are normalized for Cyclophillin A (Ppia). Expression is shown as fold change compared to Csf1$^{+/+}$ levels on chow diet. * P < 0.05 versus Csf1$^{+/+}$ mice (Mann-Whitney U Test); ** P < 0.05 versus chow diet (two-way ANOVA test).*

mice (Fig. 4C). As increased synthesis of fatty acids via the *de novo* lipogenesis pathway may also result in hepatic lipid accumulation, we next assessed the fractional C16:0 and C18 synthesis in liver homogenates from these mice following an oral load of [1-^{13}C]-acetate. Mass isotopomer distribution analysis (MIDA) showed that fractional C16:0 (palmitate), C18:0 (stearate) and C18:1 (oleate) (Fig. 4D) syntheses were no different in *Csf1$^{op/+}$* mice than *Csf1$^{+/+}$* mice. Taken together, these results indicate that the increased hepatic lipid accumulation is mainly due to reduced VLDL-TG secretion in the *Csf1$^{op/+}$* mice.

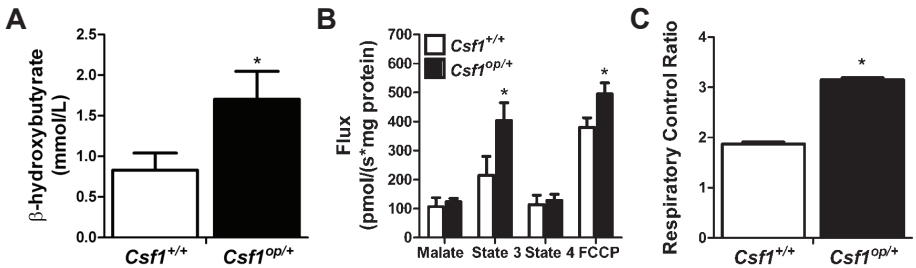

Figure 3. *Fasting triggers β-oxidation in Csf1$^{op/+}$ mice. Plasma β-hydroxybutyrate levels were determined as an overall measure of β–oxidation in chow-fed Csf1$^{+/+}$ and Csf1$^{op/+}$ mice (**A**). Respiratory analysis of liver-derived mitochondria of chow-fed Csf1$^{+/+}$ and Csf1$^{op/+}$ mice were measured by an Oxygraph. State 3 and 4o respiration levels (**B**) and respiratory control ratio (RCR) (**C**) were measured using malate as substrate. (□) = Csf1$^{+/+}$ mice and (■) = Csf1$^{op/+}$ mice. Data are expressed as mean ± SEM, n = 6 per group * P < 0.05 versus Csf1$^{+/+}$ mice (Mann-Whitney U Test).*

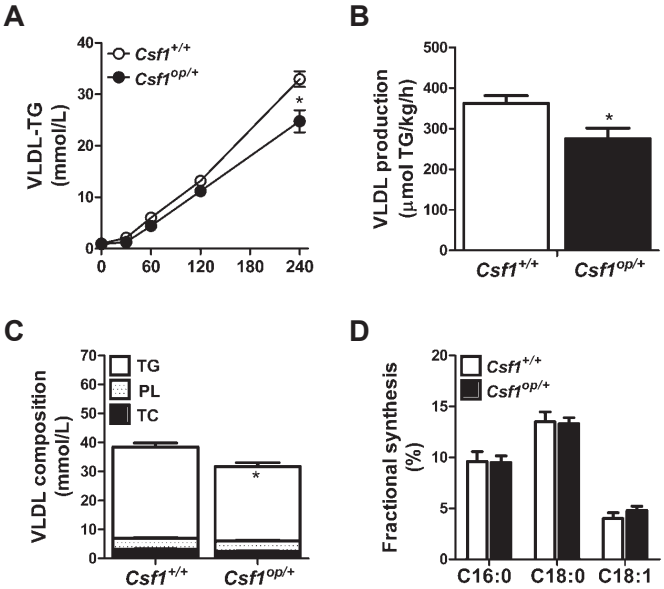

Figure 4. *Reduced VLDL-TG synthesis contributes to hepatic steatosis in Csf1$^{op/+}$ mice. An intraperitoneal injection with Poloxamer 407 was performed to measure the in vivo very-low density lipoprotein-triglyceride (VLDL-TG) production. Plasma VLDL triglyceride levels (**A**) and VLDL-TG production rates (**B**) were determined in chow-fed Csf1$^{+/+}$ and Csf1$^{op/+}$ mice; (□) = Csf1$^{+/+}$ mice and (■) = Csf1$^{op/+}$ mice. The composition of VLDL (**C**) was determined in chow-fed Csf1$^{+/+}$ and Csf1$^{op/+}$ mice; (□) = triglycerides (TG), (■) = phospholipids (PL) and (■) = cholesterol (TC). Fractional synthesis of C16:0 (palmitate), C18:0 (stearate) and C18:1 (oleate) as a measurement of de novo lipogenesis were measured by giving [1-^{13}C]-acetate in drinking water of chow-fed Csf1$^{op/+}$ and Csf1$^{op/+}$ mice (**D**). (□) = Csf1$^{+/+}$ mice and (■) = Csf1$^{op/+}$ mice. Data are expressed as mean ± SEM, n = 6 per group. * P < 0.05 versus Csf1$^{+/+}$ mice (Mann-Whitney U Test).*

Csf1op/+ mice are not protected from diet-induced obesity.

As obesity is associated with macrophage accumulation in adipose tissue (29) and adipocyte Csf1 is a mediator of adipose tissue growth (17), we next assessed the diet-induced weight gain in *Csf1*$^{+/+}$ and *Csf1*$^{op/+}$ mice. Although body weight did not differ between the mice on chow or HFC diet, Dual-Energy X-ray Absorptiometry (DEXA) scan analyses demonstrated a reduced lean body mass and much increased fat mass (Fig. 5A) in *Csf1*$^{op/+}$ mice compared to *Csf1*$^{+/+}$ mice on both diets. Despite an increased adiposity in *Csf1*$^{op/+}$ mice, the weight gain was similar in both mice following HFC feeding (data not shown). This confirmed that *Csf1*$^{op/+}$ mice are not protected from diet-induced weight gain. A trend for increased adipocyte count was observed in *Csf1*$^{op/+}$ mice fed a chow diet; however, adipocyte counts did not differ between the genotypes on a HFC diet (Fig. 5B, C). Next, we determined expression of genes governing macrophage function and cytokine production in the adipose tissue of *Csf1*$^{+/+}$ and *Csf1*$^{op/+}$ mice. Adipose tissue inflammation was decreased in HFC-fed *Csf1*$^{op/+}$ mice as shown by reduced mRNA expression levels of *Mcp1*, *Cd11b* and *Tnfα* compared to *Csf1*$^{+/+}$ mice (Fig. 5D).

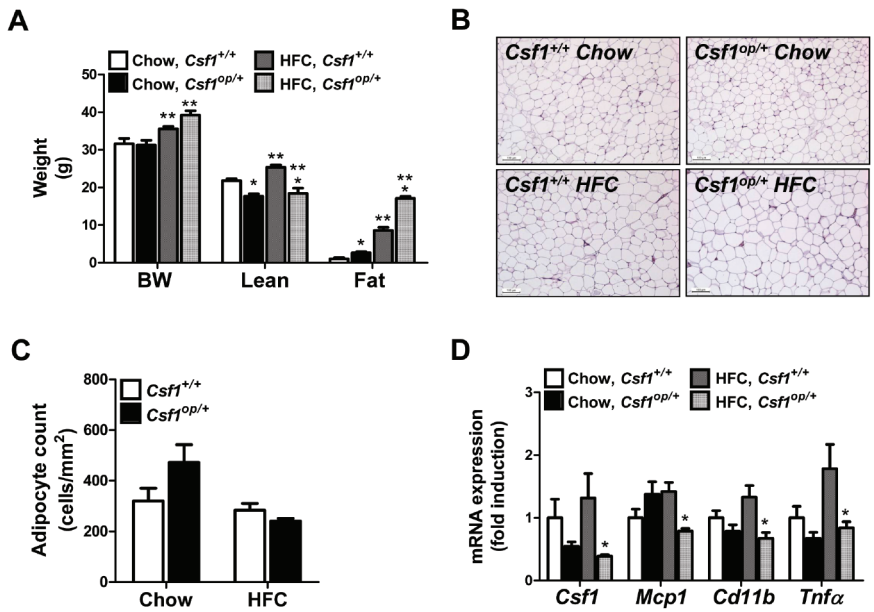

Figure 5. *Csf1*$^{op/+}$ *mice are not protected from diet-induced obesity. Body weight of Csf1*$^{+/+}$ *and Csf1*$^{op/+}$ *mice fed a standard chow or high-fat cholesterol (HFC) diet and dual energy x-ray absorptiometry (DEXA) scan analysis was performed to assess lean mass and fat mass (**A**); (□) = Csf1*$^{+/+}$ *mice on chow diet, (■) = Csf1*$^{op/+}$ *mice on chow diet, (■) = Csf1*$^{+/+}$ *mice on HFC diet and (■) = Csf1*$^{op/+}$ *mice on HFC diet. Representative pictures of the adipose tissue sections (**B**) and adipocyte counts (**C**); (□) = Csf1*$^{+/+}$ *mice and (■) = Csf1*$^{op/+}$ *mice. Real time-polymerase chain reaction (RT-PCR) analysis was performed to measure mRNA expression levels of inflammatory genes in the adipose tissue including colony stimulating factor (Csf-1), monocyte chemoattractant protein 1 (Mcp1), integrin, alpha M (Cd11b) and tumor necrosis factor α (Tnfα) (**D**); (□) = Csf1*$^{+/+}$ *mice on chow diet, (■) = Csf1*$^{op/+}$ *mice on chow diet, (■) = Csf1*$^{+/+}$ *mice on HFC diet and (■) = Csf1*$^{op/+}$ *mice on HFC diet. Data are expressed as mean ± SEM, n = 6 per group. * P < 0.05 versus Csf1*$^{+/+}$ *mice (Mann-Whitney U Test); ** P < 0.05 versus chow diet (two-way ANOVA test).*

Csf1$^{op/+}$ mice have a lower metabolic rate and reduced heat production.
To determine whether this altered body composition is associated with an aberrant metabolic rate, mice were analyzed using indirect calorimetry. Consistent with a lower lean body mass, oxygen consumption (VO_2; Fig. 6A) and carbon dioxide production (VCO_2; Fig. 6B) were greatly reduced in *Csf1$^{op/+}$* mice compared to *Csf1$^{+/+}$* mice. In addition, heat production (Fig. 6C) was decreased in *Csf1$^{op/+}$* mice compared to *Csf1$^{+/+}$* mice, whereas food intake (Fig. 6D) and activity (Fig. 6E) did not differ between the two genotypes on either diet. No differences in substrate use were found in *Csf1$^{op/+}$* mice when fed a chow diet (Supplemental Fig. 2A). However, the respiratory exchange ratio (RER) was markedly reduced in the dark phase following HFC feeding in *Csf1$^{op/+}$* mice (Fig. 6F), indicating that these mice oxidized more fatty acids than *Csf1$^{+/+}$* mice during this active period. Since *Csf1$^{op/+}$* mice have reduced lean body mass, we corrected VO_2 consumption, VCO_2 production, and heat production for lean mass. After this correction, there was no difference in VO_2 consumption (Supplemental Fig. 3A), VCO_2 production (Supplemental Fig. 3B), or heat production (Supplemental Fig. 3C). Taken together, our data indicate that *Csf1$^{op/+}$* mice have a lower metabolic rate and reduced heat production than *Csf1$^{+/+}$* mice, which corresponds to the reduced lean body mass observed in these mice.

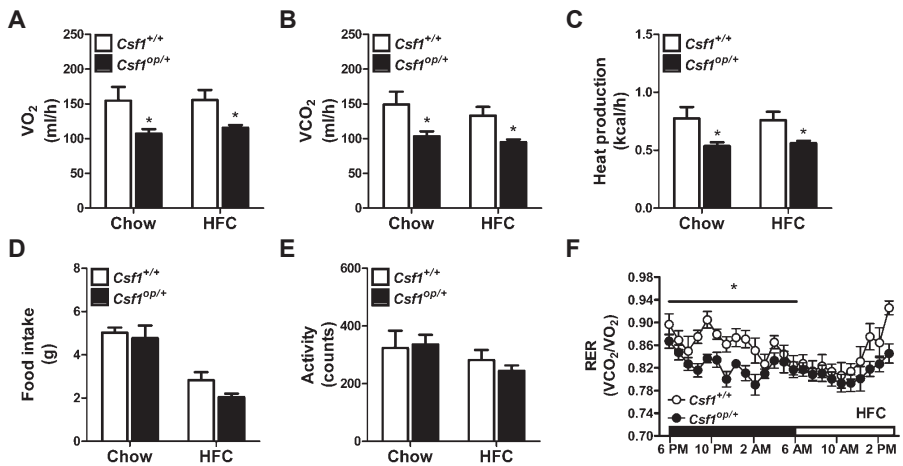

Figure 6. *Csf1$^{op/+}$ mice have a lower metabolic rate and reduced heat production. Indirect calorimetric cage analysis was performed to measure VO_2 consumption (**A**), VCO_2 production (**B**), heat production (**C**), food intake (**D**), total activity (**E**) in chow- and high-fat cholesterol (HFC)-fed Csf1$^{+/+}$ and Csf1$^{op/+}$ mice, and respiratory exchange ratio (RER) in Csf1$^{+/+}$ and Csf1$^{op/+}$ mice on a HFC diet (**F**). (□) = Csf1$^{+/+}$ mice and (■) = Csf1$^{op/+}$ mice. Data are expressed as mean ± SEM, n = 6 per group. * P < 0.05 versus Csf1$^{+/+}$ mice (unpaired Student's two-tailed t-test). A two-way ANOVA test was performed for RER and indicated the main effect for Csf1$^{op/+}$ mice.*

Csf-1 haploinsufficient mice are not protected from developing insulin resistance.
Work in the last few decades has shown that inflammatory pathways are involved in the mechanisms underlying the development of insulin resistance and type 2 diabetes

(3,4). As *Csf1*$^{op/+}$ mice exhibit lower levels of inflammation in the liver (Fig 1A, 1B) and adipose tissue (Fig. 5D), as well as a marked reduction in many inflammatory mediators in the circulation, including TNFα, IL1α, MIP1α, MIP1β and MCP1 (Fig. 7A, 7B), we hypothesized that *Csf1*$^{op/+}$ mice are protected from the development of insulin resistance. To this end, *Csf1*$^{+/+}$ and *Csf1*$^{op/+}$ mice were subjected to an oral glucose tolerance test following 10 weeks of chow and HFC feeding. Despite the lower inflammatory tone in *Csf1*$^{op/+}$ mice, whole-body glucose tolerance (Fig. 7C) and fasted insulin levels (Fig. 7E) were no different between the genotypes. However, fasted glucose levels were lower in HFC-fed *Csf1*$^{op/+}$ mice than controls (Fig. 7D), and may reflect the slight increase in plasma insulin levels seen in these mice ($p = 0.52$). Indeed, the calculated homeostasis model of assessment-insulin resistance (HOMA-IR) index, a marker of insulin resistance, revealed no differences between *Csf1*$^{+/+}$ and *Csf1*$^{op/+}$ mice on either diet (Fig. 7F). This confirms that *Csf1*$^{op/+}$ mice are not protected against the development of insulin resistance.

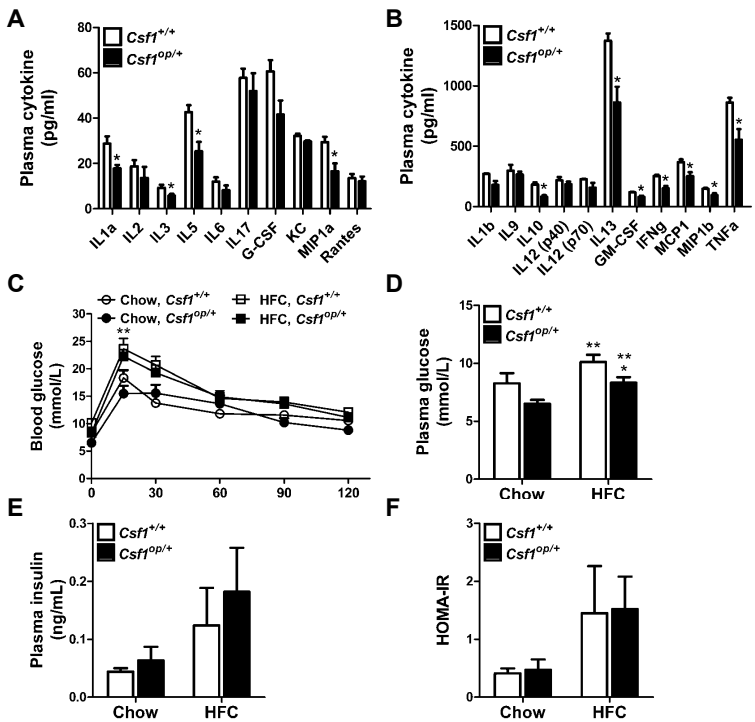

Fig. 7. Csf1 haploinsufficient mice are not protected from developing insulin resistance. Plasma cytokine levels in Csf1$^{+/+}$ *and Csf1*$^{op/+}$ *mice on a high-fat cholesterol (HFC) diet (**A, B**). Glucose tolerance test (**C**) was performed in Csf1*$^{+/+}$ *and Csf1*$^{op/+}$ *mice on chow or HFC diet following a 9-h fast. Plasma glucose (**D**) and insulin (**E**) were measured in Csf1*$^{+/+}$ *and Csf1*$^{op/+}$ *mice after an overnight fast. Homeostasis model of assessment-insulin resistance (HOMA-IR) as a surrogate marker of insulin resistance (**F**). (□) = Csf1*$^{+/+}$ *mice and (■) = Csf1*$^{op/+}$ *mice. Data are expressed as mean ± SEM, n = 6 per group. * P < 0.05 versus Csf1*$^{+/+}$ *mice (Mann-Whitney U Test); ** P < 0.05 versus chow diet (two-way ANOVA test).*

Discussion

As macrophages have been implicated in the development of metabolic disease, we aimed to gain more insight into the role of macrophages in these pathologies by studying the role of Csf1, a macrophage growth factor, in the development of hepatic steatosis and insulin resistance. Using mice heterozygous for a *Csf1* null allele, we demonstrated that Csf1 is important for the metabolic control of lipid metabolism in the liver. However, it does not offer protection against the development of insulin resistance in these mice.

Csf1 is an essential regulator of macrophage survival, proliferation and activation (11,12) and it has frequently been hypothesized but never experimentally addressed that macrophages via Csf1 regulation may contribute to the pathogenesis of obesity-related disorders. We show that Csf1 haploinsufficiency contributes to reduced hepatic, adipose tissue and systemic inflammation (Fig. 2A, 2B, 5D, 7A, 7B). This is in line with previous studies highlighting a therapeutic benefit for depletion of CSFs, including Csf1, in many inflammatory and/or autoimmune conditions in animal models (13). Our data also show that Csf1 haploinsufficiency results in reduced liver inflammation driven by Kupffer cells (Fig. 2D), thus allowing us to investigate the role of Csf1 in the development of hepatic steatosis. Here, we show that reduced hepatic inflammation in *Csf1*$^{op/+}$ mice is associated with increased hepatic triglyceride accumulation (Fig. 1). Of note, increased hepatic lipid accumulation in these mice was only apparent after an overnight fast and not in the fed state. As fasting increases hepatic TG accumulation in rodents (30), our data show that Csf1 haploinsufficiency contributes to increased fasting-induced hepatic steatosis. Our results, therefore, suggest that Csf1-induced macrophages are important for protection against the development of hepatic steatosis and unravel an unexpected, beneficial role of Csf1 in hepatic lipid homeostasis.

To better define the mechanisms that might underlie the increased fasting-induced steatosis in livers of *Csf1*$^{op/+}$ mice, we assessed the processes of *de novo* lipogenesis, VLDL-TG secretion, and β-oxidation in mice fed a chow diet and fasted overnight. We saw no difference in *de novo* lipogenesis between *Csf1*$^{+/+}$ and *Csf1*$^{op/+}$ mice (Fig. 4D). However, hepatic VLDL-TG synthesis and secretion (Fig. 4A, 4B) was markedly reduced in *Csf1*$^{op/+}$ mice. Since the hepatic steatosis was observed in the periportal region (Fig. 1D), and VLDL-TG synthesis has been shown to occur in periportal hepatocytes (31), a decline in the process of VLDL-TG synthesis and secretion (Fig. 4A, 4B), might explain the increase in fasting-induced steatosis observed in these mice. In line with the increased hepatic fatty acid oxidation in the metabolic response to fasting (28), we also show that mitochondrial β-oxidation is enhanced in *Csf1*$^{op/+}$ mice compared to *Csf1*$^{+/+}$ mice (Fig. 3A-C). However, it does not explain the hepatic steatosis observed in these mice. We therefore speculate that the increase in mitochondrial β-oxidation is likely a consequence of increased hepatic steatosis rather than a cause.

Macrophages play and important role in innate immunity and inflammation and are associated with the development of obesity-induced insulin resistance (5), our

observation that Csf1 haploinsufficiency increases fasting-induced hepatic steatosis may seem counterintuitive. However, it has been demonstrated that alternatively activated Kupffer cells protect hepatocytes from the development of inflammation and the subsequent steatosis associated with high-fat diet-induced obesity (27,32). In line with this, myeloid-specific deletion of peroxisome proliferator activator receptor δ (*Ppar*δ), which impairs alternative activation of Kupffer cells, contributes to increased lipid accumulation in the liver (26,27). In addition, co-culture of Kupffer cells and hepatocytes with lipopolysaccharides (LPS) to induce M1 polarization results in increased hepatocyte triglyceride accumulation (33). Furthermore, systemic loss of Il-10, a cytokine that drives macrophages to the M2 phenotype, results in hepatic triglyceride accumulation associated with obesity (32,34). In addition, it has recently been shown that fasting induces a response in liver that is associated with an increased number of Mac-2 positive crown-like structures, and involves an increase in M2-type macrophages (35). Since, Csf1-induced macrophages are associated with alternatively activated M2 properties (36), it is likely that the increased fasting-induced steatosis we observed may reflect the reduced ability of Csf1 to control metabolic pathways during fasting. Nevertheless, as Csf1 haploinsufficiency resulted in an overall reduction of M1 (pro-inflammatory) and M2 (ant-inflammatory) markers in the liver, we cannot confirm that a shift in M1/M2 balance is responsible for the observed aberrant lipid metabolism in *Csf1*$^{op/+}$ mice. Nor do our studies delineate which Kupffer cell-derived factors are important for this effect in the liver. However, previous data from co-culture studies with Kupffer cells and hepatocytes have shown that factors derived from Kupffer cells work in a trans-acting manner to maintain hepatic lipid homeostasis (33). In addition, Csf1-induced Kupffer cells play a key role in liver regeneration as a source of Il-6 in the liver after partial hepatectomy (37), this provides further support of an important role for Csf1 in the metabolic control of lipid homeostasis in the liver.

As macrophage activation in the liver and adipose tissue is linked to the development of obesity-induced insulin resistance, we also assessed the role of Csf1 in the development of insulin resistance (5). Although, Csf1 haploinsufficiency did not affect the level of obesity or diet-induced weight gain, DEXA scan analysis showed that adiposity was markedly increased in *Csf1*$^{op/+}$ mice, both on chow and when following a HFC diet for 10 weeks (Fig. 5A). Of note, Csf1 is upregulated in adipose tissue from humans gaining weight with overfeeding and has been shown to contribute to adipose tissue deposition in humans (17). This is in contrast to our finding that Csf1 haploinsufficiency triggers fat mass accumulation in the adipose tissue compartment. Although we cannot explain this discrepancy, another study also showed no effect of haploinsufficiency of Csf1 on diet-induced obesity in mice (20). In this study lean and fat mass were not assessed, nor its effect on the pathogenesis of obesity-associated diseases, like insulin resistance or NAFLD (20). Despite a marked increase in fat mass and a major reduction in systemic, adipose tissue and hepatic inflammation in *Csf1*$^{op/+}$ mice, insulin resistance developed similarly over time in both WT and *Csf1*$^{op/+}$ mice (Fig. 7C-F). Therefore, our results do not support a role for Csf1 in the pathology of insulin resistance in mice.

In summary, we have shown that Csf1 haploinsufficiency leads to reduced

Kupffer cell-driven inflammation and increased fasting-induced hepatic steatosis, although it does not appear to protect from the development of insulin resistance. Our results therefore suggest that Csf1-induced macrophages are important for protection against the development of hepatic steatosis, but do not affect the etiology of insulin resistance. We have shown that Csf1 has a beneficial role in lipid metabolism, suggesting that caution should be exercised with using CSF-blockade or neutralization agents in the treatment of inflammatory diseases, since they may lead to harmful side-effects in the liver.

References

1. Berrington de Gonzalez A, Hartge P, Cerhan JR, Flint AJ, Hannan L, MacInnis RJ, et al. Body-mass index and mortality among 1.46 million white adults. N Engl J Med 2010;363:2211-2219.
2. Flegal KM, Graubard BI, Williamson DF, Gail MH. Cause-specific excess deaths associated with underweight, overweight, and obesity. JAMA 2007;298:2028-2037.
3. Hotamisligil GS, Shargill NS, Spiegelman BM. Adipose expression of tumor necrosis factor-alpha: direct role in obesity-linked insulin resistance. Science 1993;259:87-91.
4. Feinstein R, Kanety H, Papa MZ, Lunenfeld B, Karasik A. Tumor necrosis factor-alpha suppresses insulin-induced tyrosine phosphorylation of insulin receptor and its substrates. J Biol Chem 1993;268:26055-26058.
5. Qatanani M, Lazar MA. Mechanisms of obesity-associated insulin resistance: many choices on the menu. Genes Dev 2007;21:1443-1455.
6. Bhargava P, Lee CH. Role and function of macrophages in the metabolic syndrome. Biochem J 2012;442:253-262.
7. Cai D, Yuan M, Frantz DF, Melendez PA, Hansen L, Lee J, et al. Local and systemic insulin resistance resulting from hepatic activation of IKK-beta and NF-kappaB. Nat Med 2005;11:183-190.
8. Tilg H, Moschen AR. Insulin resistance, inflammation, and non-alcoholic fatty liver disease. Trends Endocrinol Metab 2008;19:371-379.
9. Ferrante AW, Jr. Obesity-induced inflammation: a metabolic dialogue in the language of inflammation. J Intern Med 2007;262:408-414.
10. Stanley ER, Cifone M, Heard PM, Defendi V. Factors regulating macrophage production and growth: identity of colony-stimulating factor and macrophage growth factor. J Exp Med 1976;143:631-647.
11. Pixley FJ, Stanley ER. CSF-1 regulation of the wandering macrophage: complexity in action. Trends Cell Biol 2004;14:628-638.
12. Chitu V, Stanley ER. Colony-stimulating factor-1 in immunity and inflammation. Curr Opin Immunol 2006;18:39-48.
13. Hamilton JA. Colony-stimulating factors in inflammation and autoimmunity. Nat Rev Immunol 2008;8:533-544.
14. Naito M, Hasegawa G, Takahashi K. Development, differentiation, and maturation of Kupffer cells. Microsc Res Tech 1997;39:350-364.
15. Yamamoto T, Naito M, Moriyama H, Umezu H, Matsuo H, Kiwada H, et al. Repopulation of murine Kupffer cells after intravenous administration of liposome-encapsulated dichloromethylene diphosphonate. Am J Pathol 1996;149:1271-1286.
16. Hume DA, Macdonald KP. Therapeutic applications of macrophage colony-stimulating factor-1 (CSF-1) and antagonists of CSF-1 receptor (CSF-1R) signaling. Blood 2012;119:1810-1820.
17. Levine JA, Jensen MD, Eberhardt NL, O'Brien T. Adipocyte macrophage colony-stimulating factor is a mediator of adipose tissue growth. J Clin Invest 1998;101:1557-1564.
18. Rajavashisth T, Qiao JH, Tripathi S, Tripathi J, Mishra N, Hua M, et al. Heterozygous osteopetrotic (op) mutation reduces atherosclerosis in LDL receptor- deficient mice. J Clin Invest 1998;101:2702-2710.
19. Kodama H, Nose M, Niida S, Yamasaki A. Essential role of macrophage colony-stimulating factor in the osteoclast differentiation supported by stromal cells. J Exp Med 1991;173:1291-1294.
20. Sugita S, Kamei Y, Oka J, Suganami T, Ogawa Y. Macrophage-colony stimulating factor in obese adipose tissue: studies with heterozygous op/+ mice. Obesity (Silver Spring) 2007;15:1988-1995.

21. Taura K, De Minicis S, Seki E, Hatano E, Iwaisako K, Osterreicher CH, et al. Hepatic stellate cells secrete angiopoietin 1 that induces angiogenesis in liver fibrosis. Gastroenterology 2008;135:1729-1738.
22. Bligh EG, Dyer WJ. A rapid method of total lipid extraction and purification. Can J Biochem Physiol 1959;37:911-917.
23. Gautier T, Tietge UJ, Boverhof R, Perton FG, Le Guern N, Masson D, et al. Hepatic lipid accumulation in apolipoprotein C-I-deficient mice is potentiated by cholesteryl ester transfer protein. J Lipid Res 2007;48:30-40.
24. Oosterveer MH, van Dijk TH, Tietge UJ, Boer T, Havinga R, Stellaard F, et al. High fat feeding induces hepatic fatty acid elongation in mice. PLoS One 2009;4:e6066.
25. Wynn TA, Chawla A, Pollard JW. Macrophage biology in development, homeostasis and disease. Nature 2013;496:445-455.
26. Kang K, Reilly SM, Karabacak V, Gangl MR, Fitzgerald K, Hatano B, et al. Adipocyte-derived Th2 cytokines and myeloid PPARdelta regulate macrophage polarization and insulin sensitivity. Cell Metab 2008;7:485-495.
27. Odegaard JI, Ricardo-Gonzalez RR, Red EA, Vats D, Morel CR, Goforth MH, et al. Alternative M2 activation of Kupffer cells by PPARdelta ameliorates obesity-induced insulin resistance. Cell Metab 2008;7:496-507.
28. Kersten S, Seydoux J, Peters JM, Gonzalez FJ, Desvergne B, Wahli W. Peroxisome proliferator-activated receptor alpha mediates the adaptive response to fasting. J Clin Invest 1999;103:1489-1498.
29. Weisberg SP, McCann D, Desai M, Rosenbaum M, Leibel RL, Ferrante AW, Jr. Obesity is associated with macrophage accumulation in adipose tissue. J Clin Invest 2003;112:1796-1808.
30. Hashimoto T, Cook WS, Qi C, Yeldandi AV, Reddy JK, Rao MS. Defect in peroxisome proliferator-activated receptor alpha-inducible fatty acid oxidation determines the severity of hepatic steatosis in response to fasting. J Biol Chem 2000;275:28918-28928.
31. Aspichueta P, Perez S, Ochoa B, Fresnedo O. Endotoxin promotes preferential periportal upregulation of VLDL secretion in the rat liver. J Lipid Res 2005;46:1017-1026.
32. Clementi AH, Gaudy AM, van Rooijen N, Pierce RH, Mooney RA. Loss of Kupffer cells in diet-induced obesity is associated with increased hepatic steatosis, STAT3 signaling, and further decreases in insulin signaling. Biochim Biophys Acta 2009;1792:1062-1072.
33. Huang W, Metlakunta A, Dedousis N, Zhang P, Sipula I, Dube JJ, et al. Depletion of liver Kupffer cells prevents the development of diet-induced hepatic steatosis and insulin resistance. Diabetes 2010;59:347-357.
34. den Boer MA, Voshol PJ, Schroder-van der Elst JP, Korsheninnikova E, Ouwens DM, Kuipers F, et al. Endogenous interleukin-10 protects against hepatic steatosis but does not improve insulin sensitivity during high-fat feeding in mice. Endocrinology 2006;147:4553-4558.
35. Asterholm IW, McDonald J, Blanchard PG, Sinha M, Xiao Q, Mistry J, et al. Lack of “immunological fitness” during fasting in metabolically challenged animals. J Lipid Res 2012;53:1254-1267.
36. Brocheriou I, Maouche S, Durand H, Braunersreuther V, Le Naour G, Gratchev A, et al. Antagonistic regulation of macrophage phenotype by M-CSF and GM-CSF: implication in atherosclerosis. Atherosclerosis 2011;214:316-324.
37. Amemiya H, Kono H, Fujii H. Liver regeneration is impaired in macrophage colony stimulating factor deficient mice after partial hepatectomy: the role of M-CSF-induced macrophages. J Surg Res 2011;165:59-67.

Supplemental Information

Materials and methods

Oral Glucose Tolerance Test. Chow- and HFC-fed *Csf1*$^{+/+}$ and *Csf1*$^{op/+}$ mice were fasted overnight for 9 h and a glucose bolus (2g/kg body weight) was given by oral gavage. Glucose levels were detected in blood collected from the tail tip prior to and at 15, 30, 60, 90 and 120 minutes after the gavage using an OneTouch Ultra glucometer (Lifescan Benelux, Beerse, Belgium).

Metabolic analysis in vivo. Mice were placed individually in indirect calorimetric cages (LabMaster TSE systems, Bad Homburg, Germany). Following an initial 24-h acclimatization period, mice were monitored every 13 min for 24 h for 3 consecutive days.

Analysis of plasma parameters. Plasma β-hydroxybutyrate levels were determined using a commercially available kit (Diasys Diagnostic Systems GmbH, Holzheim, Germany). Insulin was determined in plasma from overnight fasted mice using an enzyme-linked immunosorbent assay kit (Insulin (mouse) Ultrasensitive EIA, Alpco Diagnostics, Salem, NH, USA). Free fatty acids (FFA), triglycerides (TG), total cholesterol (TC), alanine aminotransferase (ALT) and aspartate aminotransferase (AST) were determined by commercially available kits, according to the manufacturer's instructions (FFA: NEFA-HR, Wako Chemicals GmbH, Neuss, Germany; TG: Hitachi, Roche, the Netherlands; TC: cholesterol CHOD-PAP, Roche, the Netherlands; ALT and AST: Spinreact, Santa Coloma, Spain).

Tissue Preparation and Histology. Mice were euthanized and the livers were excised. Frozen-cut liver sections (5 µm) were fixated in liquid nitrogen and stained with Cd68 antibody (Abcam, Cambridge, UK) to reveal activated macrophages. Photographs were taken with a LEICA camera mounted on a LEICA DM3000 microscope.

Real-Time Quantitative RT-PCR. Total RNA was isolated from the liver with QIAzol Lysis reagent (QIAGEN, Venlo, the Netherlands) according to the manufacturer's instructions and homogenised. Total RNA (1 µg) from each individual mouse was converted into cDNA with Quantitect Reverse Transcription kit (QIAGEN, Venlo, the Netherlands) according to the manufacturer's instructions. Quantification of gene expression was done by quantitative PCR on a Taqman (7900HT, Applied Biosystems, Warrington, UK) with SDS software (Applied Biosystems) by using SYBR Green Master Mix (Bio-Rad Laboratories B.V., Veenendaal, the Netherlands). The results were normalized to Cyclophillin A (*Ppia*) mRNA levels. The primers which are used are listed in Supplemental Table 1.

VLDL composition. VLDL-TG and cholesterol contents were determined as described (23). Phospholipid content was determined using a commercial kit (Diasys Diagnostic Systems GmbH, Holzheim, Germany).

Supplemental Table 1. *Primer sequences used for RT-PCR.*

Gene	Forward primer 5'-3'	Reverse primer 5'-3'
Csf1	AGTGGAGGAGCCATCGAGAC	GGCAGTTCCACCTGTCTGTC
Cd68	TGACCTGCTCTCTCTAAGGCTACA	TCACGGTTGCAAGAGAAACATG
Mcp1	GCTGGAGAGCTACAAGAGGATCA	ACAGACCTCTCTCTTGAGCTTGGT
Cd11b	TCAGAGAATGTCCTCAGCAG	TGAGACAAACTCCTTCATCTTC
Tnfα	CATCTTCTCAAAATTCGAGTGACAA	TGGGAGTAGACAAGGTACAACCC
Il-1β	TGCAGCTGGAGAGTGTGG	TGCTTGTGAGGTGCTGATG
Il-6	GCTACCAAACTGGATATATAATCAGGAAA	CTTGTTATCTTTTAAGTTGTTCTTCATGTACTG
Fizz1	TCCCAGTGAATACTGATGAGA	CCACTCTGGATCTCCCAAGA
Ym1	AGAAGGGAGTTTCAAACCTGGT	GTCTTGCTCATGTGTGTAAGTGA
ApoA1	CCCAGTCCCAATGGGACA	CAGGAGATTCAGGTTCAGCTGTT
Ppia	TTCCTCCTTTCACAGAATTATTCCA	CCGCCAGTGCCATTATGG

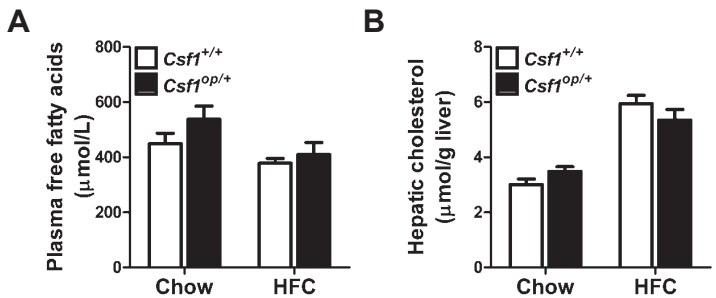

Supplemental Figure 1. *No differences in plasma FFA and hepatic cholesterol levels between Csf1$^{+/+}$ and Csf1$^{op/+}$ mice. Plasma free fatty acids (**A**) and hepatic cholesterol (**B**) levels were determined biochemically in chow- and high-fat cholesterol (HFC)-fed Csf1$^{+/+}$ and Csf1$^{op/+}$ mice. (□) = Csf1$^{+/+}$ mice and (■) = Csf1$^{op/+}$ mice. Data are expressed as mean ± SEM, n = 6 per group. * P < 0.05 versus Csf1$^{+/+}$ mice (Mann-Whitney U Test).*

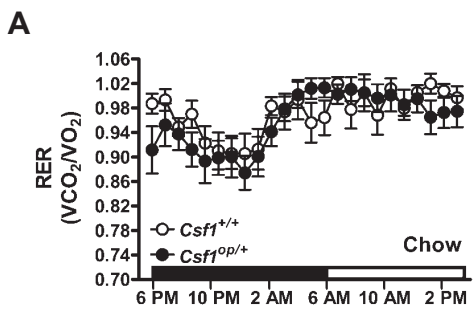

Supplemental Figure 2. *No differences in RER between chow-fed Csf1$^{+/+}$ and Csf1$^{op/+}$ mice. Indirect calorimetric cage analysis was performed to measure respiratory exchange ratio (RER) in chow-fed Csf1$^{+/+}$ and Csf1$^{op/+}$ mice (**A**). (□) = Csf1$^{+/+}$ mice and (■) = Csf1$^{op/+}$ mice. Data are expressed as mean ± SEM, n = 6 per group. * P < 0.05 versus Csf1$^{+/+}$ mice (Mann-Whitney U Test).*

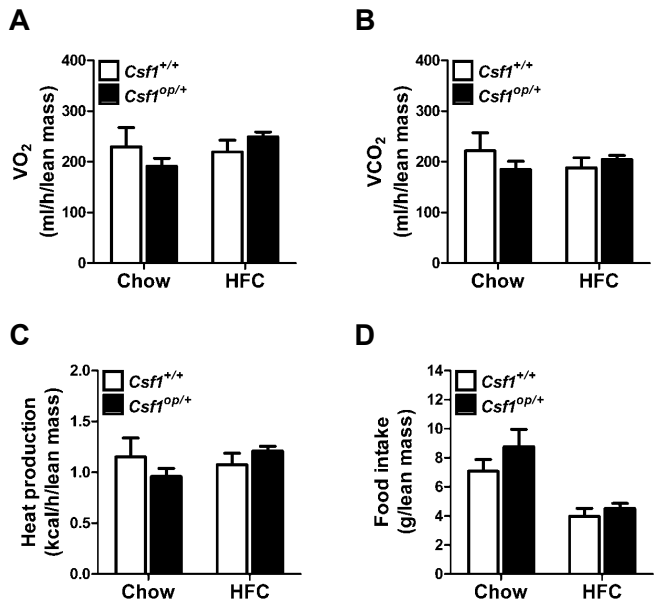

Supplemental Figure 3. *No difference in metabolic rate between Csf1$^{+/+}$ and Csf1$^{op/+}$ mice after correction for lean mass. Indirect calorimetric cage analysis was performed to measure VO_2 consumption (**A**), VCO_2 production (**B**), heat production (**C**), and food intake (**D**) after correction for lean mass in chow- and high-fat cholesterol (HFC)-fed Csf1$^{+/+}$ and Csf1$^{op/+}$ mice. (□) = Csf1$^{+/+}$ mice and (■) = Csf1$^{op/+}$ mice. Data are expressed as mean ± SEM, n = 6 per group. * P < 0.05 versus Csf1$^{+/+}$ mice (Mann-Whitney U Test).*

Chapter 5

The iminosugar AMP-DNM protects against hepatic steatosis and promotes whole-body fat oxiation in methionine and choline-deficient-pair fed mice

Anouk Funke, Tanit Lizama, Marijke Schreurs, Marcela Aparicio-Vergara, Niels J. Kloosterhuis, Elisa Lombardo, Florence Bietrix, Johannes M.F.G. Aerts, Marten H. Hofker, Albert K. Groen, Marco van Eijk, Debby P.Y. Koonen

Submitted

Abstract

Background Ceramide and derived glycosphingolipids have been implicated in the pathogenesis of obesity-induced insulin resistance. Pharmacological lowering of glycosphingolipid metabolism by the iminosugar AMP-DNM has shown promising results in improving glucose homeostasis and correcting hepatic steatosis in mice. However, AMP-DNM is associated with enhanced fat oxidation and a simultaneous reduction in food intake, which in theory could explain the lipid-lowering effects of AMP-DNM. As this has never been experimentally addressed, this study aims to unravel on the short-term effects of AMP-DNM on lipid metabolism and food intake in *ad libitum*- and pair-fed mice.

Methods We used C57BL/6J mice fed a methionine and choline-deficient (MCD) diet to induce hepatic steatosis. Mice were *ad libitum*-fed for 4 days with chow, MCD and MCD diet supplemented with 100 mg/kg/day AMP-DNM and subjected to metabolic cage analysis. In addition, to investigate the effect of AMP-DNM treatment on fat oxidation in the absence of differences in food intake, MCD-fed mice were pair-fed with AMP-DNM treated MCD-fed mice. Energy metabolism *in vivo* was assessed by indirect calorimetry, and by immunoblot analysis of AMPK and ACC and RT-PCR. Biochemical parameters in plasma and liver were measured.

Results AMP-DNM treatment inhibits glucosylceramide synthase, reduces food intake, increases whole-body fatty acid oxidation and diminishes hepatic lipid accumulation in *ad libitum*-MCD-fed mice. Moreover, using a pair-fed feeding strategy, we confirm that AMP-DNM promotes whole-body and hepatic fat oxidation in MCD-fed mice, which is not related to the appetite suppressor effect of AMP-DNM on fat oxidation.

Conclusion These data show that AMP-DNM has a direct effect on whole-body and hepatic fat oxidation unrelated to AMP-DNM's inhibitory effect on food intake, supporting the reported value of AMP-DNM as a therapeutic target for obesity-associated metabolic disease.

Introduction

Despite an increased understanding of the importance of a healthy lifestyle, obesity and its related disorders, such as insulin resistance, non-alcoholic fatty liver disease (NAFLD) and type 2 diabetes (T2D) continue to rise (1). As current preventative and pharmacological therapeutic approaches have had limited success so far, it is evident that new strategies for treating these diseases are urgently needed.

Ceramides and its glycosphingolipid metabolites have been implicated in the pathogenesis of obesity-induced insulin resistance (2,3). Consistent with this, pharmacological lowering of glycosphingolipid metabolism by the iminosugar *N*-(5'-adamantane-1'-yl-methoxy)-pentyl-1-deoxynojirimycin (AMP-DNM) significantly improves glucose homeostasis and insulin signaling in rodent models of insulin resistance and T2D (4–6). In addition, AMP-DNM has been shown to restore hepatic insulin sensitivity and reverse hepatic steatosis as well as improve adipocyte function, and attenuate metabolic inflammation in both adipose tissue and liver in different mouse models (5–8). Although, these data suggest that AMP-DNM may hold great promise as novel therapeutic target in metabolic disease, it has been suggested that some of the metabolic effects of AMP-DNM are not directly related to glucosylceramide (GlcCer) synthase inhibition (8,9). Indeed, lowering of glycosphingolipids by genetic knockdown of GlcCer synthase in hepatocytes does not reduce liver triglycerides in mice exposed to a high-fat diet (9). In addition, AMP-DNM treatment has been demonstrated to lower lipid accumulation by promoting fat oxidation in the liver (7), thus providing an alternative mechanism for the lipid-lowering effect of AMP-DNM treatment on lipid homeostasis in the liver.

AMP-DNM treatment is also associated with reduced food intake and significant weight loss in mice (7,8,10). This suggests that AMP-DNM, in addition to GlcCer synthase inhibition, may also acts like a calorie restriction mimetic. Indeed, calorie restriction has been demonstrated to enhance fat oxidation, improve hepatic and systemic insulin sensitivity, and decrease the incidence of diabetes and atherosclerosis (11–13). Of note, AMP-DNM therapy leads to responses that overlap with these effects of calorie restriction mentioned above (4–8,14). Therefore, it is likely that AMP-DNM may mediate part of its effects on lipid metabolism through fasting-induced stimulation of fat oxidation initiated by suppression of appetite.

To unravel the short-term effects of AMP-DNM treatment on lipid metabolism and to identify if AMP-DNM may act like a calorie restriction mimetic, we made use of a methionine and choline-deficient (MCD) diet previously shown to induce hepatic steatosis in C57BL/6J mice (15). Our study shows that inhibition of GlcCer synthase in MCD-fed mice results in reduced food intake, increased whole-body fat oxidation and protection against hepatic steatosis. Using a pair-fed feeding strategy, we also confirm that AMP-DNM treatment promotes whole-body fat oxidation, and that this is unrelated to the appetite suppressor effect of AMP-DNM on fat oxidation. Collectively, our data suggest that the iminosugar AMP-DNM directly targets whole-body fat oxidation in mice, supporting the beneficial use of AMP-DNM as therapeutic strategy to alleviate obesity-associated metabolic disease.

Materials and Methods

Mice. All procedures were performed with approval of the University of Groningen Ethics Committee for Animal Experiments, which adheres to the principles and guidelines established by the European Convention for the Protection of Laboratory Animals. Experiments were carried out on male C57Bl/6J mice (Charles River, JAX laboratories, France), individually housed in a temperature-controlled room under a 12 h light-dark cycle with *ad libitum* access to water and food, unless stated otherwise. Animals were fed a chow diet (RMH-B; Hope Farms, Woerden, NL) or a methionine-choline deficient diet (MCD; ICN Biomedicals, Illkirch Cedex, France) supplemented with or without 100 mg AMP-DNM/kg body weight per day for 4 days. A run-in period of 2 days with chow+AMP-DNM was used to let the mice adjust to the compound.

In the pair-fed feeding study, the animals were fed the same amount of MCD diet as consumed by the AMP-DNM-treated MCD-fed animals. This was divided into two meals and given at 8:00 AM and 6:00 PM to avoid long durations of fasting.

Iminosugar. AMP-DNM was synthesized as described previously (16).

Metabolic analysis in vivo. Mice were placed individually in indirect calorimetric cages (LabMaster TSE systems, Bad Homburg, Germany). Following an initial 24-h acclimatization period, mice were monitored every 13 min for 24 h for 3 consecutive days. The respiratory exchange ratio (RER = VCO_2/VO_2) was used to estimate the percent contribution of fat and carbohydrates to whole-body energy metabolism in mice *in vivo*.
Fat oxidation rates were calculated by the equation 1,695 * (VO_2) – 1,701 * (VCO_2) according to Perronnet and Massicote (17).

Analysis of plasma parameters. Free fatty acids (FFA), triglycerides (TG), and total cholesterol (TC) were determined by commercially available kits, according to the manufacturer's instructions (FFA: NEFA-HR, Wako Chemicals GmbH, Neuss, Germany; TG: Hitachi, Roche, Woerden, the Netherlands; TC: cholesterol CHOD-PAP, Roche, Woerden, the Netherlands).

Liver lipids. Total liver lipids were extracted from the liver according to Bligh and Dyer (18). Hepatic free and total cholesterol (respectively FC and TC) and triglycerides (TG) were quantified using commercially available kits (FC: DiaSys Diagnostic Systems GmbH, Holzheim, Germany; Cholesterol CHOD-PAP, Roche, Woerden, the Netherlands and Triglycerides Hitachi, Roche, Woerden, the Netherlands), respectively. Ceramide and glucosylceramide (GlcCer) were determined in plasma and liver samples after lipid extraction according to Folch (19) by high-performance liquid chromatography analysis of orthophtaldehyde-conjugated lipids as described (4).

Real-Time Quantitative RT-PCR. Total RNA was isolated from the liver with QIAzol reagent (QIAGEN, Venlo, the Netherlands) according to the manufacturer's

instructions. Total RNA (1 µg) from each individual mouse was converted into cDNA with Quantitect Reverse Transcription kit (QIAGEN, Venlo, the Netherlands) according to manufacturer's instructions. Real time PCR (RT-PCR) was performed using a 7900HT system (Applied Biosystems, Warrington, UK) by using Power SYBR Green Master Mix (Biorad, Veenendaal, the Netherlands). For each gene, a standard curve was generated with a serial dilution of a liver cDNA pool. Values were corrected using the housekeeping gene Cyclophillin A (*Ppia*). Primer sequences of *Pdk4*: forward TTGACTCCCACATTGGTTGA and reverse TCATGTGCACAAACTCAGAGC.

Immunoblot analysis. Livers were rapidly removed and frozen with liquid nitrogen. Powdered tissue was lysed by homogenization in buffer (150 mM NaCL, 50 mM Tris-HCl (pH 7.5), 5 mM EDTA, 30 mM pyrophosphate, 50 mM NaF supplemented with protease (Complete, Roche Molecular Biochemicals, Almere, the Netherlands) and phosphatase inhibitor cocktails (Sigma, Zwijndrecht, the Netherlands), 1% Triton X-100 and 100 mM PMSF). Equal amounts of protein were separated by SDS-PAGE and transferred to nitrocellulose (Bio-Rad, Veenendaal, the Netherlands). Antibodies against phospho and total AMP kinase (AMPK), phospho and total acetyl CoA carboxylase (ACC) and tubulin were purchased from Cell Signaling (Leiden, the Netherlands). The immune-complex was visualized using the molecular imager ChemiDoc xrs+ system (Bio-Rad, Veenendaal, the Netherlands). The densitometric analysis of bands was done with Image Lab software (Bio-Rad, Veenendaal, the Netherlands).

Statistical analysis. Data are expressed as means ± SEM. Data were statistically analyzed by performing a non-parametric Mann-Whitney test using GraphPad Prism to compare experimental groups (version 5.00 for Windows, GraphPad Software, San Diego, CA, USA). The level of significance was set at $P<0.05$.

Results

AMP-DNM protects against hepatic steatosis in MCD-fed mice.

To investigate the short-term effects of AMP-DNM on lipid metabolism in the liver, C57BL/6J mice were fed *ad libitum* with chow, MCD or MCD diet supplemented with AMP-DNM (100 mg/kg body weight/day) for 4 days. As expected, hepatic steatosis was observed in MCD-fed mice when compared to chow-fed mice, and this was prevented by AMP-DNM treatment in MCD-fed mice (Fig. 1A). In addition, plasma triglycerides (Fig. 1B) and cholesterol levels (Fig. 1C) were significantly reduced in MCD-fed mice compared to chow-fed mice. AMP-DNM therapy resulted in a further decrease in plasma triglycerides (Fig. 1B) and cholesterol (Fig. 1C) levels compared to MCD-fed control mice. No differences were observed in plasma free fatty acids (FFA; Fig. S1A), hepatic free (Fig. S1B) and total cholesterol levels (Fig. S1C) between the groups. Moreover, no differences were observed in plasma ceramide (Fig. 1D) and glucosylceramide (Fig. 1E) levels between chow- and MCD-fed mice. In line with AMP-DNM treatment in *Ldlr*$^{-/-}$ and APOE*3 Leiden mice on a high cholesterol diet (8,14), plasma ceramide (Fig. 1D) and glucosylceramide (Fig. 1E) levels were significantly reduced in AMP-DNM treated MCD-fed mice compared to MCD-fed control mice. Hepatic ceramide levels were not changed between the groups (Table 1) and liver glucosylceramide levels were not different between chow- and MCD-fed mice and between AMP-DNM treated MCD- and MCD-fed mice (Table 1). Taken together these data indicate that AMP-DNM treatment reduces plasma lipids and improves hepatic steatosis in *ad libitum*-MCD-fed mice.

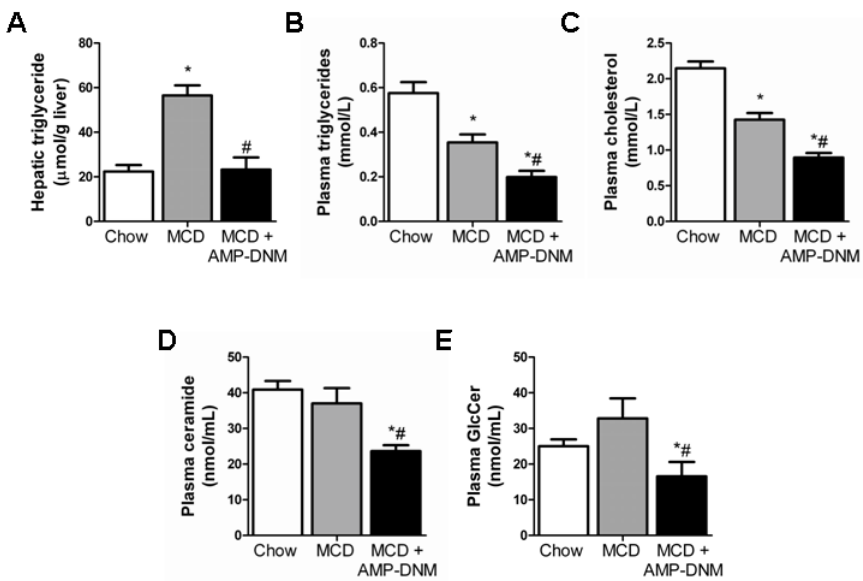

Figure 1. *AMP-DNM protects against hepatic steatosis in MCD-fed mice. C57BL/6J mice were ad libitum fed a chow, MCD or MCD diet supplemented with 100 mg/kg/day AMP-DNM for 4 days. Hepatic triglyceride content (**A**) was determined. Plasma concentrations of triglycerides (**B**) and cholesterol (**C**) were quantified biochemically. Plasma ceramide (**D**) and glucosylceramide (Glccer) (**E**) were assessed. Data are expressed as means ± SEM, n = 12-14 mice in each group. * P<0.05 versus chow diet; # versus MCD diet.*

Table 1. *Liver glycosphingolipid levels in ad libitum-fed mice.*

	Chow	MCD	MCD+AMP-DNM
GlcCer (nmol/g liver)	29.3 ± 2.5	48.1 ± 6.8	79.7 ± 11.2*
Ceramide (nmol/g liver)	306.6 ± 5.5	315.0 ± 13.8	336.3 ± 14.2

Liver glucosylceramide (GlcCer) and ceramide levels in ad libitum-fed C57BL/6J mice with a chow diet, MCD diet or MCD diet supplemented with 100 mg/kg/day of AMP-DNM for 4 days.

AMP-DNM reduces food intake and enhances whole-body fat oxidation in MCD-fed mice.

We next determined the effect of AMP-DNM on food intake and body weight in *ad libitum*-fed mice. Caloric intake was not different between chow- and MCD-fed mice, however, was significantly decreased in AMP-DNM treated MCD-fed mice compared to MCD-fed mice (Fig. 2A). Body weight was significantly lower in MCD-fed mice compared to chow-fed mice (Fig. 2B); however, AMP-DNM treated MCD-fed mice did not lose more weight than MCD-fed control mice (Fig. 2B). Next, we used indirect calorimetry to assess the effect of AMP-DNM treatment on whole body energy metabolism in these mice. No differences in VO_2 consumption (Fig. 2C), VCO_2 production (Fig. 2C), heat production (Fig. 2D), activity (Fig. 2E), and respiratory exchange ratio (RER; Fig. 2F) were observed between chow- and MCD-fed mice. Although, AMP-DNM treatment did not alter VO_2 consumption in MCD-fed mice, VCO_2 production was significantly reduced in AMP-DNM treated MCD-fed mice compared to MCD-fed controls (Fig. 2C). This was not accompanied by a significant reduction in heat production in (Fig. 2D), however, activity levels (Fig. 2E) were markedly lower throughout the dark, active phase in AMP-DNM treated MCD-fed mice compared to MCD-fed mice. In addition, exposure to AMP-DNM led to consistent lower RER values throughout the entire dark phase in MCD-fed mice (Fig. 2F, p=0.004), indicating a relative shift in substrate use from carbohydrate to fat oxidation in AMP-DNM treated MCD-fed mice. Indeed, calculation of the fat and carbohydrate oxidation rates in these mice (7) confirmed an increased contribution of fat oxidation to total fuel oxidation in AMP-DNM treated MCD-fed mice compared to MCD-fed control mice (Fig. 2G).

AMP-DNM has a direct effect on fat oxidation unrelated to food intake.

To investigate whether the effect of AMP-DNM treatment on fat oxidation in MCD-fed mice is a result of reduced food intake, MCD-fed mice were pair-fed with AMP-DNM treated MCD-fed mice. For this, MCD-fed mice were calorie restricted to a level of 55% of their normal food intake. As expected from pair-fed feeding, food intake (Fig. 3A) was not different between MCD- and AMP-DNM treated MCD-fed mice. In addition, body weight did not differ between both groups (Fig. 3B). Consistent with the observed effects of AMP-DNM treatment in *ad libitum*-fed mice (Fig. 2), VO_2 consumption (Fig. 3C) was unaltered between both groups of mice, and VCO_2 production (Fig. 3D) was significantly reduced in the light phase in AMP-DNM treated MCD-fed mice compared to MCD-fed controls. Moreover, heat production and activity levels were not different between pair-fed mice (data not shown). Of note, calorie restriction in MCD-fed mice resulted in a significant drop in RER levels (Fig. 3E) in the dark phase to ~0.73, indicative of a fasting-induced increase in fat oxidation. This

was not observed in AMP-DNM treated MCD-fed mice as AMP-DNM treated MCD-fed mice maintained an RER of ~0.86-0.9 throughout the entire day (Fig. 3E). This may indicate that AMP-DNM treated mice are not energy-compromised, suggesting that AMP-DNM might exert a direct effect on fat oxidation unrelated to food intake.

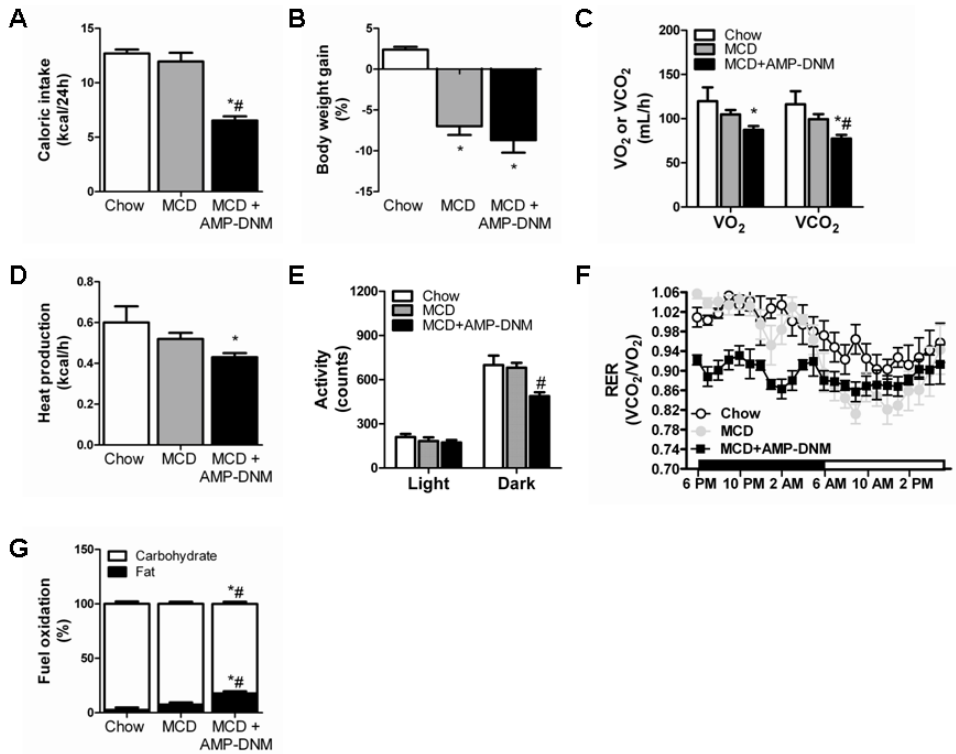

Figure 2. *AMP-DNM reduces food intake and enhances whole-body fat oxidation in MCD-fed mice. Food intake (**A**) and body weight (**B**) were measured. Indirect calorimetry was performed to measure VO_2 consumption or VCO_2 production (**C**), heat production (**D**), total activity (**E**), respiratory exchange ratio (RER) (**F**) and fuel oxidation (**G**) in C57BL/6J mice fed ad libitum with chow, MCD or MCD diet supplemented with 100 mg/kg/day AMP-DNM for 4 days. Data are expressed as means ± SEM, n = 5 mice in each group. * P<0.05 versus chow diet; # P<0.05 versus MCD diet.*

AMP-DNM leads to increased hepatic steatosis in pair-fed mice.

We next investigated the effect of AMP-DNM treatment on lipid metabolism in pair-fed mice. Plasma free fatty acids (FFA) were increased in AMP-DNM treated MCD-fed mice compared to MCD-fed control mice (Fig. 4A). Whereas AMP-DNM treated MCD-fed mice showed a reduction in plasma cholesterol levels compared to MCD-fed mice (Fig. 4B), plasma triglyceride levels were not different between the groups (Fig. 4C). However, hepatic fat accumulation was elevated in the AMP-DNM treated MCD-fed mice compared to MCD-fed mice (Fig. 4D). In addition, plasma ceramide levels were not changed between MCD- and AMP-DNM treated MCD-fed mice (Fig. 4E). As expected, plasma glucosylceramide levels were reduced in AMP-DNM treated MCD-fed mice compared to MCD control mice (Fig. 4F), whereas

liver ceramide and glucosylceramide levels were not altered between both groups of mice (Table 2).

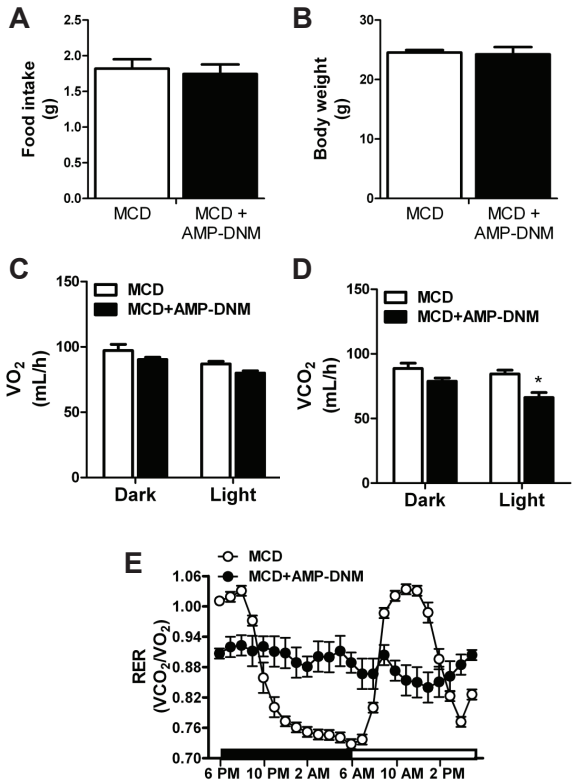

Figure 3. *AMP-DNM has a direct effect on whole-body fat oxidation which is unrelated to food intake. C57BL/6J mice were pair-fed with MCD with and without supplemented AMP-DNM to the diet. Food intake (**A**) and body weight were measured (**B**). Indirect calorimetry was performed to measure VO_2 consumption (**C**) VCO_2 production (**D**), and respiratory exchange ratio (RER) (**E**). Data are expressed as means ± SEM, n = 4-5 mice in each group. * P<0.05 versus MCD diet.*

Table 2. *Liver glycosphingolipid levels in pair-fed mice.*

	MCD	MCD+AMP-DNM
GlcCer (nmol/g liver)	50.7 ± 3.2	58.3 ± 15.5
Ceramide (nmol/g liver)	212.2 ± 9.5	258.5 ± 14.8

Liver glucosylceramide (GlcCer) and ceramide levels in pair-fed mice with MCD or MCD diet supplemented with 100 mg/kg/day of AMP-DNM for 4 days.

AMP-DNM treatment directly targets hepatic fat oxidation in pair-fed mice.

To further investigate the effect of AMP-DNM treatment on hepatic fat oxidation in pair-fed mice, we examined gene expression of pyruvate dehydrogenase kinase isozyme 4 (*Pdk4*) in livers of MCD- and AMP-DNM treated MCD-fed mice. Hepatic mRNA expression of *Pdk4* was increased in AMP-DNM treated MCD-fed

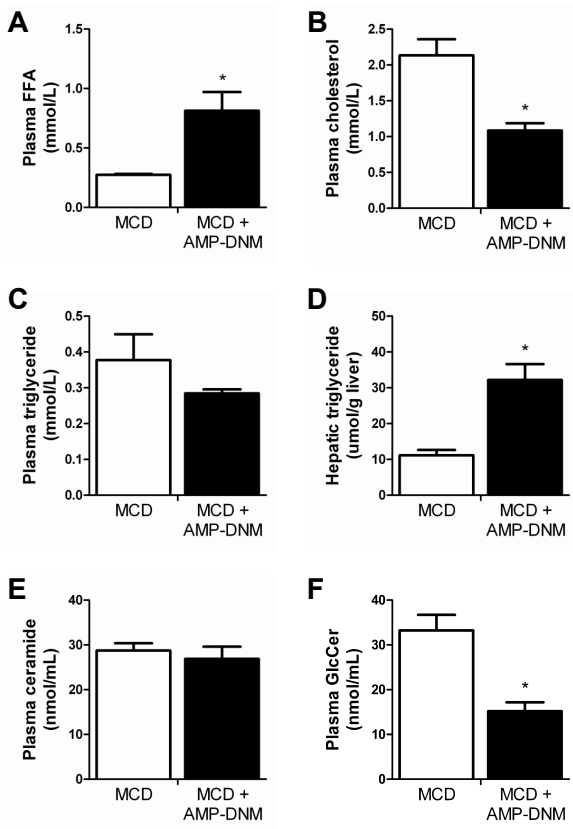

Figure 4. *AMP-DNM leads to increased hepatic steatosis in pair-fed mice. C57BL/6J mice were pair-fed with MCD with and without supplemented AMP-DNM to the diet for 4 days. Plasma concentrations of free fatty acids (FFA) (**A**), cholesterol (**B**), and triglycerides (**C**) were quantified biochemically. Triglyceride content in the liver (**D**) was determined. Plasma ceramide (**E**) and glucosylceramide (GlcCer) (**F**) concentrations were measured. Data are expressed as means ± SEM, n = 4-5 mice in each group. * P<0.05 versus MCD diet.*

mice compared to MCD-fed mice (Fig 5A). In addition, plasma β-hydroxybutyrate levels were significantly increased in AMP-DNM treated MCD-fed mice compared to MCD-fed mice, indicating that hepatic fat oxidation is enhanced in AMP-DNM treated MCD-fed mice. Moreover, AMP-DNM-treated MCD-fed mice have increased β-hydroxybutyrate levels compared to MCD-fed mice (Fig. 5B). Next we examined the energy-sensing kinase, AMP-activated protein kinase (AMPK), which is a crucial cellular nutrient and energy sensor, and regulates glucose and lipid metabolism (20). No differences in the phosphorylation status of AMPK (Fig. 5C) and total AMPK levels (Fig. 5D) between *ad libitum*-fed and MCD-restricted mice were observed. However, the phosphorylation status of AMPK was significantly increased in AMP-DNM treated MCD-fed mice compared to both pair- and *ad libitum-fed* control mice (Fig. 5C). In addition, AMP-DNM treatment resulted in a significant reduction in total AMPK levels (Fig. 5D). Next we assessed the phosphorylation status of acetyl CoA carboxylase (ACC), the downstream target of AMPK that indirectly regulates fatty

acid entry into the mitochondria and ultimately β-oxidation. AMP-DNM did not alter the phosphorylation status of ACC in livers of MCD-fed mice (Fig. 5E). However, we observed a significant drop in both phospho and total levels of both ACC isoforms following AMP-DNM treatment in MCD-fed mice (Fig. 5E; pACC, MCD 1.02 ± 0.07 *vs* MCD+AMP-DNM 0.58 ± 0.05, p<0.01; ACC, MCD 1.13 ± 0.08 *vs* MCD+AMP-DNM 0.57 ± 0.06, p<0.01). This may suggest that AMP-DNM directly affects the processes of fat acid oxidation and synthesis in livers of MCD-fed mice, independent from the observed appetite suppressor effect of AMP-DNM.

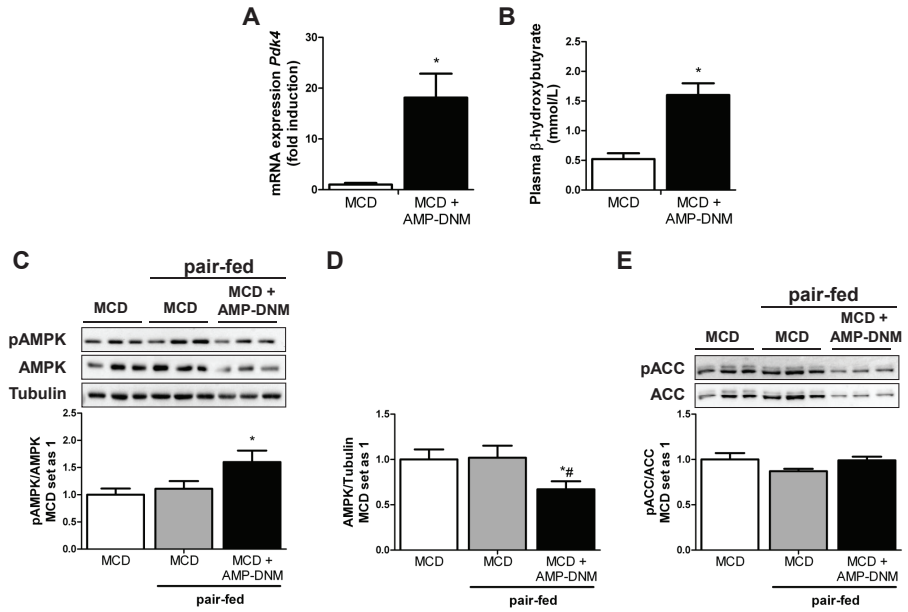

Figure 5. *AMP-DNM treatment directly targets hepatic fat oxidation in pair-fed mice. C57BL/6J mice were pair-fed with MCD with and without supplemented AMP-DNM to the diet for 4 days. Gene expression in whole liver homogenate of pyruvate dehydrogenase kinase, isoenzyme 4 (Pdk4) (**A**) was determined by RT-PCR and expressed as fold induction versus MCD diet. Plasma β-hydroxybutyrate levels were measured as a marker for beta-oxidation (**B**). Phosphorylation status of AMPK at threonine 172 (**C**) and ACC at serine 79 (**E**) were detected using immunoblot analysis with phospho-specific antibodies. Immunoblots were quantified by densitometry and normalized against total protein levels of AMPK (**D**) and ACC (**C**). Data are expressed as means ± SEM, n = 4-5 mice in each group. * P<0.05 versus MCD diet.*

Discussion

In this study, we aimed to gain more insight into the short-term effects of AMP-DNM on lipid metabolism. We wanted to identify if AMP-DNM mediates part of its lipid-lowering effects through acting as a caloric restriction mimetic. Using a MCD diet to induce hepatic steatosis in *ad libitum*-fed mice, we demonstrated that short-term AMP-DNM treatment results in reduced food intake, increased whole-body fat oxidation and protection against the development of hepatic steatosis. Using a pair-fed feeding strategy, we confirmed that AMP-DNM directly induces whole-body and hepatic fat oxidation, which is not related to the appetite suppressor effect of AMP-DNM on fat oxidation. Therefore, our data suggest that the iminosugar AMP-DNM might directly stimulate whole-body and hepatic fat oxidation, supporting the beneficial role of AMP-DNM as a therapeutic target in metabolic disease.

In line with previous reports in *ad libitum*-fed mice (5,7,8), we show that glucosylceramide synthase inhibition by the iminosugar AMP-DNM results in a reduction of hepatic steatosis in MCD-fed mice (Fig. 1A). In addition, we have also shown that AMP-DNM treatment of MCD-fed mice results in a 45% reduction of food intake (Fig. 2A) and this is accompanied by a significant increase in whole-body fat oxidation (Fig. 2F, 2G) compared to untreated MCD-fed mice. As similar observations of AMP-DNM on food intake and fat oxidation have been observed previously (7,8) and caloric restriction is known to induce fat oxidation (21,22), our results in *ad libitum*-MCD-fed mice suggest that this increase in whole-body fat oxidation might be a result of the severe reduction in food intake in AMP-DNM treated MCD-fed mice. However, using a pair-fed feeding strategy, we demonstrate that AMP-DNM treatment directly promotes whole-body fat oxidation, as reflected by an RER that is distinct from the normal response to starvation (Fig. 3E). Indeed, the calorie restriction-induced effect on fat oxidation was significantly more dramatic in pair-fed MCD-fed mice compared to AMP-DNM-treated mice (Fig. 3E), suggesting that AMP-DNM-treated mice are not energy compromised in comparison to the MCD-pair-fed mice. This indicates that the enhanced fat oxidation observed in *ad libitum*-fed mice is independent of the appetite suppressing effect of AMP-DNM.

In addition to the stimulation of whole body fat oxidation, AMP-DNM treatment increased hepatic fat oxidation, which was associated with enhanced mRNA expression of *Pdk4* (Fig. 5A) and increased production of ketone bodies in the circulation (ketogenesis) (Fig. 5B). In addition, we observed an increased phosporylation of pAMPK/AMPK (Fig. 5C) associated with a significant reduction in protein expression of both ACC isoforms (Fig. 5E) following AMP-DNM treatment in MCD-fed mice compared to both *ad libitum*- and MCD-pair-fed mice. Given their regulatory roles in both lipogenesis (ACC1), β-oxidation and ketogenesis (ACC2) (23,24), and the reported continuous fat oxidation in *Acc2*$^{-/-}$ mice (25), this may further provide evidence for a direct role AMP-DNM in the stimulation of fat oxidation in the liver. However, enhanced fat oxidation following AMP-DNM treatment in MCD-fed mice was associated with increased hepatic steatosis compared to pair-fed controls (Fig. 4D). This is in contrast to the lipid-lowering effect of AMP-DNM on hepatic steatosis in *ad libitum*-fed mice, both in our study as reported by many others

(5,7,8,10). Although we can't explain this controversial finding, it may be suggested that during starvation dietary fatty acids are immediately oxidized and thus not preferentially stored in the liver as triglycerides. Since, we show a starvation effect on fat oxidation in MCD-pair-fed but not in AMP-DNM treated mice, this may thus explain why hepatic steatosis is in fact *increased* in AMP-DNM-treated MCD-fed mice compared to MCD-pair-fed mice.

Although our data indicates that the effect of AMP-DNM on fat oxidation and food intake are seemingly unrelated, they could still be intertwined and thus it remains to be clarified how AMP-DNM integrates these effects on food intake and fat oxidation. Although it is not known of AMP-DNM is able to cross the blood brain barrier, AMP-DNM has previously been shown to stimulate the production of plasma peptide YY (PYY), a satiety-regulating hormone released from the L cells in the intestine in response to food intake (7). PYY has been demonstrated to reduce appetite and slow gastric emptying, most likely due to stimulation of the Y2 receptor in the hypothalamus (26,27), the central regulator of food intake (28). Furthermore, it has been shown to increase fat oxidation following acute and chronic PPY administration in C57BL/6 mice (29), suggesting that PYY may modulate the integration between food intake and fat oxidation in *ad libitum*-fed mice. However, as the effect of AMP-DNM on food intake in our study is secondary to the alteration in substrate metabolism, and since there is unambiguous evidence to support a role for the liver in the control of food intake (30,31), we propose an alternative explanation involving an hepatic site of action for the observed effects of AMP-DNM on fat oxidation and food intake in AMP-DNM treated mice. The liver is an important metabolic sensor involved in the relay of humoral and neural signals via the brain stem to the hypothalamus (32). It has been postulated that hepatic fat oxidation could modulate vagal afferent activity and thus food intake by alterations in the hepatic membrane potential that cause a reduction in afferent spike frequency resulting in transmission of a satiety signal to the brain (30,31). In addition, hepatic fat oxidation may control food intake by producing ketones like 3-hydroxybutyrate that are used as fuels by peripheral nerve fibers (33). Given that AMP-DNM stimulates hepatic fat oxidation and plasma ketones are elevated in our study, it is therefore plausible that AMP-DNM may indeed mediate the control of food intake by directly enhancing hepatic fatty acid oxidation and ketogenesis. However, further studies should be directed to support this hypothesis.

Based on the reduction in food intake in AMP-DNM treated mice, it might be suggested that AMP-DNM could be used as anti-obesity therapeutic. Although, AMP-DNM treatment did not result in a further decrease in body weight compared to both MCD-fed (Fig. 2B) and pair-fed mice (Fig. 3B), it might be that 4 days of AMP-DNM treatment is too short to lead to a reduction in body weight. Indeed, prolonged treatment with AMP-DNM did result in reduced body weight (gain) (7,8), suggesting that AMP-DNM may hold therapeutic value as an anti-obesity agent.

In summary, our study demonstrates that AMP-DNM inhibits GlcCer synthase, reduces food intake, increases whole-body fat oxidation and protects against the development of hepatic steatosis in MCD-fed mice. Moreover, in the paired feeding

study, we confirm that AMP-DNM enhances whole-body fat oxidation and this is unrelated to the appetite suppressor effect of AMP-DNM on fat oxidation. Therefore this study suggests that AMP-DNM directly targets whole-body and hepatic fat oxidation in MCD-fed mice, supporting a beneficial role of AMP-DNM as a therapeutic strategy for obesity-associated metabolic disease.

References

1. Parekh S, Anania FA (2007) Abnormal lipid and glucose metabolism in obesity: implications for nonalcoholic fatty liver disease. Gastroenterology 132: 2191-2207.
2. Aerts JM, Boot RG, van Eijk M, Groener J, Bijl N, Lombardo E, Bietrix FM, Dekker N, Groen AK, Ottenhoff R, van Roomen C, Aten J, Serlie M, Langeveld M, Wennekes T, Overkleeft HS (2011) Glycosphingolipids and insulin resistance. Adv Exp Med Biol 721: 99-119.
3. Chavez JA, Summers SA (2012) A ceramide-centric view of insulin resistance. Cell Metab 15: 585-594.
4. Aerts JM, Ottenhoff R, Powlson AS, Grefhorst A, van Eijk M, Dubbelhuis PF, Aten J, Kuipers F, Serlie MJ, Wennekes T, Sethi JK, O'Rahilly S, Overkleeft HS (2007) Pharmacological inhibition of glucosylceramide synthase enhances insulin sensitivity. Diabetes 56: 1341-1349.
5. Bijl N, Sokolovic M, Vrins C, Langeveld M, Moerland PD, Ottenhoff R, van Roomen CP, Claessen N, Boot RG, Aten J, Groen AK, Aerts JM, van Eijk M (2009) Modulation of glycosphingolipid metabolism significantly improves hepatic insulin sensitivity and reverses hepatic steatosis in mice. Hepatology 50: 1431-1441.
6. van Eijk M, Aten J, Bijl N, Ottenhoff R, van Roomen CP, Dubbelhuis PF, Seeman I, Ghauharali-van der Vlugt K, Overkleeft HS, Arbeeny C, Groen AK, Aerts JM (2009) Reducing glycosphingolipid content in adipose tissue of obese mice restores insulin sensitivity, adipogenesis and reduces inflammation. PLoS One 4: e4723.
7. Langeveld M, van den Berg SA, Bijl N, Bijland S, van Roomen CP, Houben-Weerts JH, Ottenhoff R, Houten SM, van Dijk KW, Romijn JA, Groen AK, Aerts JM, Voshol PJ (2012) Treatment of genetically obese mice with the iminosugar N-(5-adamantane-1-yl-methoxy-pentyl)-deoxynojirimycin reduces body weight by decreasing food intake and increasing fat oxidation. Metabolism 61: 99-107.
8. Lombardo E, van Roomen CP, van Puijvelde GH, Ottenhoff R, van Eijk M, Aten J, Kuiper J, Overkleeft HS, Groen AK, Verhoeven AJ, Aerts JM, Bietrix F (2012) Correction of liver steatosis by a hydrophobic iminosugar modulating glycosphingolipids metabolism. PLoS One 7: e38520.
9. Jennemann R, Rothermel U, Wang S, Sandhoff R, Kaden S, Out R, van Berkel TJ, Aerts JM, Ghauharali K, Sticht C, Grone HJ (2010) Hepatic glycosphingolipid deficiency and liver function in mice. Hepatology 51: 1799-1809.
10. Bijl N, van Roomen CP, Triantis V, Sokolovic M, Ottenhoff R, Scheij S, van Eijk M, Boot RG, Aerts JM, Groen AK (2009) Reduction of glycosphingolipid biosynthesis stimulates biliary lipid secretion in mice. Hepatology 49: 637-645.
11. Corton JC, Apte U, Anderson SP, Limaye P, Yoon L, Latendresse J, Dunn C, Everitt JI, Voss KA, Swanson C, Kimbrough C, Wong JS, Gill SS, Chandraratna RA, Kwak MK, Kensler TW, Stulnig TM, Steffensen KR, Gustafsson JA, Mehendale HM (2004) Mimetics of caloric restriction include agonists of lipid-activated nuclear receptors. J Biol Chem 279: 46204-46212.
12. Frame LT, Hart RW, Leakey JE (1998) Caloric restriction as a mechanism mediating resistance to environmental disease. Environ Health Perspect 106 Suppl 1: 313-324.
13. Weindruch R, Keenan KP, Carney JM, Fernandes G, Feuers RJ, Floyd RA, Halter JB, Ramsey JJ, Richardson A, Roth GS, Spindler SR (2001) Caloric restriction mimetics: metabolic interventions. J Gerontol A Biol Sci Med Sci 56 Spec No 1: 20-33.
14. Bietrix F, Lombardo E, van Roomen CP, Ottenhoff R, Vos M, Rensen PC, Verhoeven AJ, Aerts JM, Groen AK (2010) Inhibition of glycosphingolipid synthesis induces a profound reduction of plasma cholesterol and inhibits atherosclerosis development in APOE*3 Leiden and low-density lipoprotein receptor-/- mice. Arterioscler Thromb Vasc Biol 30: 931-937.

15. Leclercq IA, Lebrun VA, Starkel P, Horsmans YJ (2007) Intrahepatic insulin resistance in a murine model of steatohepatitis: effect of PPARgamma agonist pioglitazone. Lab Invest 87: 56-65.
16. Overkleeft HS, Renkema GH, Neele J, Vianello P, Hung IO, Strijland A, van der Burg AM, Koomen GJ, Pandit UK, Aerts JM (1998) Generation of specific deoxynojirimycin-type inhibitors of the non-lysosomal glucosylceramidase. J Biol Chem 273: 26522-26527.
17. Peronnet F, Massicotte D (1991) Table of nonprotein respiratory quotient: an update. Can J Sport Sci 16: 23-29.
18. Bligh EG, Dyer WJ (1959) A rapid method of total lipid extraction and purification. Can J Biochem Physiol 37: 911-917.
19. Folch J, Lees M, Sloane Stanley GH (1957) A simple method for the isolation and purification of total lipides from animal tissues. J Biol Chem 226: 497-509.
20. Hardie DG, Carling D (1997) The AMP-activated protein kinase--fuel gauge of the mammalian cell? Eur J Biochem 246: 259-273.
21. Bruss MD, Khambatta CF, Ruby MA, Aggarwal I, Hellerstein MK (2010) Calorie restriction increases fatty acid synthesis and whole body fat oxidation rates. Am J Physiol Endocrinol Metab 298: E108-E116.
22. Kersten S, Seydoux J, Peters JM, Gonzalez FJ, Desvergne B, Wahli W (1999) Peroxisome proliferator-activated receptor alpha mediates the adaptive response to fasting. J Clin Invest 103: 1489-1498.
23. Abu-Elheiga L, marza-Ortega DB, Baldini A, Wakil SJ (1997) Human acetyl-CoA carboxylase 2. Molecular cloning, characterization, chromosomal mapping, and evidence for two isoforms. J Biol Chem 272: 10669-10677.
24. Abu-Elheiga L, Brinkley WR, Zhong L, Chirala SS, Woldegiorgis G, Wakil SJ (2000) The subcellular localization of acetyl-CoA carboxylase 2. Proc Natl Acad Sci U S A 97: 1444-1449.
25. Abu-Elheiga L, Matzuk MM, bo-Hashema KA, Wakil SJ (2001) Continuous fatty acid oxidation and reduced fat storage in mice lacking acetyl-CoA carboxylase 2. Science 291: 2613-2616.
26. Batterham RL, Cowley MA, Small CJ, Herzog H, Cohen MA, Dakin CL, Wren AM, Brynes AE, Low MJ, Ghatei MA, Cone RD, Bloom SR (2002) Gut hormone PYY(3-36) physiologically inhibits food intake. Nature 418: 650-654.
27. Karra E, Chandarana K, Batterham RL (2009) The role of peptide YY in appetite regulation and obesity. J Physiol 587: 19-25.
28. Morton GJ, Cummings DE, Baskin DG, Barsh GS, Schwartz MW (2006) Central nervous system control of food intake and body weight. Nature 443: 289-295.
29. van den Hoek AM, Heijboer AC, Voshol PJ, Havekes LM, Romijn JA, Corssmit EP, Pijl H (2007) Chronic PYY3-36 treatment promotes fat oxidation and ameliorates insulin resistance in C57BL6 mice. Am J Physiol Endocrinol Metab 292: E238-E245.
30. Scharrer E (1999) Control of food intake by fatty acid oxidation and ketogenesis. Nutrition 15: 704-714.
31. Friedman MI (1997) An energy sensor for control of energy intake. Proc Nutr Soc 56: 41-50.
32. Richardson RA, Garden OJ, Davidson HI (2001) Chronic liver disease and transplantation- uncovering the role of the liver in ingestive behaviour. Clinical Nutrition 20, Supplement 1: 141-145.
33. Greene DA, Winegrad AI (1979) In vitro studies of the substrates for energy production and the effects of insulin on glucose utilization in the neural components of peripheral nerve. Diabetes 28: 878-887.

Supplemental Figure

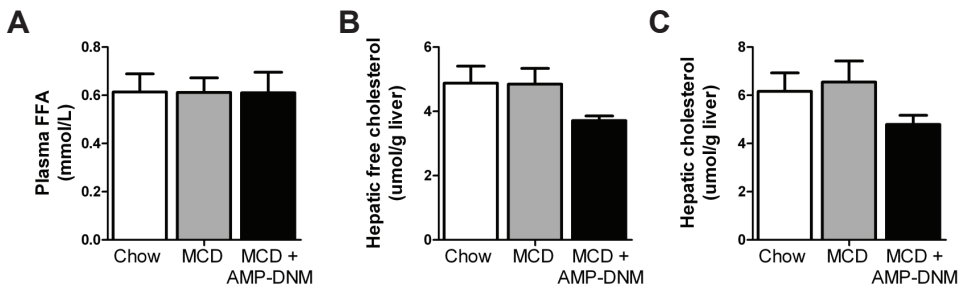

***Figure S1**. Effect of 4 days of AMP-DNM treatment on plasma and liver lipids. C57BL/6J mice were fed ad libitum a chow, MCD or MCD diet supplemented with 100 mg/kg/day AMP-DNM for 4 days. Plasma concentrations of free fatty acids (FFA) (**A**) and liver free cholesterol (**B**) and total cholesterol (**C**) content were measured biochemically. Data are expressed as means ± SEM, n = 12-14 mice in each group. *P < 0.05 versus chow diet.*

Chapter 6

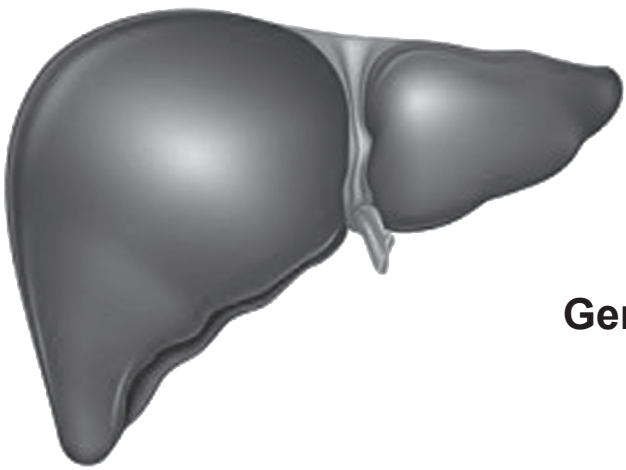

General Discussion

It is generally assumed that inflammation plays a crucial role in the etiology of obesity-induced insulin resistance and type 2 diabetes (T2D). Inflammation in obesity is largely driven by tissue macrophages, and particularly the activated macrophages in metabolic tissues like adipose tissue and liver are believed to cause insulin resistance. Although, most studies have focussed on the role of adipose tissue macrophages, the liver has the largest population of macrophages, which includes the resident macrophages of the liver also known as Kupffer cells. In my thesis, we aimed to establish the role of Kupffer cells on the development of insulin resistance. Insulin resistance is the most important therapeutic target for the metabolic syndrome and therefore insulin resistance is the focus of this discussion. Of note, some of our hypotheses seemed to conflict with the current ideas about the role of inflammation as a cause for the development of insulin resistance. These findings indicate that our current view is still in its infancy, limiting the use of inflammation as a preventive and therapeutic target. Below I will review the role of hepatic inflammation in the development of insulin resistance and discuss the caveats in obesity-induced insulin resistance.

1. Current state of the art

1.1. Mechanism of insulin resistance

Obesity is the most common cause of insulin resistance in humans. Therefore, obesity-induced insulin resistance is one of the dominant factors underlying both metabolic syndrome and the rising frequency of T2D. It is clear that T2D is a heterogeneous disease, making the etiology of insulin resistance complex (1). Chronic, low-grade tissue inflammation is a well-known cause of obesity-induced insulin resistance (2,3). In humans, obesity is associated with increased levels of inflammatory cytokines, including tumor necrosis factor alpha (TNFα) and interleukin-6 (IL-6) (4) and increased levels of C-reactive protein (CRP) (5). Two transcription factor signaling pathways have been linked to the pro-inflammatory effects of obesity and insulin resistance: the nuclear factor-κB (NF-κB) pathway, which is activated by inhibitor of NF-κB (IκB) kinase β (IKKβ), and the c-Jun NH_2-terminal kinase (JNK) pathway. Obesity and high-fat diets activate IKKβ/NF-κB and JNK pathways in different cell types including adipocytes, hepatocytes and macrophages (6). These pathways are activated by pro-inflammatory stimuli including cytokines such as TNFα and interleukin-1 (IL-1) and toll-like receptors (TLRs). Moreover, intracellular stressors like reactive oxygen species (ROS), endoplasmic reticulum (ER) stress, ceramides and various protein kinase C (PKC) isoforms have also been shown to activate JNK and NF-κB (7-10). Phosphorylation of insulin receptor substrate (IRS) 1 and/or 2 at serine sites by either JNK or IKKβ potently inhibits insulin action (Fig. 1; reviewed in (11,12)). Pharmacological or genetic inhibition of IKKβ/NF-κB and JNK signaling have been found to protect experimental animals and humans from diet-induced insulin resistance (13,14). In addition, heterozygous *IKKβ*$^{+/-}$ mice fed a high-fat diet or crossed with obese *ob/ob* mice, are protected against the development of insulin resistance (15). Moreover, genetic deletion of JNK-1 in mice results in protection against diet-induced or genetically-induced (*ob/ob*) insulin resistance (16)

demonstrating the importance of JNK signaling in obesity-induced inflammation and insulin resistance.

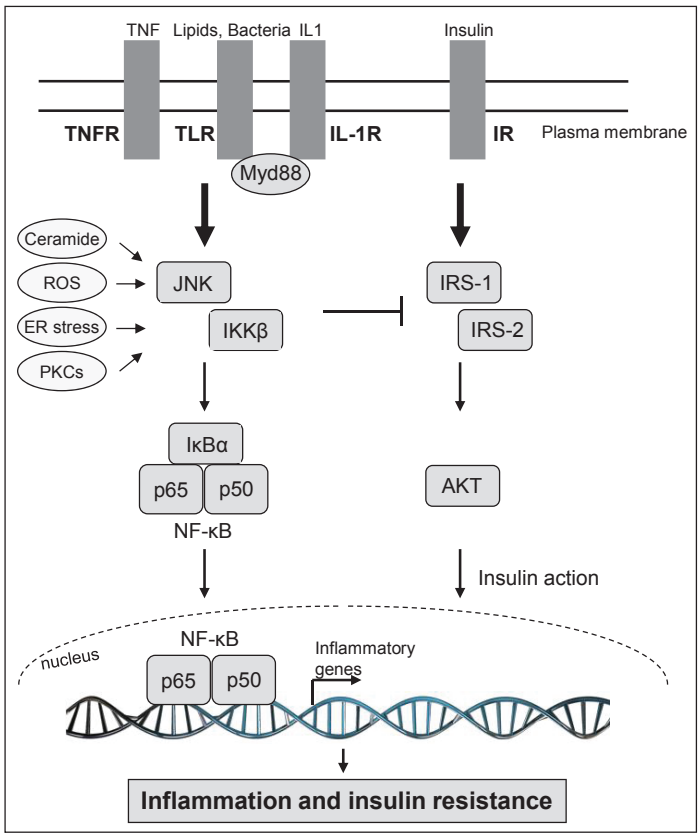

Figure 1. *Cellular mechanisms for activating inflammatory signaling. The IKKβ/NF-κB and JNK pathways ahave been linked to the pro-inflammatory effects of obesity and insulin resistance. These pathways are activated by cytokines, TLRs or intracellular stressors, including ceramides, ROS, ER stress and PKCs. IKKβ and JNK activation leads to serine phosphorylation of IRS-1 and IRS-2, and consequently inhibits insulin signaling.*

1.2. Inflammation and insulin resistance in adipose tissue and liver

Adipose tissue is an important initiator of the inflammatory response to obesity. The discovery of adipose tissue being infiltrated with increasing numbers of macrophages in obese mice and humans has led to a major mechanistic breakthrough into the understanding of how obesity and inflammation are connected (17,18). As part of the chronic inflammatory process, activation of adipose tissue macrophages (ATMs) results in the secretion of chemokines, which attract pro-inflammatory macrophages into the adipose tissue where they form crown-like structures (19). These tissue macrophages then release pro-inflammatory cytokines that further

activate the inflammatory pathway in neighbouring adipocytes, thereby exacerbating inflammation and insulin resistance (reviewed in (20)).

In addition to inflammation and insulin resistance within the adipose tissue, the same process can occur in the liver. Hepatocyte-driven inflammation has been demonstrated to play a role in the etiology of insulin resistance. Expression of constitutively-active IKKβ in the liver resulted in hepatic and systemic insulin resistance (21). Moreover, mice lacking IKKβ in the hepatocytes retain insulin responsiveness in the liver in response to high-fat feeding, obesity or aging, but these mice develop insulin resistance in skeletal muscle and adipose tissue (22). Moreover, secretion of pro-inflammatory cytokines by the Kupffer cells, the resident macrophages of the liver, are linked to disruption of hepatic insulin signaling (23). Consistent with this, enhanced expression of inflammatory genes in the liver following high-fat feeding is associated with reduced insulin sensitivity in mice (21,24). These studies suggest that insulin resistance is causally related to hepatic inflammation (21-23).

Although activation of pro-inflammatory pathways in insulin target tissues (adipose tissue, liver and muscle) is strongly associated with the development of systemic insulin resistance, recent reports, including this thesis, have raised doubt on the causality of this association. Hence, the general role of inflammation as inducer of insulin resistance may be questioned and it has become of significant interest to precisely understand the link between inflammation and insulin resistance. Only then, it will be possible to design the much-needed novel therapies to combat T2D.

2. The controversial role of hepatic inflammation and insulin resistance

2.1. Discrepancies in the models used to study the role of inflammation in the pathogenesis of insulin resistance

In this thesis, we have demonstrated using 3 different mouse models that hepatic inflammation does not necessarily cause insulin resistance. We have assessed the role of inflammation in the development of insulin resistance by making use of a high-fat cholesterol (HFC) diet, which is known to induce hepatic inflammation already after 7 days of treatment (25). First, we have established that short-term HFC feeding results in pronounced Kupffer cell-driven hepatic inflammation in low-density lipoprotein receptor knockout (*Ldlr*$^{-/-}$) mice **(Chapter 2**). However, we did not observe any signs of systemic or hepatic insulin resistance in these mice during the onset of obesity. In addition, sustained hepatic inflammation induced by 15 weeks of HFC feeding did not aggravate the development of hepatic or systemic insulin resistance in *Ldlr*$^{-/-}$ mice compared to mice fed the high-fat control diet without excess cholesterol (HFnC) and a regular high-fat (HF)-diabetogenic diet. As we do not find a correlation between the level of hepatic inflammation, insulin resistance and/or obesity, our data, suggest that HFC-induced hepatic inflammation does not contribute to insulin resistance in *Ldlr*$^{-/-}$ mice (**Chapter 2**). Second, global deletion of myeloid differentiation primary response gene 88 (Myd88), an essential signaling

adaptor for most TLRs and IL-1 receptor family members, results in reduced hepatic inflammation but does not lead to protection from obesity-induced insulin resistance (**Chapter 3**). In fact, insulin resistance was even exacerbated in high-fat fed *Myd88*$^{-/-}$ mice, while body weight or adiposity remained unaffected (26,27). Third, colony stimulating factor 1 insufficient (*Csf1*$^{op/+}$) mice show lower inflammatory levels in the liver, adipose tissue and plasma, but still develop systemic insulin resistance (**Chapter 4**).

In support of this, more studies have shown a disconnection between insulin resistance and hepatic inflammation (28-30). In contrast, hepatic insulin resistance is not necessarily associated with the presence of inflammation in the liver as mice overexpressing diacylglycerol O-acyltransferase 2 (DGAT2) in the liver displayed hepatic insulin resistance in the absence of liver inflammation on a chow diet (30). Kupffer cell depletion, by clodronate encapsulated liposomes, has shown to reduce hepatic inflammation, but these mice still develop insulin resistance (29).

Different experimental approaches (genetically engineered mouse models, Kupffer cell depletion, and dietary intervention studies) may be an explanation for the discrepancies about the role of inflammation in the development of insulin resistance. Hepatic inflammation could be studied by 2 different approaches, including hepatocyte- or Kupffer cell-driven hepatic inflammation. However, the question now rises whether hepatocyte-driven inflammation is functionally different from Kupffer cell-driven inflammation and whether or not there is a distinctive role in their control of insulin resistance. A caveat of our experiments could be that the reduced hepatic inflammation is solely due to decreased expression of inflammatory genes in the Kupffer cells and not due to hepatocytes. This would explain why insulin signaling remains unaffected (**Chapter 4**). Nevertheless, the overall inflammatory tone in the liver is high, and does not affect insulin signalling. Hence, it should be clear that inflammation in the adipose tissue, rather than liver is likely to be the dominant mechanism in insulin resistance. In *Ldlr*$^{-/-}$ (**Chapter 2**) and *Myd88*$^{-/-}$ (**Chapter 3**) mice we did not assess the role of adipose tissue inflammation in the development of insulin resistance. Therefore these studies cannot answer the question whether total adiposity may be the driving force behind the development of insulin resistance in our model. However, Csf1 insufficient mice have reduced adipose tissue inflammation but still develop insulin resistance. So the adipose tissue cannot explain the development of insulin resistance in *Csf1*$^{op/+}$ mice (**Chapter 4**).

In contrast to global Myd88 deficiency, deletion of Myd88 from the hematopoietic compartment results in the protection from inflammation-induced insulin resistance (**Chapter 3**). In our global *Myd88*$^{-/-}$ mouse we cannot rule out the role of other cell types including the hepatocytes in the development of inflammation-induced insulin resistance. However, in our hematopoietic deficient Myd88 model Myd88 is depleted in all bone-marrow derived cells, including the Kupffer cells (**Chapter 3**). Therefore these suggest that Kupffer cell-mediated hepatic inflammation is indeed involved in the development of insulin resistance. In addition, mice with brain-specific deletion of Myd88 are protected from hypothalamic inflammation as well as peripheral insulin resistance induced by either palmitate or a HF diet (31).

A better understanding why the above mentioned models do not exhibit (hepatic) inflammation-induced insulin resistance is of significant interest, as these mechanisms of insulin resistance.

2.2. The controversial role of TNFα in inflammation-induced insulin resistance

As described above, TNFα, derived from the expanding adipose tissue, is one of the cytokines that has been linked to the development of obesity and insulin resistance (32). However, several studies question a role for this cytokine and its signaling pathway in the development of insulin resistance (33-36). *Ob/ob* mice that lack TNFα or its receptors (p55 or p75) show a partial protection against the development of insulin resistance (34). Remarkably, using the same mice, Schreyer et al. showed that mice lacking the TNF receptors, p55 and p75, demonstrated an exacerbation of insulin resistance (37). In addition, insulin sensitivity in *ob/ob* mice that only lack the p75 TNFR2 is not affected (38). Other studies also do not support a role for the TNFR in the development of insulin resistance in mice (35). In contrast, it has been suggested that deletion of the TNFR1 exacerbates insulin resistance (33). Moreover, in a gain of function mutant mice expressing the nonsheddable TNFR1 (p55delta ns mice), resulting in chronic low-grade inflammation, we have shown that hepatic inflammation is not associated with insulin resistance (28). Subsequently, these mice were fed a chow diet for one year and were not prone to develop insulin resistance, nor did 12 weeks of HF feeding at the age of one year accelerate the onset of insulin resistance in these mice (28). Although it has been demonstrated that the pro-inflammatory cytokine TNFα was able to induce insulin resistance in rodents (32), neutralizing antibodies against TNFα do not significantly improve insulin sensitivity in obese type 2 diabetic patients (39). In contrast to what has been suggested by others (40,41), circulating concentrations of TNFα are not increased in patients with insulin resistance (42,43). Thus, while initial studies described a causal link between TNF receptor signaling and insulin resistance, recent data cannot confirm this, and also patient data using TNFR receptor blockers to improve insulin signaling are not encouraging.

A possible explanation for the lack of *in vivo* efficacy of TNFα treatment in patients with insulin resistance could be the large difference between circulating and tissue levels of TNFα. TNFα exerts its effects in a paracrine fashion. Given that interstitial adipose tissue levels are 1-2 orders of magnitude higher than circulating TNFα concentrations (44), the possibility arises that that TNFα blocking agents may neutralize the TNFα levels in the circulation only. This leaves the TNFα concentrations in the adipose tissue virtually unaffected. As a result, the effects of TNFα to cause decreased insulin sensitivity are not inhibited because of insufficient penetration into the tissues (45). Nevertheless, treatment of rheumatoid arthritis patients with TNFα inhibitors improved insulin resistance and led to a decreased rate of progression to T2D (46).

It has been suggested that the level of inflammation is important in the pathogenesis

of insulin resistance. Previous reports have revealed that lipopolysaccharide (LPS) levels are increased following a high-fat diet and induce hepatic steatosis and insulin resistance in obese mice (47). Moreover, treatment with antibiotics resulted in a reduction of LPS levels and improved the steatosis and insulin resistance in obese mice (48). In addition, administration of TNFα induces acute hepatitis (49); however, it does not mimic the chronic low-grade inflammation associated with obesity. Mice expressing non-sheddable TNFR1 have hepatic inflammatory gene expression level of approximately 10- to 100-fold lower than mice receiving a single injection with TNFα (28). Both LPS and TNFα induce an acute inflammatory response, while in our studies we have a more physiologically relevant situation of chronic low-grade hepatic inflammation. Therefore the level of inflammation is of significant importance in the development of insulin resistance.

2.3. The controversial role of IKKε in obesity-induced insulin resistance

In addition to the involvement of the classical IκB kinases, IKKα and IKKβ, IKKε has been suggested as novel player in the etiology of obesity-related insulin resistance (50). Interestingly, studies addressing a role of IKKε in obesity and insulin resistance have also shown conflicting results. In a study by Chiang *et al.*, *IKKε*$^{-/-}$ mice appear to be protected from diet-induced weight gain, adipose tissue inflammation and whole-body insulin resistance (50). However, Scheja *et al.*, did not confirm this finding. Indeed, insulin resistance developed to a similar extent in *IKKε*$^{-/-}$ and WT mice following 19 weeks of HF diet feeding (51). Moreover, body weight, fasting glucose and insulin levels, and homeostasis model of assessment-insulin resistance (HOMA-IR) did not differ between WT and *IKKε*$^{-/-}$ mice (51). In addition, inflammatory levels in the adipose tissue, liver, and the circulation were not decreased in *IKKε*$^{-/-}$ mice (51). A possible explanation that could underlie this discrepancy between the two studies could be variations in the degree of diet-induced obesity observed between both studies. For instance, insulin sensitivity was only maintained in *IKKε*$^{-/-}$ mice protected against HF-induced weight-gain (50), whereas *IKKε*$^{-/-}$ mice that gained weight following HF feeding also developed insulin resistance (51). This could be due to the higher fat content of the diet (59 cal% (50) versus 45 cal% (51)) or the earlier onset of the dietary regimen (6 weeks of age (50) vs 14-18 weeks (51)).

Despite these controversies, amlexanox, a high-affinity inhibitor of IKKε used in the clinic to treat asthma, allergic rhinitis and aphthous ulcers, has recently been tested as a potential treatment option for obesity and related disorders in mice (52). Daily administration of amlexanox revealed that HFD-induced weight gain was prevented in mouse models of obesity. Moreover, amlexanox improved insulin sensitivity, attenuated hepatic steatosis and reduced adipose tissue inflammation. In addition, amlexanox promoted energy expenditure in adipose tissue through increased thermogenesis (52). Amlexanox may thus be an interesting candidate for clinical evaluation in the treatment of obesity and related disorders.

3. Balance between inflammatory mediators for metabolic control

Despite the ambiguities discussed above, macrophages are important players in the development of insulin resistance. Some of the ambiguities may be due to the fact that not all studies have thoroughly investigated the macrophage subtypes that may be more relevant for their role in diseases than measuring their cytokine production. Macrophages show heterogeneity in their function, as local environmental factors shape their properties and activation state (53,54). Macrophage are able to produce cytokines and their activation has been roughly defined across 2 separate polarization states, M1 and M2 (53,54). M1 or "classically activated" macrophages are induced by pro-inflammatory mediators such as LPS and IFN-γ. M1 macrophages have enhanced production of the pro-inflammatory cytokines TNFα and IL-6. *In vitro*, M2 or "alternatively activated" macrophages are generated by stimulation of macrophages with IL-4 and/or IL-13 (55). M2 macrophages have low pro-inflammatory cytokine expression and instead these macrophages produce high levels of anti-inflammatory cytokines like IL-10. In the normal situation there is a balance between M1 and M2 macrophages, and between pro- and anti-inflammatory cytokines. The balance between M1 and M2 macrophage populations within visceral adipose tissue appears to be crucially involved in the development of obesity-associated insulin resistance (56). It has been demonstrated that adipose tissue macrophages (ATMs) in lean mice are polarized towards the alternatively activated M2 state, whereas ATMs in obese mice have a classically activated M1 profile (57). Not only in the adipose tissue, but also the macrophages in the liver, the Kupffer cells, have these M1 or M2 properties (55,58). Moreover, previous reports have suggested that alternatively activated M2 macrophages protect hepatocytes from the development of inflammation and steatosis associated with high-fat diet-induced obesity (29,59). CSF-1-induced macrophages are known to be associated with alternatively activated M2 properties (60). We have shown that Csf1 insufficiency resulted in reduced Kupffer cell-mediated hepatic inflammation and fasting-induced hepatic steatosis. This increased liver accumulation is likely due to a decrease in very-low density lipoprotein- triglyceride (VLDL-TG) synthesis and not to differences in *de novo* lipogenesis or β-oxidation (**Chapter 4**). In line with this, genetic ablation of *Pparδ* impairs alternative activation of Kupffer cells, leading to the development of hepatic steatosis (59,61). Moreover, co-culture of Kupffer cells with LPS to induce M1 polarization results in increased hepatic triglyceride accumulation (62). In addition, Kupffer cell depletion studies show that Kupffer cells are important in liver lipid metabolism and triglyceride accumulation (29,62-64). Moreover, deletion of IL-10 results in hepatic triglyceride accumulation associated with obesity (29,65). Altogether these data demonstrate that Kupffer cells play an important role in the development of hepatic steatosis. In addition, it has been suggested that a shift in the resident macrophage polarization is sufficient to induce metabolic dysregulation (61). Together these results indicate a crucial role for alternatively activated Kupffer cells in control of metabolic homeostasis (**Chapter 4**). Hence, a proper balance between pro- and anti-inflammatory mediators is necessary for the optimal metabolic control of the liver.

4. Novel targets to restore insulin sensitivity

Since many studies showed that inflammation plays a crucial role in the etiology of obesity-induced insulin resistance, anti-inflammatory drugs would be a likely choice in restoring insulin sensitivity. However, the use of experimental anti-inflammatory therapies has not been overly successful. In rodents, TNFα blocking agents have been shown to improve insulin sensitivity and lower blood glucose levels, but have been either ineffective or modestly efficacious in humans (66,67). Moreover, Il-1β inhibitors have also been used in the treatment of T2D, again with only moderate success (68,69). Until a specific anti-inflammatory agent shows efficacy in humans, the role of inflammation in causing insulin resistance in obese and T2D subjects remains incompletely established (45). Discussion of anti-inflammatory therapy raises the fundamental question of whether we should inhibit inflammation in the first place. Inflammation is a host response to danger, usually in the form of a pathogen or injury, which is necessary for wound repair and survival. Removing this inflammatory signal could make the system vulnerable to continuing damage and subsequent exposures (2).

Given that obesity is the most common cause of insulin resistance in man and the obesity epidemic underlies the increasing prevalence of T2D, it is obvious that the most effective form of therapy would be to prevent or treat the underlying obesity (45). In this thesis we have shown that *Ldlr*$^{-/-}$ (**Chapter 2**), *Myd88*$^{-/-}$ (**Chapter 3**) and *Csf1*$^{op/+}$ (**Chapter 4**) mice all become obese and develop insulin resistance. Body weight reduction leads to a loss of adipose tissue as well as liver triglycerides, which further leads to improvements in peripheral and hepatic insulin sensitivity, and prevention of hepatic injury (70,71). In addition to lifestyle changes, current therapies utilize bariatric surgery for morbidly obese patients to treat insulin resistance (70,71). The results of gastric bypass surgeries is rapid improvements in insulin resistance and decreased hyperglycemia in T2D patients well in advance of the onset of significant weight reduction (45). A possible explanation might be that the gut microbiota is altered in these patients. Of note, gut microbiota are altered in mice with a Roux-en-Y gastric bypass (RYGB) that resemble many of the metabolic outcomes in humans. Moreover, these changes were independent of weight change or caloric restriction. In addition, transfer of gut mirobiota from RYGB-treated mice to non-operated, germ-free mice resulted in weight loss and decreased fat mass. These data provide evidence that changes in the gut microbiota contribute to reduced weight gain and adiposity after gastric bypass surgery (72). Unfortunately, we did not assess the role of gut microbiota in our models. Therefore we cannot exclude if gut microbiota plays an important role in our models. However, it has already been suggested that the intestinal microbiota is associated with obesity in both mice and humans and plays a role in the development of NAFLD (73). Therefore, therapeutic purposes to modify the gastrointestinal microbiota would be very important in treating metabolic disease. Gnobiotic (germ-free) mice are resistant to HFD-induced obesity (74) and colonization of gnobiotic mice with conventional mouse microbiota increases adipose tissue mass (75). In addition, increased levels of circulating bacteria or bacterial products, including LPS, have been associated with insulin

resistance (76). It is known that antibiotics, which modify the intestinal flora, have an effect on metabolism. Indeed, animals that receive antibiotics gain more weight than animals without antibiotic treatment (77). In line with this, early exposure to oral antibiotics in infants was associated with overweight in later childhood (78,79). It remains to be established how well these processes or mechanisms observed in mice can be extrapolated to humans. Despite marked differences between mice and humans, some promising clinical investigative studies have emerged. For example, the blood levels of bacterial DNA are elevated in pre-diabetic patients and can be predictive of diabetes development in subsequent years, raising the possibility that blood bacterial DNA may be a biomarker for disease progression (80). Furthermore, a recent clinical trial revealed that even though body weight was unaffected, insulin sensitivity was improved in obese individuals receiving fecal transplants from lean subjects (81).

In **Chapter 5** we have shown that the iminosugar *N*-(5'-adamantane-1'-yl-methoxy)-pentyl-1-deoxynojirimycin (AMP-DNM) acts as a caloric restriction mimetic in the presence of glucosylceramide synthase inhibition. Glucosylceramide (GlcCer) synthase inhibitors, like AMP-DNM, have been shown to have great promise as novel therapeutics in metabolic disease, including T2D, insulin resistance, NAFLD, non-alcoholic steatohepatitis (NASH) and atherosclerosis (82-86). We and others have shown that AMP-DNM reduced food intake (85,87,88). Caloric restriction (CR) is known to increase longevity in diverse species (89,90), including mice and humans. In experimental models, CR decreases circulating levels of cholesterol, triglyceride, and glucose, increased insulin sensitivity in the liver and peripheral tissue and decreases the incidence of diabetes and atherosclerosis (91,92). AMP-DNM exhibits many effects that are also observed following caloric restriction, making AMP-DNM a potential target in treating NASH and insulin resistance. However, additional research is needed to investigate if AMP-DNM could be used as a therapeutic target in the development of insulin resistance.

5. Shortcomings and new approaches to study the role inflammation in the development of insulin resistance

All of the mechanistic research that describes the role of inflammation in the development of insulin resistance is performed in high-fat diet-fed C57BL/6 mice. In response to a high-fat diet or aging, C57BL/6 mice become obese, hyperinsulinemic and severely insulin resistant, whereas 129S6 mice do not develop hyperinsulinemia and insulin resistance (93,94). All diet-induced obesity models develop both obesity and inflammation, making it difficult to dissect the role of either obesity or inflammation in the development of insulin resistance. Moreover, it is also hard to assess inter-organ effects in obesity-induced insulin resistance because in diet-induced obesity models the high-fat diet affects all organs at the same time. It has been demonstrated that diabetes-prone C57BL/6 and diabetes-resistant 129S6 mice at 6 weeks of age already show pre-existing differences in the inflammatory milieu in metabolic active tissues before differences in metabolic parameters can be detected. These pre-existing differences may represent an important component of the genetic

background as a risk factor to metabolic disease (95). These observations clearly impact the choice of models and dietary strategy for metabolic studies, as high-fat diets rapidly induce obesity in mice. Future studies may include the use of a systems biology approach in investigating the role of inflammation-induced insulin resistance. For this, different and/or more time points should be considered. The novelty of this systems biology approach is that by comparing young animals using a sensitive computational approach, the focus is on factors that can potentially predispose from disease in a prospective manner and avoid findings that are mainly secondary to obesity or metabolic differences. With this approach, differences between C57BL/6 and 129S6 mice in multiple organs were examined, allowing them to conclude that inflammation in the adipose tissue, and to a lesser extent in liver, is associated with the predisposition to insulin resistance. Moreover, gene network enrichment analysis was able to identify gene sets involved in signal transduction, protein secretion pathways, and glucose metabolism which were differentially expressed between the mouse strains in adipose tissue at 6 week of age (95). It is known that many of these pathways can interact with inflammatory pathways, and this crosstalk could represent an entry point to the manifestation of metabolic diseases.

Concluding remarks

Although, it has been suggested that there is synergy between obesity and inflammation in the development of insulin resistance, we have shown in this thesis that hepatic inflammation is not under all circumstances causally linked to the pathogenesis of insulin resistance. Our data clearly show that the current knowledge about the role of inflammation in the development of insulin resistance is far from understood. This might also explain why anti-inflammation therapy has, so far, failed to translate into meaningful therapeutic advances. In addition, we have also shown that cross-talk between Kupffer cells and hepatocytes is important for protecting hepatocytes from the development of hepatic steatosis These data suggest that a fine balance of inflammatory mediators is necessary for the optimal metabolic control in the liver.

In order to further unravel the role of (hepatic) inflammation in the development of insulin resistance we could benefit from the use of alternative approaches, including a systems biology approach with more or different time points. In addition, research needs to be performed in studying the role of crosstalk between different organs, but also in cell-cell interaction within metabolic tissues.

References

1. Moller DE, Kaufman KD. Metabolic syndrome: a clinical and molecular perspective. Annu Rev Med 2005;56:45-62.
2. Gregor MF, Hotamisligil GS. Inflammatory mechanisms in obesity. Annu Rev Immunol 2011;29:415-445.
3. Lumeng CN, Saltiel AR. Inflammatory links between obesity and metabolic disease. J Clin Invest 2011;121(6):2111-2117.
4. Kern PA, Ranganathan S, Li C, Wood L, Ranganathan G. Adipose tissue tumor necrosis factor and interleukin-6 expression in human obesity and insulin resistance. Am J Physiol Endocrinol Metab 2001;280(5):E745-E751.
5. Visser M, Bouter LM, McQuillan GM, Wener MH, Harris TB. Elevated C-reactive protein levels in overweight and obese adults. JAMA 1999;282(22):2131-2135.
6. Shoelson SE, Lee J, Goldfine AB. Inflammation and insulin resistance. J Clin Invest 2006;116(7):1793-1801.
7. Furukawa S, Fujita T, Shimabukuro M, Iwaki M, Yamada Y, Nakajima Y, et al. Increased oxidative stress in obesity and its impact on metabolic syndrome. J Clin Invest 2004;114(12):1752-1761.
8. Ozcan U, Cao Q, Yilmaz E, Lee AH, Iwakoshi NN, Ozdelen E, et al. Endoplasmic reticulum stress links obesity, insulin action, and type 2 diabetes. Science 200415;306(5695):457-461.
9. Gao Z, Zhang X, Zuberi A, Hwang D, Quon MJ, Lefevre M, et al. Inhibition of insulin sensitivity by free fatty acids requires activation of multiple serine kinases in 3T3-L1 adipocytes. Mol Endocrinol 2004;18(8):2024-2034.
10. Summers SA. Ceramides in insulin resistance and lipotoxicity. Prog Lipid Res 2006;45(1):42-72.
11. Odegaard JI, Chawla A. Pleiotropic actions of insulin resistance and inflammation in metabolic homeostasis. Science 2013;339(6116):172-177.
12. Hotamisligil GS. Inflammation and metabolic disorders. Nature 2006;444(7121):860-867.
13. Schenk S, Saberi M, Olefsky JM. Insulin sensitivity: modulation by nutrients and inflammation. J Clin Invest 2008;118(9):2992-3002.
14. Wellen KE, Hotamisligil GS. Inflammation, stress, and diabetes. J Clin Invest 2005;115(5):1111-1119.
15. Yuan M, Konstantopoulos N, Lee J, Hansen L, Li ZW, Karin M, et al. Reversal of obesity- and diet-induced insulin resistance with salicylates or targeted disruption of Ikkbeta. Science 2001;293(5535):1673-1677.
16. Hirosumi J, Tuncman G, Chang L, Gorgun CZ, Uysal KT, Maeda K, et al. A central role for JNK in obesity and insulin resistance. Nature 2002;420(6913):333-336.
17. Weisberg SP, McCann D, Desai M, Rosenbaum M, Leibel RL, Ferrante AW, Jr. Obesity is associated with macrophage accumulation in adipose tissue. J Clin Invest 2003;112(12):1796-1808.
18. Wellen KE, Hotamisligil GS. Obesity-induced inflammatory changes in adipose tissue. J Clin Invest 2003;112(12):1785-1788.
19. Cinti S, Mitchell G, Barbatelli G, Murano I, Ceresi E, Faloia E, et al. Adipocyte death defines macrophage localization and function in adipose tissue of obese mice and humans. J Lipid Res 2005;46(11):2347-2355.
20. de Luca C, Olefsky JM. Inflammation and insulin resistance. FEBS Lett 2008;582(1):97-105.
21. Cai D, Yuan M, Frantz DF, Melendez PA, Hansen L, Lee J, et al. Local and systemic insulin resistance resulting from hepatic activation of IKK-beta and NF-kappaB. Nat Med 2005;11(2):183-190.
22. Arkan MC, Hevener AL, Greten FR, Maeda S, Li ZW, Long JM, et al. IKK-beta links

inflammation to obesity-induced insulin resistance. Nat Med 2005;11(2):191-198.
23. Tilg H, Moschen AR. Insulin resistance, inflammation, and non-alcoholic fatty liver disease. Trends Endocrinol Metab 2008;19(10):371-379.
24. Lee YS, Li P, Huh JY, Hwang IJ, Lu M, Kim JI, et al. Inflammation is necessary for long-term but not short-term high-fat diet-induced insulin resistance. Diabetes 2011;60(10):2474-2483.
25. Wouters K, Van Gorp PJ, Bieghs V, Gijbels MJ, Duimel H, Lutjohann D, et al. Dietary cholesterol, rather than liver steatosis, leads to hepatic inflammation in hyperlipidemic mouse models of nonalcoholic steatohepatitis. Hepatology 2008;48(2):474-486.
26. Hosoi T, Yokoyama S, Matsuo S, Akira S, Ozawa K. Myeloid differentiation factor 88 (MyD88)-deficiency increases risk of diabetes in mice. PLoS One 2010;5(9): e12537.
27. Kennedy DJ, Kuchibhotla S, Westfall KM, Silverstein RL, Morton RE, Febbraio M. A CD36-dependent pathway enhances macrophage and adipose tissue inflammation and impairs insulin signalling. Cardiovasc Res 2011;89(3):604-613.
28. Aparicio-Vergara M, Hommelberg PP, Schreurs M, Gruben N, Stienstra R, Shiri-Sverdlov R, et al. Tumor necrosis factor receptor 1 gain-of-function mutation aggravates nonalcoholic fatty liver disease but does not cause insulin resistance in a murine model. Hepatology 2013;57(2):566-576.
29. Clementi AH, Gaudy AM, van Rooijen N, Pierce RH, Mooney RA. Loss of Kupffer cells in diet-induced obesity is associated with increased hepatic steatosis, STAT3 signaling, and further decreases in insulin signaling. Biochim Biophys Acta 2009;1792(11):1062-1072.
30. Jornayvaz FR, Birkenfeld AL, Jurczak MJ, Kanda S, Guigni BA, Jiang DC, et al. Hepatic insulin resistance in mice with hepatic overexpression of diacylglycerol acyltransferase 2. Proc Natl Acad Sci U S A 2011;108(14):5748-5752.
31. Kleinridders A, Schenten D, Konner AC, Belgardt BF, Mauer J, Okamura T, et al. MyD88 signaling in the CNS is required for development of fatty acid-induced leptin resistance and diet-induced obesity. Cell Metab 2009;10(4):249-259.
32. Hotamisligil GS, Shargill NS, Spiegelman BM. Adipose expression of tumor necrosis factor-alpha: direct role in obesity-linked insulin resistance. Science 1993;259(5091):87-91.
33. Toda K, Hayashi Y, Saibara T. Deletion of tumor necrosis factor-alpha receptor type 1 exacerbates insulin resistance and hepatic steatosis in aromatase knockout mice. Biochim Biophys Acta 2010;1801(6):655-664.
34. Uysal KT, Wiesbrock SM, Marino MW, Hotamisligil GS. Protection from obesity-induced insulin resistance in mice lacking TNF-alpha function. Nature 1997;389(6651):610-614.
35. Pamir N, McMillen TS, Kaiyala KJ, Schwartz MW, LeBoeuf RC. Receptors for tumor necrosis factor-alpha play a protective role against obesity and alter adipose tissue macrophage status. Endocrinology 2009;150(9):4124-4134.
36. Romanatto T, Roman EA, Arruda AP, Denis RG, Solon C, Milanski M, et al. Deletion of tumor necrosis factor-alpha receptor 1 (TNFR1) protects against diet-induced obesity by means of increased thermogenesis. J Biol Chem 2009;284(52):36213-36222.
37. Schreyer SA, Chua SC, Jr., LeBoeuf RC. Obesity and diabetes in TNF-alpha receptor- deficient mice. J Clin Invest 1998;102(2):402-411.
38. Uysal KT, Wiesbrock SM, Hotamisligil GS. Functional analysis of tumor necrosis factor (TNF) receptors in TNF-alpha-mediated insulin resistance in genetic obesity. Endocrinology 1998;139(12):4832-4838.
39. Ofei F, Hurel S, Newkirk J, Sopwith M, Taylor R. Effects of an engineered human anti-TNF-alpha antibody (CDP571) on insulin sensitivity and glycemic control in patients with NIDDM. Diabetes 1996;45(7):881-885.

40. Dandona P, Weinstock R, Thusu K, bdel-Rahman E, Aljada A, Wadden T. Tumor necrosis factor-alpha in sera of obese patients: fall with weight loss. J Clin Endocrinol Metab 1998;83(8):2907-2910.
41. Katsuki A, Sumida Y, Murashima S, Murata K, Takarada Y, Ito K, et al. Serum levels of tumor necrosis factor-alpha are increased in obese patients with noninsulin-dependent diabetes mellitus. J Clin Endocrinol Metab 1998;83(3):859-862.
42. Muller S, Martin S, Koenig W, Hanifi-Moghaddam P, Rathmann W, Haastert B, et al. Impaired glucose tolerance is associated with increased serum concentrations of interleukin 6 and co-regulated acute-phase proteins but not TNF-alpha or its receptors. Diabetologia 2002;45(6):805-812.
43. Bruun JM, Verdich C, Toubro S, Astrup A, Richelsen B. Association between measures of insulin sensitivity and circulating levels of interleukin-8, interleukin-6 and tumor necrosis factor-alpha. Effect of weight loss in obese men. Eur J Endocrinol 2003;148(5):535-542.
44. Hotamisligil GS, Arner P, Caro JF, Atkinson RL, Spiegelman BM. Increased adipose tissue expression of tumor necrosis factor-alpha in human obesity and insulin resistance. J Clin Invest 1995;95(5):2409-2415.
45. Johnson AM, Olefsky JM. The origins and drivers of insulin resistance. Cell 2013;152(4):673-684.
46. Solomon DH, Massarotti E, Garg R, Liu J, Canning C, Schneeweiss S. Association between disease-modifying antirheumatic drugs and diabetes risk in patients with rheumatoid arthritis and psoriasis. JAMA 2011;305(24):2525-2531.
47. Cani PD, Amar J, Iglesias MA, Poggi M, Knauf C, Bastelica D, et al. Metabolic endotoxemia initiates obesity and insulin resistance. Diabetes 2007;56(7):1761-1772.
48. Cani PD, Bibiloni R, Knauf C, Waget A, Neyrinck AM, Delzenne NM, et al. Changes in gut microbiota control metabolic endotoxemia-induced inflammation in high-fat diet-induced obesity and diabetes in mice. Diabetes 2008;57(6):1470-1481.
49. Endo M, Masaki T, Seike M, Yoshimatsu H. TNF-alpha induces hepatic steatosis in mice by enhancing gene expression of sterol regulatory element binding protein-1c (SREBP-1c). Exp Biol Med (Maywood) 2007;232(5):614-621.
50. Chiang SH, Bazuine M, Lumeng CN, Geletka LM, Mowers J, White NM, et al. The protein kinase IKKepsilon regulates energy balance in obese mice. Cell 2009;138(5):961-975.
51. Scheja L, Heese B, Seedorf K. Beneficial effects of IKKepsilon-deficiency on body weight and insulin sensitivity are lost in high fat diet-induced obesity in mice. Biochem Biophys Res Commun 2011;407(2):288-294.
52. Reilly SM, Chiang SH, Decker SJ, Chang L, Uhm M, Larsen MJ, et al. An inhibitor of the protein kinases TBK1 and IKK-varepsilon improves obesity-related metabolic dysfunctions in mice. Nat Med 2013;19(3):313-321.
53. Gordon S, Taylor PR. Monocyte and macrophage heterogeneity. Nat Rev Immunol 2005;5(12):953-964.
54. Mantovani A, Sica A, Sozzani S, Allavena P, Vecchi A, Locati M. The chemokine system in diverse forms of macrophage activation and polarization. Trends Immunol 2004;25(12):677-686.
55. Gordon S. Alternative activation of macrophages. Nat Rev Immunol 2003;3(1):23-35.
56. Fuentes L, Roszer T, Ricote M. Inflammatory mediators and insulin resistance in obesity: role of nuclear receptor signaling in macrophages. Mediators Inflamm 2010;2010:219583.
57. Lumeng CN, Bodzin JL, Saltiel AR. Obesity induces a phenotypic switch in adipose tissue macrophage polarization. J Clin Invest 2007;117(1):175-184.
58. Herbert DR, Holscher C, Mohrs M, Arendse B, Schwegmann A, Radwanska M, et al. Alternative macrophage activation is essential for survival during schistosomiasis

and downmodulates T helper 1 responses and immunopathology. Immunity 2004;20(5):623-635.
59. Odegaard JI, Ricardo-Gonzalez RR, Red EA, Vats D, Morel CR, Goforth MH, et al. Alternative M2 activation of Kupffer cells by PPARdelta ameliorates obesity-induced insulin resistance. Cell Metab 2008;7(6):496-507.
60. Brocheriou I, Maouche S, Durand H, Braunersreuther V, Le Naour G, Gratchev A, et al. Antagonistic regulation of macrophage phenotype by M-CSF and GM-CSF: implication in atherosclerosis. Atherosclerosis 2011;214(2):316-324.
61. Kang K, Reilly SM, Karabacak V, Gangl MR, Fitzgerald K, Hatano B, et al. Adipocyte-derived Th2 cytokines and myeloid PPARdelta regulate macrophage polarization and insulin sensitivity. Cell Metab 2008;7(6):485-495.
62. Huang W, Metlakunta A, Dedousis N, Zhang P, Sipula I, Dube JJ, et al. Depletion of liver Kupffer cells prevents the development of diet-induced hepatic steatosis and insulin resistance. Diabetes 2010;59(2):347-357.
63. Neyrinck AM, Cani PD, Dewulf EM, De Backer F, Bindels LB, Delzenne NM. Critical role of Kupffer cells in the management of diet-induced diabetes and obesity. Biochem Biophys Res Commun 2009;385(3):351-356.
64. Stienstra R, Saudale F, Duval C, Keshtkar S, Groener JE, van Rooijen N, et al. Kupffer cells promote hepatic steatosis via interleukin-1beta-dependent suppression of peroxisome proliferator-activated receptor alpha activity. Hepatology 2010;51(2):511-522.
65. den Boer MA, Voshol PJ, Schroder-van der Elst JP, Korsheninnikova E, Ouwens DM, Kuipers F, et al. Endogenous interleukin-10 protects against hepatic steatosis but does not improve insulin sensitivity during high-fat feeding in mice. Endocrinology 2006;147(10):4553-4558.
66. Bernstein LE, Berry J, Kim S, Canavan B, Grinspoon SK. Effects of etanercept in patients with the metabolic syndrome. Arch Intern Med 2006;166(8):902-908.
67. Dominguez H, Storgaard H, Rask-Madsen C, Steffen HT, Ihlemann N, Baunbjerg ND, et al. Metabolic and vascular effects of tumor necrosis factor-alpha blockade with etanercept in obese patients with type 2 diabetes. J Vasc Res 2005;42(6):517-525.
68. Larsen CM, Faulenbach M, Vaag A, Volund A, Ehses JA, Seifert B, et al. Interleukin-1-receptor antagonist in type 2 diabetes mellitus. N Engl J Med 2007;356(15):1517-1526.
69. van Asseldonk EJ, Stienstra R, Koenen TB, Joosten LA, Netea MG, Tack CJ. Treatment with Anakinra improves disposition index but not insulin sensitivity in nondiabetic subjects with the metabolic syndrome: a randomized, double-blind, placebo-controlled study. J Clin Endocrinol Metab 2011;96(7):2119-2126.
70. Satapathy SK, Sanyal AJ. Novel treatment modalities for nonalcoholic steatohepatitis. Trends Endocrinol Metab 2010;21(11):668-675.
71. Hammer S, Snel M, Lamb HJ, Jazet IM, van der Meer RW, Pijl H, et al. Prolonged caloric restriction in obese patients with type 2 diabetes mellitus decreases myocardial triglyceride content and improves myocardial function. J Am Coll Cardiol 2008;52(12):1006-1012.
72. Liou AP, Paziuk M, Luevano JM, Jr., Machineni S, Turnbaugh PJ, Kaplan LM. Conserved shifts in the gut microbiota due to gastric bypass reduce host weight and adiposity. Sci Transl Med 2013;5(178):178ra41.
73. Mouzaki M, Comelli EM, Arendt BM, Bonengel J, Fung SK, Fischer SE, et al. Intestinal microbiota in patients with nonalcoholic fatty liver disease. Hepatology 2013;58(1):120-127.
74. Backhed F, Manchester JK, Semenkovich CF, Gordon JI. Mechanisms underlying the resistance to diet-induced obesity in germ-free mice. Proc Natl Acad Sci U S A 2007;104(3):979-984.

75. Backhed F, Ding H, Wang T, Hooper LV, Koh GY, Nagy A, et al. The gut microbiota as an environmental factor that regulates fat storage. Proc Natl Acad Sci U S A 2004;101(44):15718-15723.
76. Burcelin R, Garidou L, Pomie C. Immuno-microbiota cross and talk: the new paradigm of metabolic diseases. Semin Immunol 2012;24(1):67-74.
77. Cho I, Yamanishi S, Cox L, Methe BA, Zavadil J, Li K, et al. Antibiotics in early life alter the murine colonic microbiome and adiposity. Nature 2012;488(7413):621-626.
78. Trasande L, Blustein J, Liu M, Corwin E, Cox LM, Blaser MJ. Infant antibiotic exposures and early-life body mass. Int J Obes (Lond) 2013;37(1):16-23.
79. Ajslev TA, Andersen CS, Gamborg M, Sorensen TI, Jess T. Childhood overweight after establishment of the gut microbiota: the role of delivery mode, pre-pregnancy weight and early administration of antibiotics. Int J Obes (Lond) 2011;35(4):522-529.
80. Amar J, Serino M, Lange C, Chabo C, Iacovoni J, Mondot S, et al. Involvement of tissue bacteria in the onset of diabetes in humans: evidence for a concept. Diabetologia 2011;54(12):3055-3061.
81. Vrieze A, Van Nood E, Holleman F, Salojarvi J, Kootte RS, Bartelsman JF, et al. Transfer of intestinal microbiota from lean donors increases insulin sensitivity in individuals with metabolic syndrome. Gastroenterology 2012;143(4):913-916.
82. Aerts JM, Ottenhoff R, Powlson AS, Grefhorst A, van Eijk M, Dubbelhuis PF, et al. Pharmacological inhibition of glucosylceramide synthase enhances insulin sensitivity. Diabetes 2007;56(5):1341-1349.
83. Bietrix F, Lombardo E, van Roomen CP, Ottenhoff R, Vos M, Rensen PC, et al. Inhibition of glycosphingolipid synthesis induces a profound reduction of plasma cholesterol and inhibits atherosclerosis development in APOE*3 Leiden and low-density lipoprotein receptor-/- mice. Arterioscler Thromb Vasc Biol 2010;30(5):931-937.
84. Bijl N, Sokolovic M, Vrins C, Langeveld M, Moerland PD, Ottenhoff R, et al. Modulation of glycosphingolipid metabolism significantly improves hepatic insulin sensitivity and reverses hepatic steatosis in mice. Hepatology 2009;50(5):1431-1441.
85. Lombardo E, van Roomen CP, van Puijvelde GH, Ottenhoff R, van Eijk M, Aten J, et al. Correction of liver steatosis by a hydrophobic iminosugar modulating glycosphingolipids metabolism. PLoS One 2012;7(10):e38520.
86. van Eijk M, Aten J, Bijl N, Ottenhoff R, van Roomen CP, Dubbelhuis PF, et al. Reducing glycosphingolipid content in adipose tissue of obese mice restores insulin sensitivity, adipogenesis and reduces inflammation. PLoS One 2009;4(3):e4723.
87. Langeveld M, van den Berg SA, Bijl N, Bijland S, van Roomen CP, Houben-Weerts JH, et al. Treatment of genetically obese mice with the iminosugar N-(5-adamantane-1-yl-methoxy-pentyl)-deoxynojirimycin reduces body weight by decreasing food intake and increasing fat oxidation. Metabolism 2012;61(1):99-107.
88. Bijl N, van Roomen CP, Triantis V, Sokolovic M, Ottenhoff R, Scheij S, et al. Reduction of glycosphingolipid biosynthesis stimulates biliary lipid secretion in mice. Hepatology 2009;49(2):637-645.
89. Anderson RM, Shanmuganayagam D, Weindruch R. Caloric restriction and aging: studies in mice and monkeys. Toxicol Pathol 2009;37(1):47-51.
90. Sinclair DA. Toward a unified theory of caloric restriction and longevity regulation. Mech Ageing Dev 2005;126(9):987-1002.
91. Frame LT, Hart RW, Leakey JE. Caloric restriction as a mechanism mediating resistance to environmental disease. Environ Health Perspect 1998;106 Suppl 1:313-324.
92. Weindruch R, Keenan KP, Carney JM, Fernandes G, Feuers RJ, Floyd RA, et al. Caloric restriction mimetics: metabolic interventions. J Gerontol A Biol Sci Med Sci 2001;56 Spec No 1:20-33.

93. Kulkarni RN, Almind K, Goren HJ, Winnay JN, Ueki K, Okada T, et al. Impact of genetic background on development of hyperinsulinemia and diabetes in insulin receptor/insulin receptor substrate-1 double heterozygous mice. Diabetes 2003;52(6):1528-1534.
94. Almind K, Kahn CR. Genetic determinants of energy expenditure and insulin resistance in diet-induced obesity in mice. Diabetes 2004;53(12):3274-3285.
95. Mori MA, Liu M, Bezy O, Almind K, Shapiro H, Kasif S, et al. A systems biology approach identifies inflammatory abnormalities between mouse strains prior to development of metabolic disease. Diabetes 2010;59(11):2960-2971.

Chapter 7

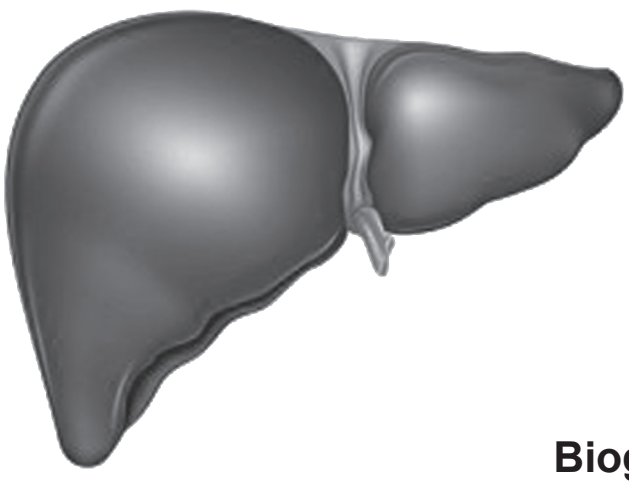

Summary
Samenvatting
Dankwoord
Biography/Biografie

Summary

Over the last decade obesity rates have reached pandemic proportions worldwide and as a result obesity has developed into a global health issue. In parallel with the obesity epidemic, obesity-related disorders, including the metabolic syndrome are rising. In **Chapter 1**, the metabolic syndrome was introduced as a cluster of metabolic disorders, largely driven by obesity, and characterized by dyslipidemia, insulin resistance, and non-alcoholic fatty liver disease (NAFLD). NAFLD is considered as the hepatic manifestation of the metabolic syndrome and refers to a spectrum of liver disorders, including hepatic steatosis, non-alcoholic steatohepatitis (NASH), advanced fibrosis, cirrhosis and ultimately liver cancer/failure. NASH is an advanced stage of NAFLD, involving both hepatic lipid accumulation (steatosis) and inflammation. The liver is comprised of different cells types, including hepatocytes, Kupffer cells, endothelial cells, stellate cells and immune cells. Kupffer cells are the resident macrophages in the liver and they play an important role in the etiology of NAFLD and NASH. Moreover, considerable evidence points towards a crucial role for low-grade inflammation as a causal factor in obesity-induced insulin resistance and type 2 diabetes (T2D). In the present thesis, we used 3 different mouse models, to study the role of inflammation in the etiology of NAFLD and insulin resistance, i.e., *Ldlr*$^{-/-}$ mice, *Myd88*$^{-/-}$ mice, and *Csf1*$^{op/+}$ mice.

Since the significance of hepatic inflammation in driving the pathogenesis of insulin resistance is unclear, we aimed to unravel the role of Kupffer cell-driven hepatic inflammation in the pathogenesis of insulin resistance (**Chapter 2)**. To this end, we used mice deficient for the low-density lipoprotein receptor (*Ldlr*$^{-/-}$) and fed these mice a high-fat cholesterol (HFC) diet to induce hepatic inflammation. We made use of short-term and long-term dietary feeding interventions to study the effect of hepatic inflammation in the absence and presence of obesity. Although we show that short-term HFC feeding leads to hepatic inflammation, systemic or hepatic insulin resistance was not introduced in lean *Ldlr*$^{-/-}$ mice fed this diet. In addition, long-term high-fat diet feeding resulted in obese *Ldlr*$^{-/-}$ mice with insulin resistance; however, this was not exacerbated by cholesterol-induced hepatic inflammation. Hence, our data dissociate hepatic inflammation from insulin resistance and suggest that hepatic inflammation is a consequence rather than a cause of metabolic dysfunction in obesity. Our data therefore provide evidence to question a direct role of Kupffer cell-driven hepatic inflammation in the development of insulin resistance in mice.

The signaling pathways of toll-like receptor (TLR) and interleukin-1 (IL-1) drive nuclear factor-κB (NF-κB)-mediated transcription of inflammatory genes and have been shown to contribute to the development of NASH and insulin resistance. Since TLR and IL-1 signaling activate NF-κB via myeloid differentiation primary response gene 88 (Myd88), we hypothesized that Myd88 might also play an important role in the development of NAFLD and insulin resistance (**Chapter 3**). In mice, we found that Myd88 deficiency resulted in decreased hepatic inflammatory levels and reduced hepatic steatosis. However, these mice were not protected from the development of systemic insulin resistance. To further investigate the role of leukocyte Myd88 in

NASH, we made use of the *Ldlr*$^{-/-}$ mouse model, a validated model to study NASH. For this purpose, we transplanted *Ldlr*$^{-/-}$ mice with bone marrow from WT or *Myd88*$^{-/-}$ mice and fed these mice a HFC diet. *Myd88*$^{-/-}$ transplanted mice showed reduced hepatic inflammation and hepatic steatosis. Of note, these mice were protected from HFC-induced insulin resistance. Next, we evaluated if hepatic *MYD88* expression could play a role in the disease progression in humans. In morbidly obese patients with different stages of NAFLD, we found a correlation between *MYD88* expression in the liver and the levels of C-reactive protein (CRP), ASAT and Kleiner score for steatosis. These data validate our findings in mice that Myd88 plays an important role in the development of NAFLD.

Macrophages are regarded as key players in metabolic homeostasis and in the pathogenesis of diet-induced obesity and insulin resistance. One essential regulator of macrophage homeostasis *in vivo* is macrophage colony-stimulating factor, or Csf1. Although, Csf1 has been suggested to contribute to the pathogenesis of obesity-related disorders, including insulin resistance and T2D, this has never been experimentally addressed. In **Chapter 4**, we investigated the role of Csf-1 in the development of fatty liver disease and insulin resistance. Our data show that *Csf1*$^{op/+}$ mice exhibit fasting-induced hepatic triglyceride accumulation, which might be explained by a reduction in VLDL-TG secretion. Moreover, indirect calorimetric analysis revealed a lower metabolic rate in *Csf1*$^{op/+}$ mice, which was in line with a decrease in lean body mass in these mice. In addition, Csf1 insufficiency resulted in reduced Kupffer cell-driven hepatic inflammation. Despite reduced inflammation in the liver, adipose tissue and the circulation, *Csf1*$^{op/+}$ mice are not protected against the development of insulin resistance. These data suggest that Csf1-induced Kupffer cells are important for protection against the development of hepatic steatosis, but do not affect the etiology of insulin resistance.

Ceramide and its glycosphingolipid metabolites have been implicated in the pathogenesis of obesity-induced insulin resistance. *N*-(5'-adamantane-1'-yl-methoxy)-pentyl-1-deoxynojirimycin (AMP-DNM), an inhibitor of the enzyme glucosylceramide synthase catalyzing glycosphingolipid biosynthesis, has been shown to improve glucose homeostasis and insulin signaling. In **Chapter 5**, we aimed to unravel the short-term effects of AMP-DNM treatment on lipid metabolism and to identify if AMP-DNM may act like a calorie restriction mimetic. To this end, we made use of a methionine and choline-deficient (MCD) diet to induce hepatic steatosis in C57BL/6J mice. Our data show that AMP-DNM treatment results in reduced food intake, increased whole-body fat oxidation and protection against hepatic steatosis in MCD-fed mice. In the paired feeding study, we have demonstrated that AMP-DNM treatment directly promotes whole-body fat oxidation, which is unrelated to the appetite suppressor effect of AMP-DNM on fat oxidation. These data suggest that the iminosugar AMP-DNM directly targets whole-body fat oxidation in mice, supporting the beneficial use of AMP-DNM as therapeutic strategy to alleviate obesity-associated metabolic disease.

The final chapter (**Chapter 6)** discusses the major findings of this thesis, places them in the context with the current state of this field and addresses the clinical

implications of the results.

In conclusion, the studies described in this thesis show that in the models used hepatic inflammation is not necessarily causally linked to the development of insulin resistance. Our data clearly suggest that the current knowledge about the role of inflammation in the development of insulin resistance is far from understood. This might also explain why anti-inflammation therapy has, so far, failed to translate into meaningful therapeutic advances. In addition, we have also shown that cross-talk between Kupffer cells and hepatocytes is important for protecting hepatocytes from the development of hepatic steatosis. These data suggest that a fine balance of inflammatory mediators is necessary for the optimal metabolic control of the liver.

Samenvatting

In de laatste decennia is overgewicht een pandemie geworden en heeft het zich ontwikkeld tot een wereldwijd gezondheidsprobleem. Parallel met deze epidemie heeft er een stijging plaatsgevonden van overgewicht gerelateerde aandoeningen, zoals het metabool syndroom. In **hoofdstuk 1** wordt het metabool syndroom geïntroduceerd als een groep van metabole aandoeningen, grotendeels gedreven door overgewicht, en gekarakteriseerd door een verandering in het lipidenprofiel (dyslipidemie), insuline resistentie en niet-alcoholische leververvetting (NAFLD). NAFLD wordt beschouwd als de lever manifestatie van het metabool syndroom en beschrijft een breed spectrum van lever aandoeningen, zoals vetophoping in de lever (lever steatose), leverontsteking (NASH), fibrose, cirrose en uiteindelijk lever kanker en/of leverfalen. NASH is een vergevorderd stadium van NAFLD waarbij zowel lever steatose als ontsteking betrokken zijn. De lever bestaat uit verschillende typen cellen, namelijk hepatocyten, Kupffer cellen, endotheel cellen, stellaat cellen en immuun cellen. Kupffer cellen zijn de macrofagen van de lever en zij spelen een belangrijke rol bij het ontstaan van NAFLD en NASH. Veel bewijsmateriaal wijst nu op een cruciale rol voor ontstekingen als oorzaak in overgewicht geïnduceerde insuline resistentie en type 2 diabetes (T2D).
In dit proefschrift hebben we drie verschillende muismodellen gebruikt om de rol van ontstekingen bij de ontwikkeling van NAFLD en insuline resistentie te bestuderen: de *Ldlr*$^{-/-}$ muis, de *Myd88*$^{-/-}$ muis en de *Csf1*$^{op/+}$ muis.

Aangezien het belang van ontstekingen in de lever in de pathogenese van insuline resistentie onduidelijk is, hebben we gekeken naar de rol van de Kupffer cel gedreven lever ontstekingen bij het ontstaan van insuline resistentie (**hoofdstuk 2**). Hiervoor hebben we *Ldlr*$^{-/-}$ muizen gebruikt die we een hoog-vet cholesterol (HFC) dieet hebben gegeven om lever ontsteking te induceren. We hebben een korte (2 wk) en lange termijn (15 wk) hoog-vet dieet (verschillend in vet en cholesterol gehalte) gegeven om het effect van lever ontstekingen in aan- en afwezigheid van overgewicht te bestuderen. Hoewel we laten zien dat korte termijn HFC voeding leidt tot lever ontsteking, ontwikkelden de slanke *Ldlr*$^{-/-}$ muizen op dit dieet geen systemische of lever insuline resistentie. Bovendien, leidde lange termijn hoog-vet dieet tot het ontstaan van insuline resistentie in dikke *Ldlr*$^{-/-}$ muizen, echter, dit was niet verergerd door cholesterol geïnduceerde lever ontsteking. Vandaar dat onze resultaten geen verband laten zien tussen lever ontsteking en insuline resistentie en het suggereert dat lever ontsteking eerder een gevolg dan een oorzaak zijn van metabole dysfunctie bij overgewicht. Onze gegevens leveren bewijs om een directe rol van lever ontsteking in het ontstaan van insuline resistentie in muizen in twijfel te trekken.

De signalerings routes van toll-like receptor (TLR) en interleukine-1 (IL-1) leiden tot activatie van nuclear factor-κB (NF-κB) gemedieerde transcriptie van ontstekingsgenen en deze routes dragen bij aan de ontwikkeling van NASH en insuline resistentie. Aangezien TLR en IL-1 signalering beide NF-κB activeren via myeloid differentiation primary response gene 88 (Myd88) veronderstelden wij dat

ook Myd88 een belangrijke rol speelt bij de ontwikkeling van NAFLD en insuline resistentie (**hoofdstuk 3)**. In muizen hebben we gevonden dat Myd88 deficiëntie leidt tot een verlaging van lever ontsteking en een vermindering van lever vervetting. Echter, deze muizen zijn niet beschermd tegen de ontwikkeling van systemische insuline resistentie. Om verder de rol van leukocyt Myd88 in NASH te onderzoeken, hebben we het *Ldlr*$^{-/-}$ muismodel gebruikt omdat het een gevalideerd model is om NASH te bestuderen. Hiervoor hebben we *Ldlr*$^{-/-}$ muizen getransplanteerd met beenmerg cellen van wildtype (WT) of *Myd88*$^{-/-}$ muizen en hebben deze muizen een HFC dieet gevoerd. *Myd88*$^{-/-}$ getransplanteerde muizen laten een verlaging zien van zowel lever ontsteking als lever vervetting. Bovendien zijn deze muizen beschermd tegen HFC geïnduceerde insuline resistentie. Vervolgens hebben we bekeken of *MYD88* expressie in de lever een rol speelt in de ziekte vooruitgang in mensen. In morbide obese patiënten met verschillende stadia van NAFLD hebben we een correlatie gevonden tussen *MYD88* expressie in de lever en de niveaus van C-reactive protein (CRP, een acuut fase eiwit en een marker voor systemische ontsteking), ASAT (marker voor lever schade) en Kleiner score voor steatose (mate van lever steatose). Deze gegevens valideren onze bevindingen in muizen dat Myd88 een belangrijke rol speelt in de ontwikkeling van NAFLD.

Macrofagen worden gezien als belangrijke spelers in metabole homeostase en in de pathogenese van dieet geïnduceerd overgewicht en insuline resistentie. Eén van de belangrijke regelaars van macrofaag homeostase *in vivo* is macrophage colony-stimulating factor, ook wel Csf1 genoemd. Hoewel er wordt gesuggereerd dat Csf1 bijdraagt aan de pathogenese van overgewicht gerelateerde aandoeningen, zoals insuline resistentie en T2D, is dit nooit experimenteel onderzocht. In **hoofdstuk 4** hebben we de rol van Csf1 bestudeerd in de ontwikkeling van vette lever ziekte en insuline resistentie. Onze resultaten laten zien dat *Csf1*$^{op/+}$ muizen een vasten geïnduceerde lever triglyceride opstapeling hebben die mogelijk verklaard kan worden door een verlaagde VLDL-TG secretie. Bovendien laat indirecte caloriemetrische analyse zien dat *Csf1*$^{op/+}$ muizen een lagere stofwisseling hebben en dit is in overeenstemming met een lagere vetvrije massa (spiermassa). Daarnaast leidt Csf1 insufficiëntie tot een verlaging van Kupffer cel gedreven ontsteking in de lever. Ondanks verminderde ontsteking in de lever, het vet weefsel en de circulatie zijn *Csf1*$^{op/+}$ muizen niet beschermd tegen de ontwikkeling van insuline resistentie. Deze resultaten suggereren dat Csf1 geïnduceerde Kupffer cellen een belangrijke rol spelen bij de bescherming tegen de ontwikkeling van lever vervetting, maar Csf1 heeft geen invloed op het ontstaan van insuline resistentie.

Ceramide en de bijbehorende glycosphingolipide metabolieten zijn betrokken bij de pathogenese van overgewicht geïnduceerde insuline resistentie. Het iminosuiker *N*-(5'-adamantane-1'-yl-methoxy)-pentyl-1-deoxynojirimycin (AMP-DNM), een remmer van het enzym glucosylceramide synthase die de biosynthese van glycosphingolipides katalyseert, laat zien dat het de glucose homeostase en insuline signalering verbeterd. In **hoofdstuk 5** hebben we ons gericht op het ontrafelen van de korte termijn effecten van AMP-DNM op de vetstofwisseling en om te identificeren of AMP-DNM als een eetlust remmer kan fungeren. Hierbij hebben we gebruik gemaakt van een methionine en choline-deficiënt (MCD) dieet

om lever steatose te induceren in C57BL/6J muizen. Onze resultaten laten zien dat behandeling met AMP-DNM resulteert in verminderde voedselinname, verhoogde vetverbranding op lichaamsniveau en bescherming tegen lever steatose in MCD gevoede muizen. Door middel van het verlagen van de voedselinname van de MCD controle muizen hebben we vervolgens aangetoond dat behandeling met AMP-DNM direct leidt tot een bevordering van ververbranding op lichaamsniveau en dit is niet gerelateerd aan de eetlust onderdrukking van AMP-DNM op de vetverbranding. Deze resultaten suggereren dat het iminosuiker AMP-DNM rechtstreeks een effect heeft op vetverbranding op lichaamsniveau in muizen en dat ondersteunt het gebruik van AMP-DNM als een mogelijke therapeutische strategie om overgewicht geassocieerde metabole ziekten te verlichten.

Het laatste hoofdstuk (**hoofdstuk 6**) bespreekt de belangrijkste bevindingen van dit proefschrift, plaatst ze in de context van het onderzoeksveld en richt zich op de klinische toepassingen van de resultaten.

In het kort, de in dit proefschrift beschreven studies tonen aan dat in de gebruikte modellen lever ontsteking niet per se causaal gekoppeld zijn aan de ontwikkeling van insuline resistentie. Onze resultaten suggereren dat de huidige kennis met betrekking tot de rol van ontsteking in de ontwikkeling van insuline resistentie verre van begrepen is. Dit zou ook verklaren waarom anti-ontstekingstherapieën tot nu toe niet hebben geleid tot betekenisvolle therapeutische vooruitgang. Verder hebben we aangetoond dat cross-talk tussen Kupffer cellen en hepatocyten belangrijk is voor de bescherming van hepatocyten bij de ontwikkeling van lever steatose. Deze resultaten suggereren dat een juiste balans van ontstekingsmediatoren belangrijk is voor een optimale metabole controle in de lever.

Dankwoord

Eindelijk is het zover, mijn proefschrift is af!! De afgelopen 6 jaar heb ik met veel plezier gewerkt op de afdeling Moleculaire Genetica. Tevens heb ik veel geleerd en al met al heeft dit geleidt tot de totstandkoming van dit proefschrift. En daarvoor wil ik iedereen bedanken die mij hierbij geholpen heeft.

Allereerst wil ik beginnen met het bedanken van mijn promotor Marten Hofker. Beste Marten, bedankt dat jij het in mij zag om mij als AIO in jouw groep op te nemen, terwijl Folkert zich afvroeg of ik er wel al klaar voor was om AIO te worden. Bedankt voor je opbeurende woorden en suggesties als het even tegen zat. We hebben niet veel manuscripten samen geschreven, maar dat hebben we op het laatste moment nog een klein beetje ingehaald met het Myd88 manuscript. Daarnaast moet ik mijn copromoter Debby Koonen bedanken. Debby, ik ben ontzettend blij geweest dat jij ons lab kwam versterken in 2009. In het begin liep het allemaal wat stroef tussen ons, maar naderhand was ik zeer blij dat jij erbij kwam met je goede ideeën en inzichten. Ik heb een hoop van je geleerd met name over het schrijven van de verschillende manuscripten en daar ben ik je erg dankbaar voor. En we hebben samen een drietal mooie manuscripten afgeleverd!! Tegen de tijd dat je dit leest, ben je aardig op weg in je zwangerschap en kun je bijna met zwangerschapsverlof. Succes met de laatste loodjes en veel plezier samen met Tim en je “5de” maar dan ‘echte’ kleine baby.

Daarnaast wil ik de leden van de leescommissie: Prof. Bert Groen, Prof. Patrick Rensen en Prof. Robert Porte, bedanken dat ze de moeite en de tijd hebben genomen om mijn proefschrift positief te beoordelen, ondanks dat de hoofdstukken niet gepubliceerd waren.

Bart en Kuif, allebei erg bedankt voor jullie kritische kijk op de lopende experimenten en de manuscripten. Bart, we hebben altijd leuke discussies gehad over voetbal en met name wie er kampioen zou worden in dat jaar. Gelukkig heb ik de afgelopen 3 jaar kunnen zeggen dat AJAX kampioen is geworden!! En hebben we daarom leuke en lekkere AJAX tompoucen kunnen eten! Beste Pascal, we hebben maar een aantal experimenten samen gedaan, maar bedankt voor je hulp met de hepatocyten en Kupffer cel isolaties en de Oroboros proeven. En bedankt voor je input op de manuscripten. Veel succes met je nieuwe baan!!

Marcel en Marcela, we zijn samen begonnen en jullie zijn inmiddels klaar en ik mag als laatste van ons de rij sluiten met het verdedigen van mijn proefschrift. Allebei bedankt voor de leuke kaas fondue avonden en het bespreken van onze dagelijkse beslommeringen.

Marijke, je was mijn steun en toeverlaat in moeilijke tijden, ik kon altijd bij je terecht voor zowel wetenschappelijke als persoonlijke zaken. Daarom ben ik ook erg blij dat jij mijn paranimf wilt zijn. Ik was blij dat jij er bij was toen ik gebeten werd door een muis en ik vervolgens naar de Eerste Hulp moest. We hebben er in ieder geval achteraf om kunnen lachen. Maar ook wil ik je bedanken voor de dagen dat er muizen gecanuleerd en geclampd moest worden. Helaas is het experiment niet gegaan zoals wij hoopten en hebben we 5 dagen voor niets zo vroeg aanwezig moeten zijn op het CDL.

Niels en Henk, bedankt dat jullie altijd klaar stonden om mij te helpen met de muizen experimenten. Van een beenmerg transplantatie tot een ip injectie, niets was jullie te gek!! Helemaal nadat ik geen injecties meer mocht geven aan de muizen. Niels, jij nog in het bijzonder bedankt voor de altijd leuke en gezellige treinritjes waarin we het altijd over van alles konden hebben. Daarnaast was alles natuurlijk niet mogelijk zonder de andere analisten Daphne, Nicolette, Bastiaan en Elinda. Elinda om maar met jou te beginnen. Bedankt dat jij mij in het begin alle technieken hebt willen leren en willen helpen met het uitvoeren van

het lab werk. Nicolette, bedankt voor je kritische blik op de uitgevoerde experimenten en de interpretatie ervan. Daphne, bedankt dat je mijn “reserve” paranimf wilde zijn en mij hebt geholpen met de voorbereidingen van de “grote” dag. Beste Bastiaan, bedankt dat je mij hebt willen hebben met de Bodipy experimenten, die we helaas niet hebben kunnen gebruiken in ons Csf1 manuscript. Maar ook bedankt voor je hulp met de layout van het proefschrift. Veel succes met je nieuwe baan als research assistent in Soupthampton!

Dear PhD students Nanda and Fareeba, I would like to thank you for all your help with the last experiments you had to perform for me while I was not working anymore at the department. Hopefully, we will be rewarded with accepted manuscripts. Paulina, Alina, Tobias, Frederico, Laser and Jan-Willem thank you for the nice time on the lab. I wish you all the best and good luck finishing your PhD.

Ingrid van der Strate bedankt voor alles wat je hebt gedaan om veel administratief en organisatie werkzaamheden uit mijn handen te houden en dat ik voor van alles bij jou terecht kon. Ingrid Engelsman, we kennen elkaar nog niet zo lang, maar bedankt dat je toch een aantal zaken voor mijn promotie hebt willen uitzoeken/regelen.

Tevens wil het lab van kindergeneeskunde bedanken voor het helpen opzetten van alle experimenten tijdens mijn 1ste jaar als AIO. Folkert en Bert jullie hebben altijd goede suggesties gehad als we even vast zaten met een experiment, zoals het voorstel om nog een experiment doen met het stofje AMP-DNM voor ons MCD manuscript. Tevens wil ik Rick bedanken voor de canulaties voor het clampen. Echter hebben deze experimenten ons niet verder kunnen helpen in het *Ldlr*$^{-/-}$ model. Theo wil ik bedanken voor alle berekeningen die er zijn gedaan voor de verschillende experimenten. Albert, bedankt voor alle hulp met betrekking tot de experimenten met de Oroboros. Dirk-Jan bedankt voor je altijd goede suggesties en opmerkingen.

Verder wil ik graag alle mensen van het CDL bedanken voor het verzorgen van mijn vele individueel gehuisveste dieren in de afgelopen 5 jaar. Arjen, ik wil jou in het bijzonder bedanken voor de dagen dat we hepatocyten hebben geïsoleerd. Ik kon bij jou altijd even mijn verhaal kwijt en het was altijd gezellig.

Daarnaast wil ik graag de leden van de “IOP” groep bedanken: Gert-Jan van Ommen, Tonnie Rijkers, Cisca Wijmenga, Timon van Haeften, Yvonne van der Schouw, Charlotte Onland-Moret, Clara Elbers, Florianne Bauer, Jana van Vliet-Ostaptchouk, Sander Rensen en Wim Buurman. Het was niet altijd even makkelijk om jullie studies in mensen te begrijpen, maar dat zal voor jullie net zo zijn geweest als ik het over de verschillende muis modellen had.

Ook wil ik natuurlijk mijn (schoon)familie bedanken, Frans en Geja, Jasper dank voor jullie vertrouwen in de goede afloop. Bianca, mijn zusje, fijn dat jij vandaag één van mijn paranimfen wilt zijn en er altijd maar in geloofd hebt dat ik het zou afronden. Ton, leuk om je in de familie te hebben en ervoor te zorgen dat mijn “kleine” zusje niet meer helemaal in haar eentje in Nijkerk woont. Pap en mam, jullie hebben altijd vertrouwen in mij gehouden, ook als het even tegen zat, dank jullie wel!!

En natuurlijk lieve Sander, bedankt voor alle ondersteuning die ik tijdens mijn gehele AIO periode van je heb gekregen. Ik weet dat het niet altijd makkelijk was voor ons allebei. Maar we hebben het gered en we gaan ervan genieten dat het nu echt af is!!

Biography

Anouk Funke was born on the 3rd of October 1982 in Emmen. In 2002 she graduated from high school (Esdal College) and started studying Biology at the University of Groningen. After a specialization in Medical Biology she performed 2 research internships with the subjects COPD and Crohn's Disease. This last internship resulted in an authorship on the publication in Clinical and Vaccine Immunology (2012) with the title 'Crohn's disease patients have more fecal IgG-binding bacteria than controls'. Anouk received her Master's degree in August 2007. In 2008 Anouk started as a PhD student at the department of Molecular Genetics at the University Medical Center Groningen under the supervision of Prof. dr. M.H. Hofker. The results obtained from her PhD studies are described in this dissertation and were financed by SenterNovem/Agentschap NL, IOP Genomics project 'The role of inflammation in obesity-induced type 2 diabetes: towards new diagnostic markers and interventional targets'.

Biografie

Anouk Funke werd geboren op 3 oktober 1982 te Emmen. Aan het Esdal College behaalde zij in 2002 haar VWO-diploma, waarna ze aan de studie Biologie begon aan de Rijksuniversiteit Groningen. Na een specialisatie in de richting Medische Biologie volgden twee wetenschappelijk stages met als onderwerpen COPD en de ziekte van Crohn. Deze laatste stage resulterende in een auteurschap op de publicatie in Clinical and Vaccine Immunology (2012) getiteld 'Crohn's disease patients have more fecal IgG-binding bacteria than controls'. Anouk heeft haar doctoraal Medische Biologie ontvangen in augustus 2007. In 2008 begon Anouk aan haar promotieonderzoek bij de afdeling Moleculaire Genetica in het Universitair Medisch Centrum Groningen onder de begeleiding van Prof. dr. M.H. Hofker. De bevindingen van haar onderzoek, gefinancierd door SenterNovem/Agentschap NL, IOP Genomics project 'The role of inflammation in obesity-induced type 2 diabetes: towards new diagnostic markers and interventional targets, worden in dit proefschrift beschreven.